Measurement Of Direct Photon Higher Order Azimuthal Anisotropy In $\sqrt{s_{NN}}$=200GeV Au+Au Collisions at RHIC-PHENIX

(RHIC-PHENIX実験における$\sqrt{s_{NN}}$=200GeV 金・金衝突での直接光子の高次方位角異方性の測定)

筑波大学
University of Tsukuba

水野 三四郎
数理物質科学研究科 物理学専攻
高エネルギー原子核衝突実験グループ
博士論文公開発表会(本審査) 3/7/2015

Outline

✓ **Introduction**
- High Energy Heavy Ion Collision
- Direct photon analysis
- Higher order azimuthal anisotropy

✓ **Analysis**
- PHENIX experiment
- Direct photon v_n measurement

✓ **Results and Discussion**
- Jet contribution for azimuthal anisotropy in high p_T
- Direct photon v_n
- Blast wave model

✓ **Conclusion**

Introduction

Quark-Gluon Plasma (QGP) at heavy ion collision

Quarks and gluons move freely at high temperature and dense matter.

High energy heavy ion collision experiment

- **RHIC at BNL (Au+Au : 200, 62.4, 39 GeV, Cu+Cu : 200 GeV)**
- **LHC at CERN (Pb+Pb : 2760 GeV, p+Pb : 5020 GeV)**

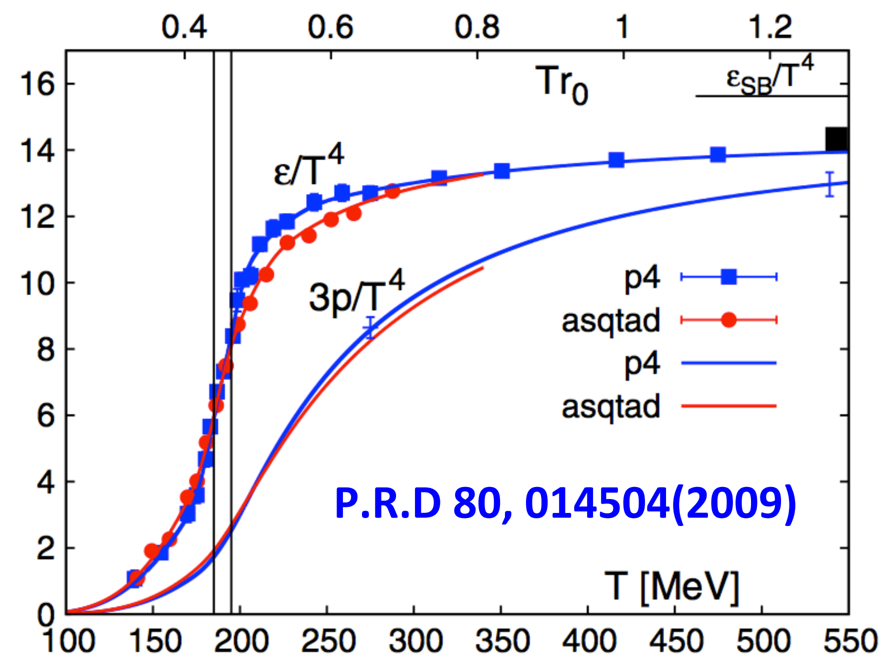

Lattice-QCD calculation predicts

$\varepsilon \approx 1 GeV/fm^3$: $T \approx 170 MeV$

History of collision and photon emission

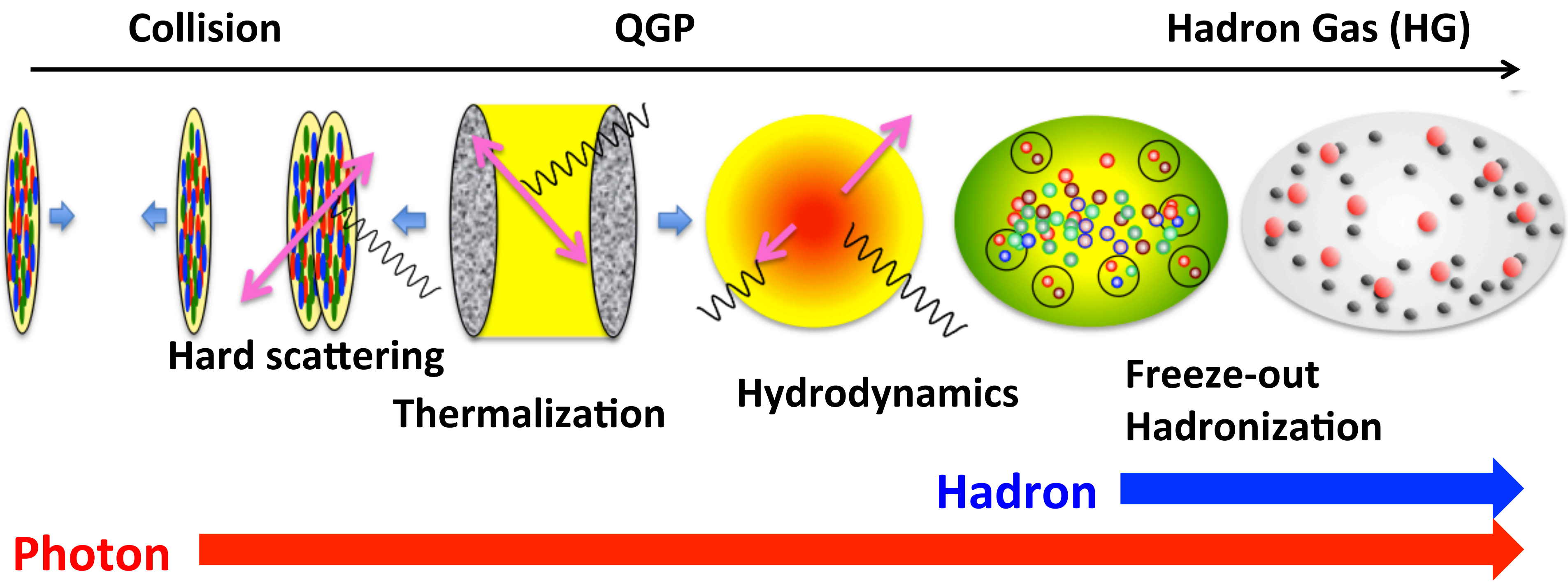

The properties of photon in high energy heavy ion collision

- **emitted during all stages of the collisions**
- **don't interact with the medium**

We can access the evolution of the collision.

Identifying direct photon sources

Direct photons are all photons except those originating from hadron decay.
It is challenging to identify photon sources.
by p_T distribution? emitting angle?

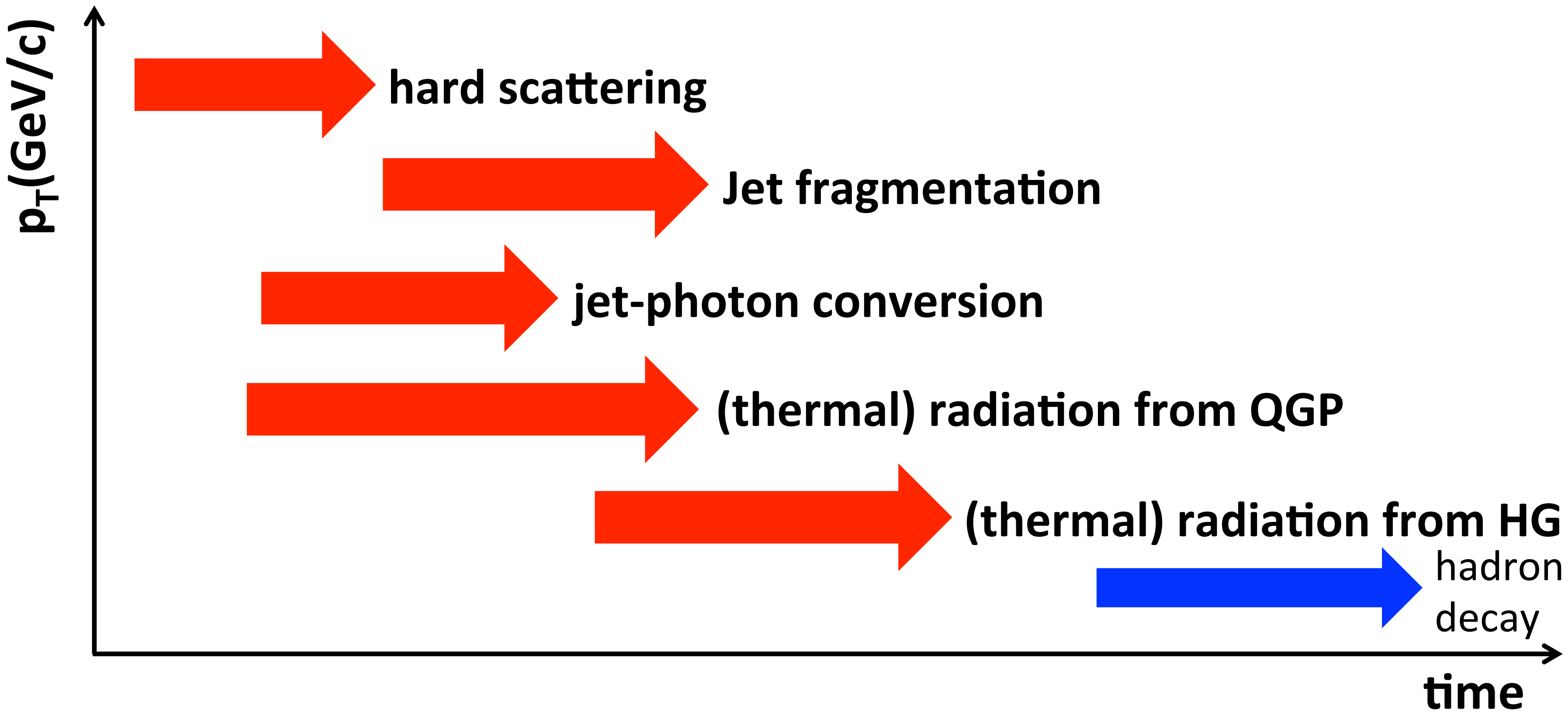

The excess of direct photon

The excess of direct photon has been measured in the wide p_T range.

The methods of virtual photon and external conversion photon are sensitive to low p_T region.

Less than 4 GeV/c, direct photons are included by 20 % in inclusive photon.

$$R_\gamma = N_{inc.}/N_{dec.}$$

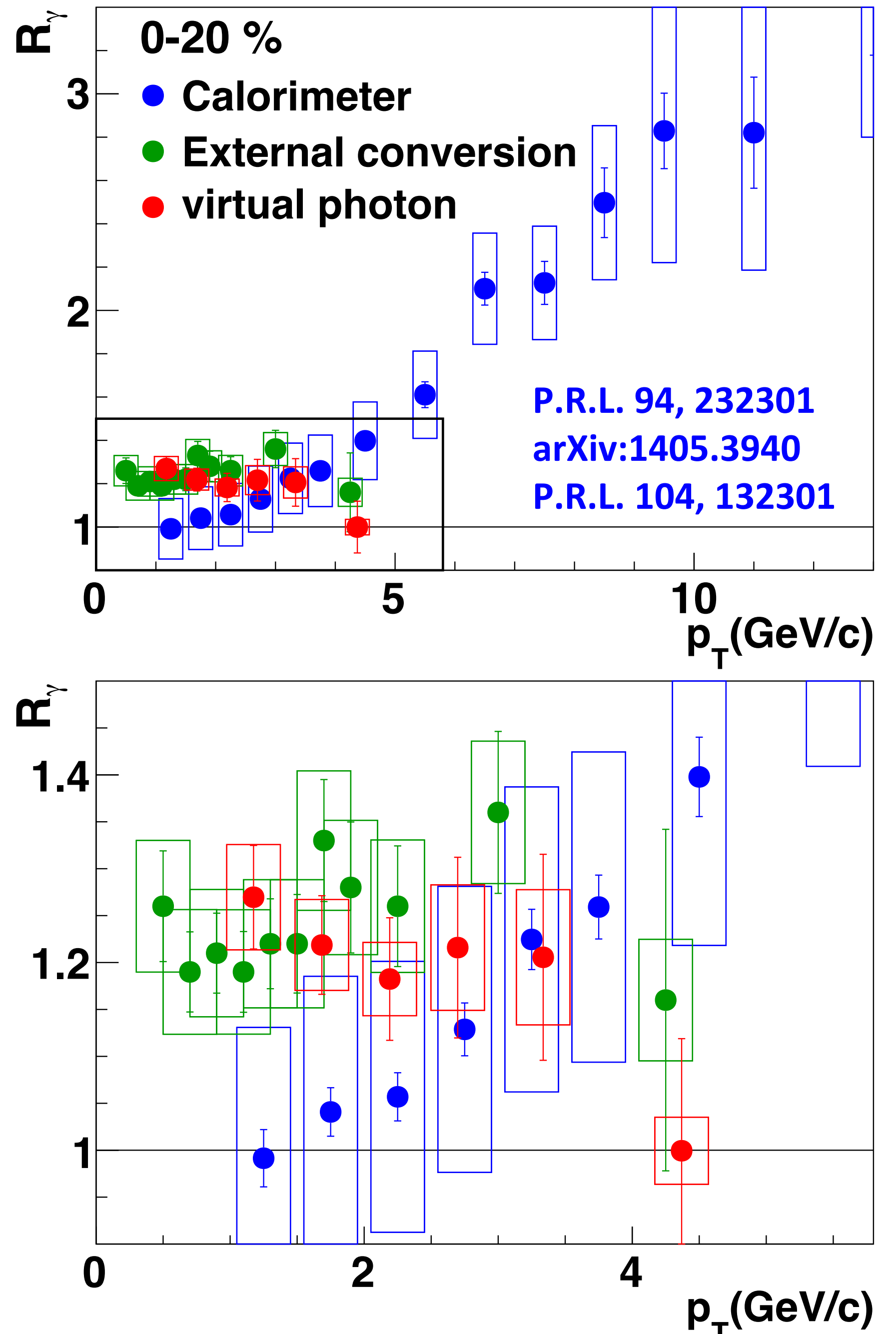

Direct photon p_T spectra

arXiv:1405.3940(2014)

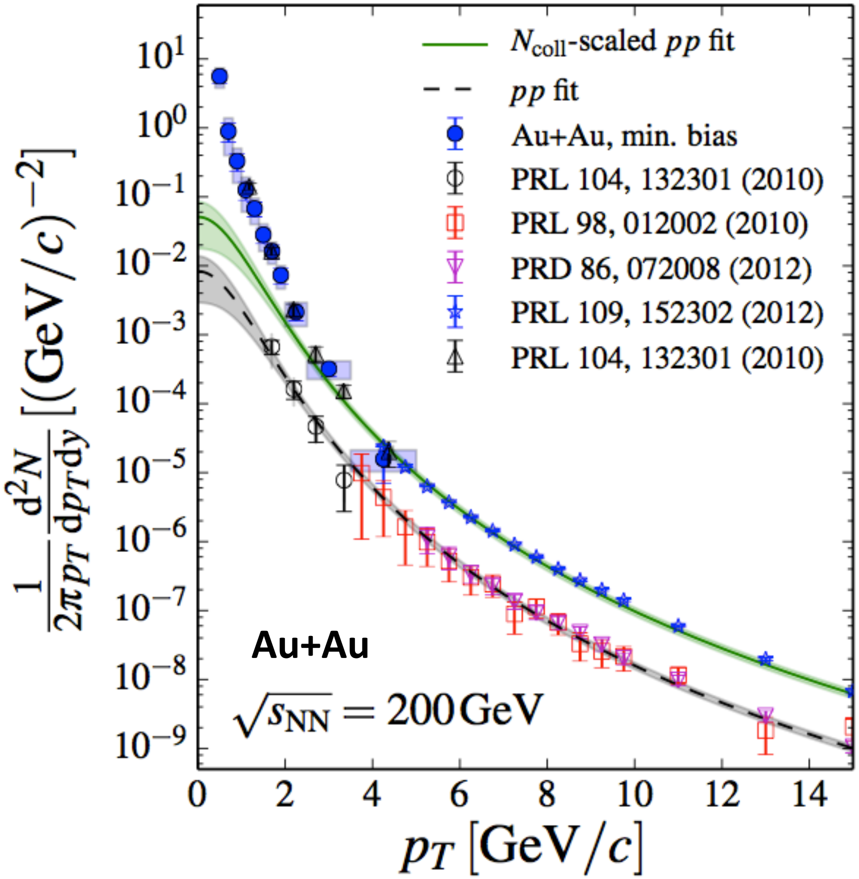

The p_T spectra in Au+Au collision is enhanced compared with that in p+p collision scaled by the number of binary collisions less than 4 GeV/c.

The excess of p_T spectra is fitted and effective temperature is extracted. (Freeze-out temperature of hadrons are about 100MeV)

Centrality	Effective temperature
0% - 20%	239 ± 25 ± 7 (MeV)
20% - 40%	260 ± 33 ± 8 (MeV)
40% - 60%	225 ± 28 ± 6 (MeV)

Photons in low p_T are mainly radiated from very hot medium at early time of collisions.

Azimuthal anisotropy (Elliptic flow)

$$N(\phi - \Psi_{R.P.}) \propto 1 + 2\sum v_n \cos\{n(\phi - \Psi_{R.P.})\}$$

$$v_2 = \langle \cos\{2(\phi - \Psi_{R.P.})\} \rangle$$

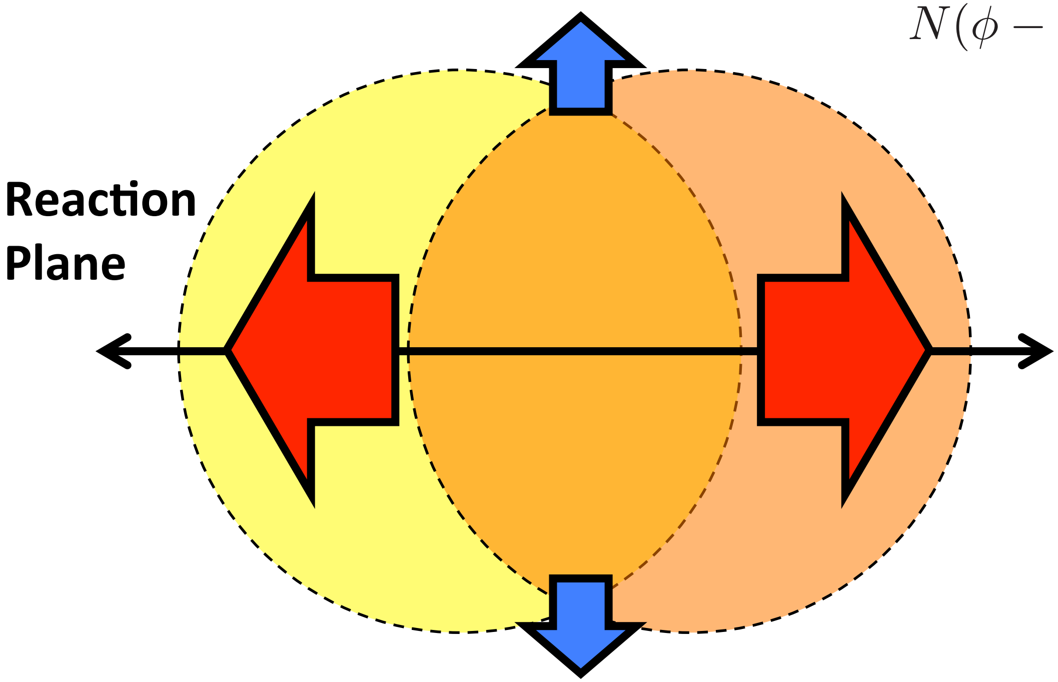

charged particle dφ distribution

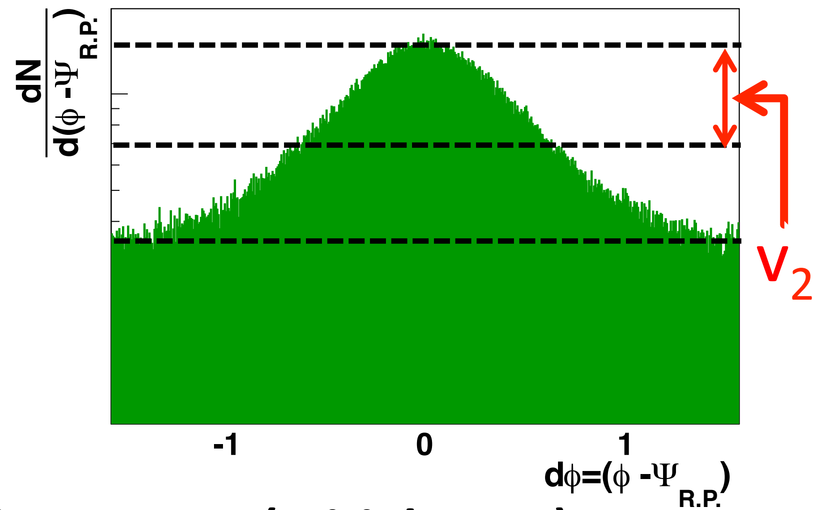

- anisotropic pressure gradient in participant zone (Initial state)
- QGP expansion (hydrodynamic motion, η/s)
  (η is shear viscosity and s is entropy density)
- hadron production mechanism (coalescence)

(1) : Initial geometry is converted into final azimuthal anisotropy
(2) : (expected to be) sensitive to η/s

Photon emitting angle dependence

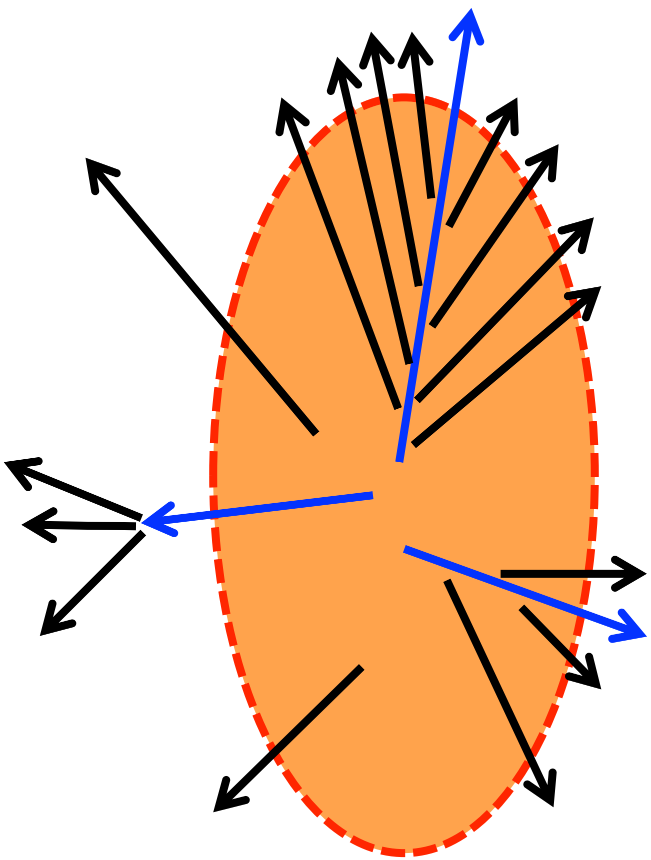

It is expected that the emitted angle of photons depends on their sources.

- Initial hard scattering : $v_2 \approx 0$
- Medium induced : $v_2 \leq 0$
- Jet fragmentation : $v_2 \geq 0$
- Radiation from expanding medium : $v_2 > 0$

The measurement of photon azimuthal anisotropy is a powerful probe to identify the photon sources.

Elliptic flow of direct photon

P.R.L. 109, 122302(2012)

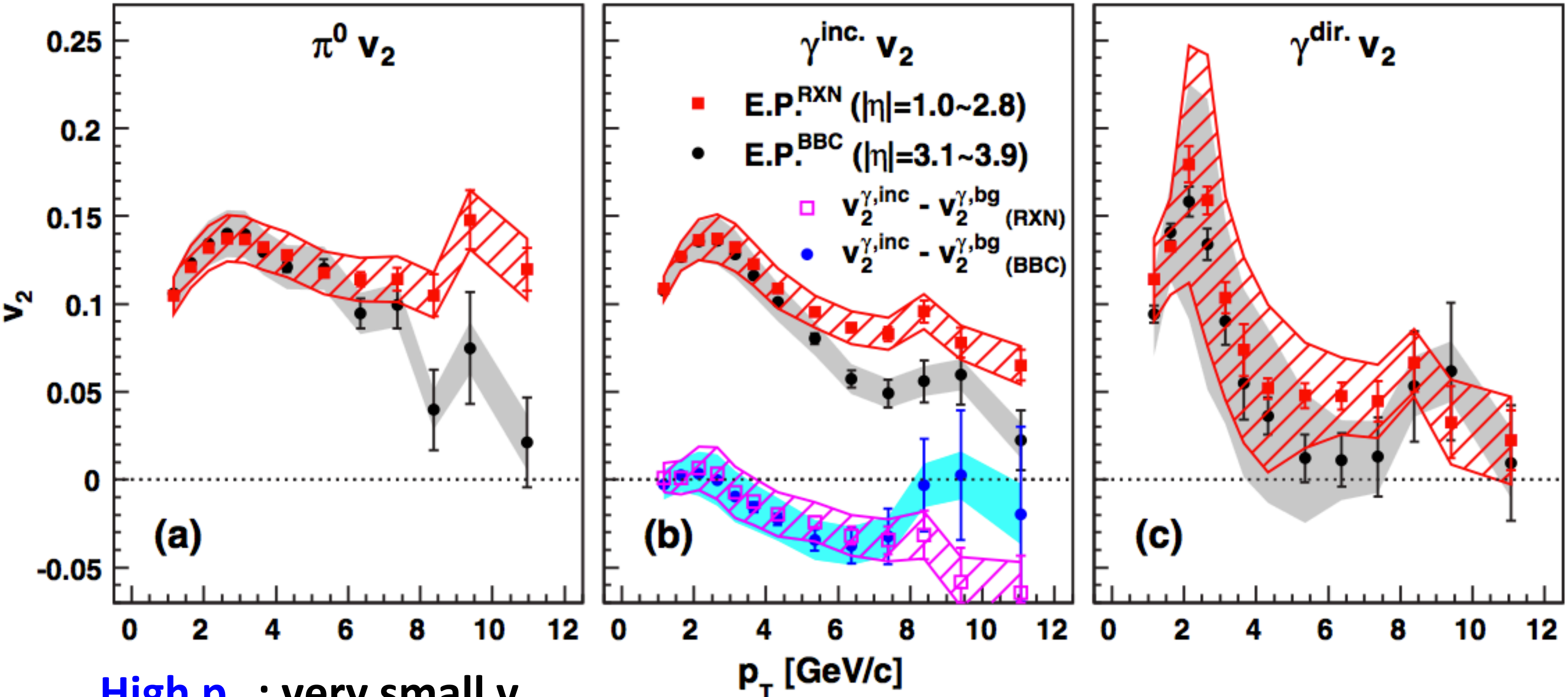

High p_T : very small v_2

It is consistent with the expectation that photons produced in the initial hard scattering are dominant plus no interaction of photon in QGP (R_{AA}≈1).

Low p_T : Comparable to hadron v_2 at around 2 GeV/c

Direct photon puzzle

Thermal radiation photons are dominant in low p_T region.

Elliptic flow :
It was expected that photon has small v_2, since it includes ones from early stage having small v_2.
-> Photons are dominantly emitted at late stage.

p_T spectra :
Emitted from very hot medium ($T_{eff} \approx 240MeV$).
-> Photons are dominantly emitted at early stage.

There is a discrepancy, and it is called "direct photon puzzle".
There is no models to explain both observables simultaneously.

Third order azimuthal anisotropy (v_3)

Ψ_n : Participant Plane

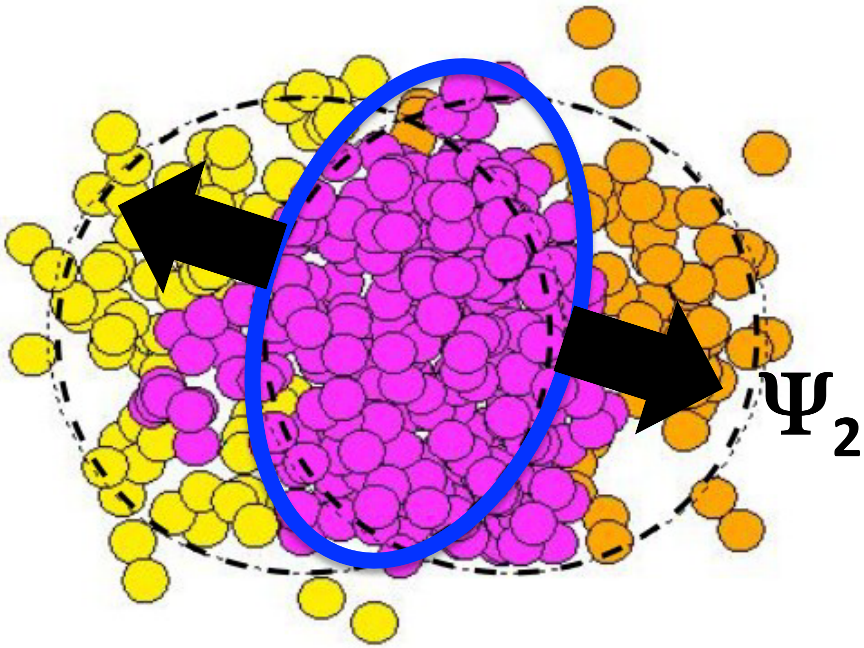

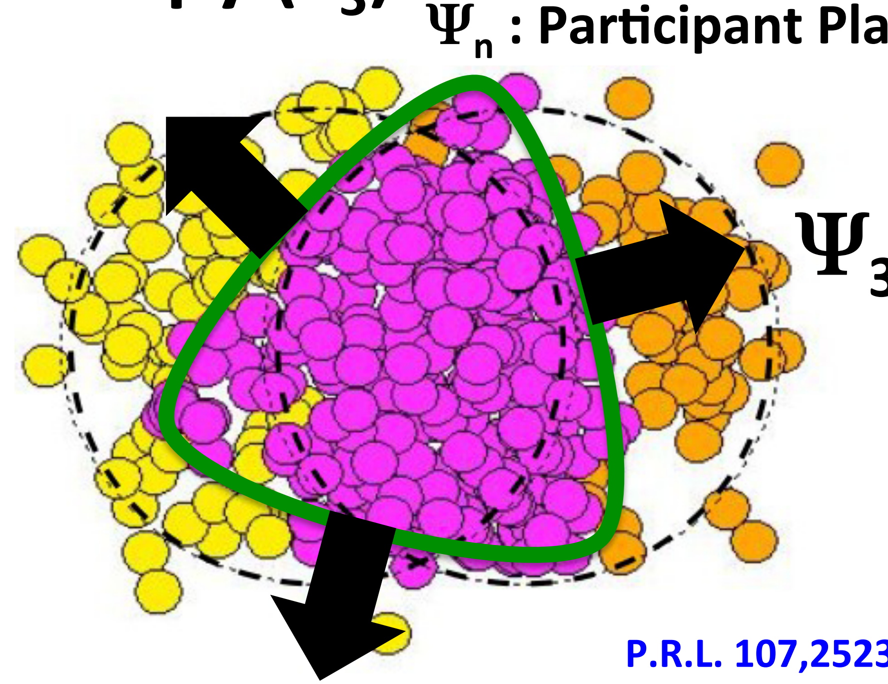

$$N(\phi - \Psi_n) \propto 1 + 2\sum v_n \cos\{n(\phi - \Psi_n)\}$$

$$v_n = \langle \cos\{n(\phi - \Psi_n)\}\rangle$$

The higher order flow is originating from the fluctuation of the shape of participant zone. It is expected to constrain the initial geometry calculating model and η/s of QGP.

P.R.L. 107,252301

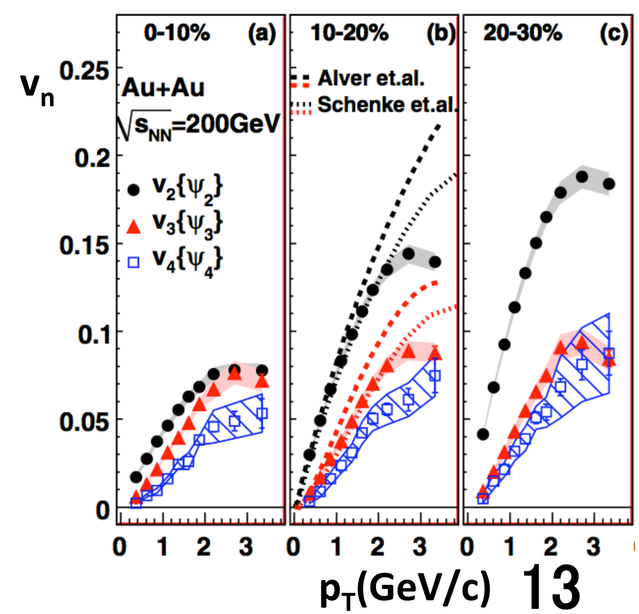

Why direct photon v_3 is measured?

$$T' = T\sqrt{\frac{1+\beta}{1-\beta}}$$

Radial flow effect (blue shift effect) :
It makes apparent temperature higher than true temperature.
Photons from late state are dominant.
$v_2>0$: $v_3>0$

P.R.C 89, 044910 (2014)

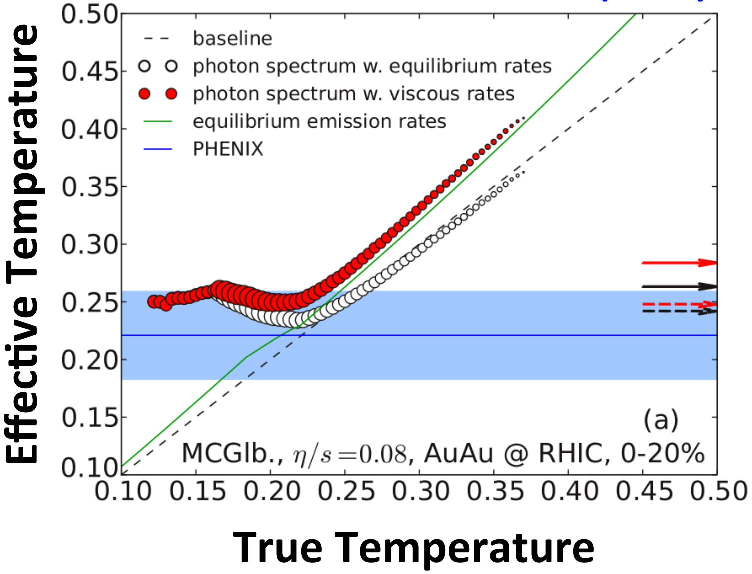

Large magnetic field :
Direction of magnetic field is strongly related with Ψ_2(R.P.) but not with Ψ_3.
$v_2>0$: $v_3\approx0$

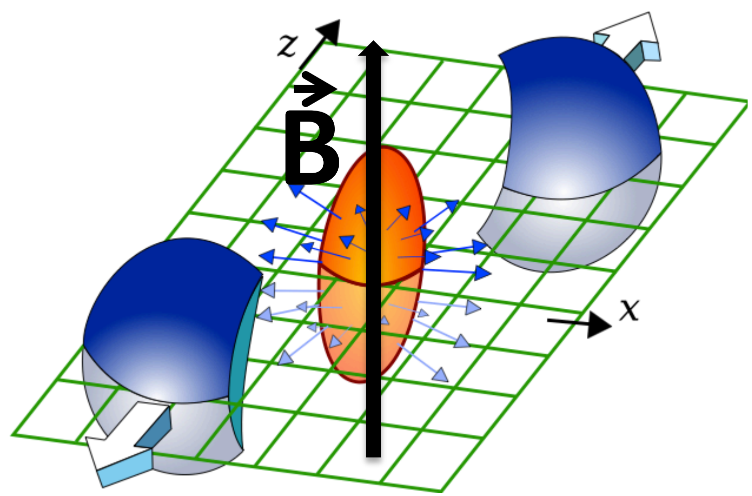

v_3 measurement could provide additional constraint on photon production mechanism.

My activity

Poster & Talk : Analysis

2012 (D1): Data taking shift and Detector expert & TOF calibration

Poster QM 2012

Talk ATHIC 2012

Talk JPS spring

Identified particle azimuthal anisotropy

2013 (D2): Data taking shift and Detector expert & TOF calibration

Talk JPS fall

Talk JPS spring

Neutral pion and direct photon azimuthal anisotropy

2014 (D3): Data taking shift and Detector expert

Talk QM 2014

Talk HIC HIP

Talk ATHIC 2014

Talk WPCF 2014

Analysis

PHENIX detector

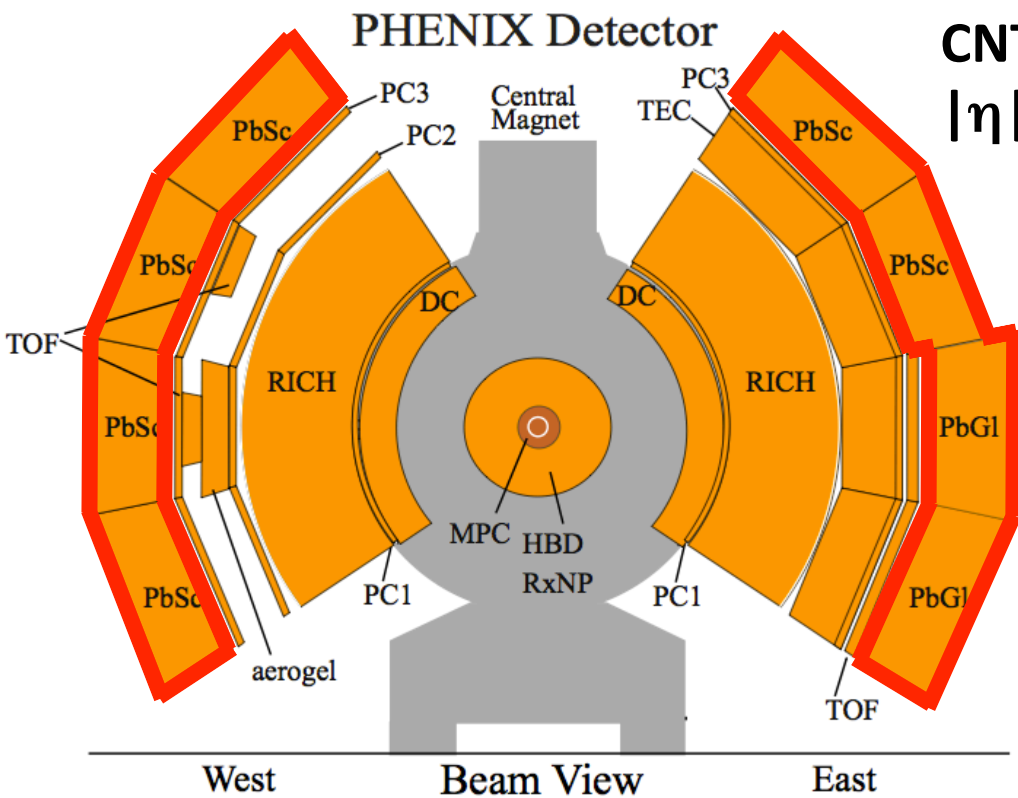

CNT
$|\eta| < 0.35$

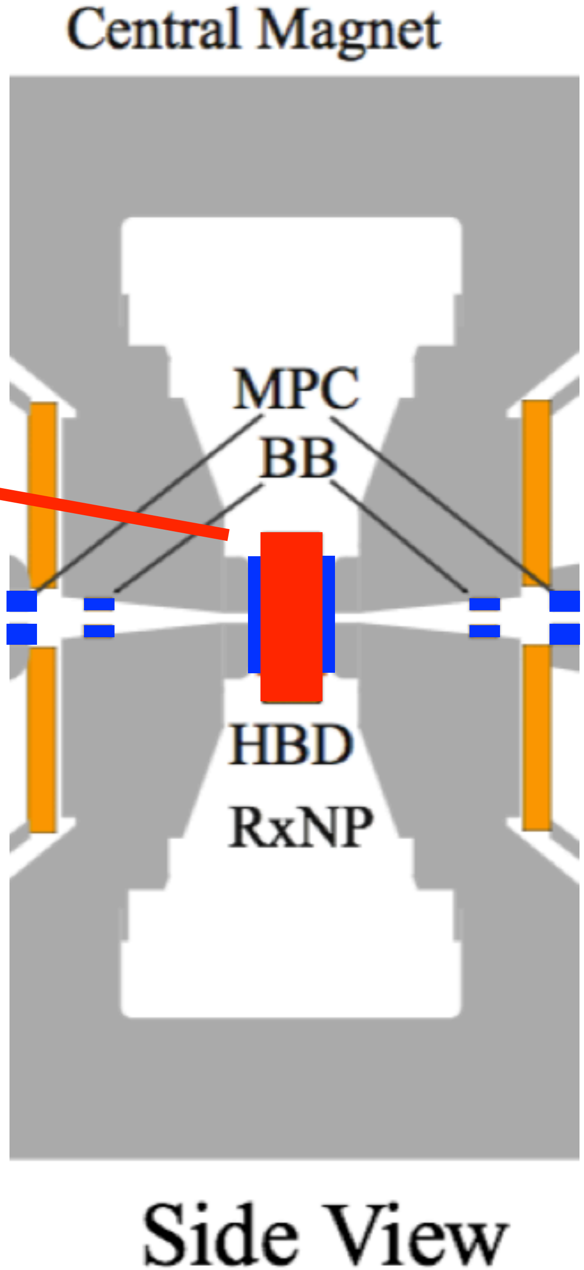

Data set : Au+Au $\sqrt{s_{NN}}$=200GeV collisions
4.4 billion events are analyzed.

$$v_n = \langle \cos\{n(\phi - \Psi_n)\}\rangle$$

Centrality determination

Centrality :
The size of participant zone is classified by multiplicity in BBC.

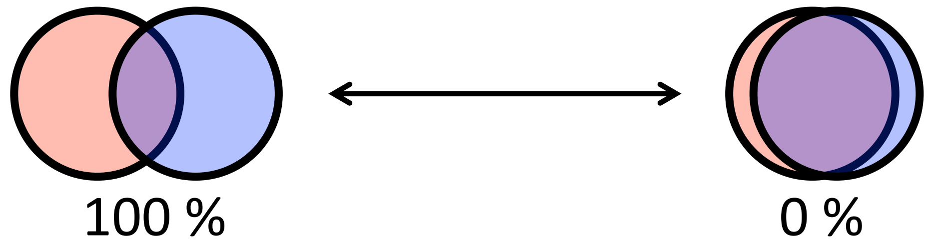

Beam-Beam Counter (BBC) :
Measures charged particles.

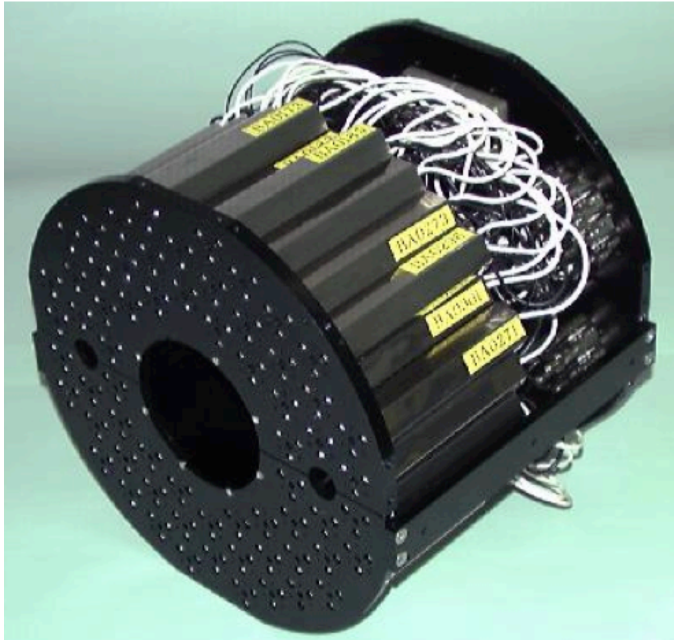

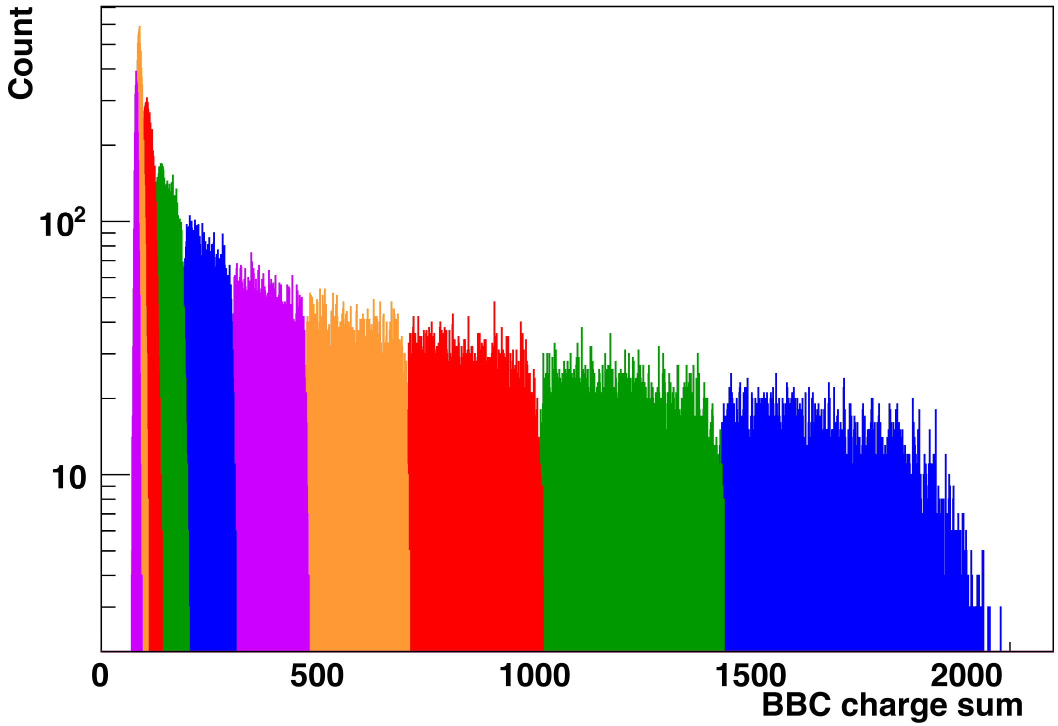

Event plane determination

Event plane is the direction defined by the number of emitted particles.
It is determined for each harmonic "n".

$$\Psi_n = \frac{1}{n}\tan^{-1}\left(\frac{\sum w_i \sin n\phi_i}{\sum w_i \cos n\phi_i}\right)$$

$$\mathrm{Res}(\Psi_n) = \langle \cos\{n(\Psi_n^{\mathrm{true}} - \Psi_n^{\mathrm{obs.}})\}\rangle$$

Reaction Plane detector(RxN)

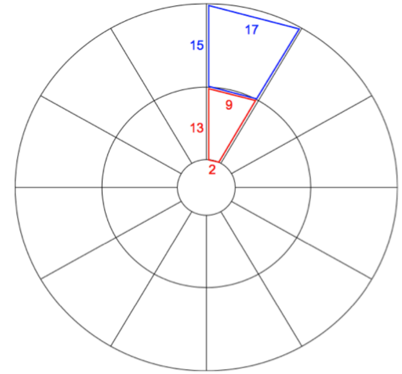

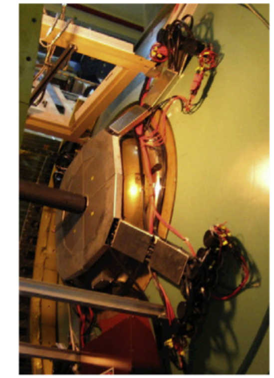

Muon Piston Calorimeter (MPC)

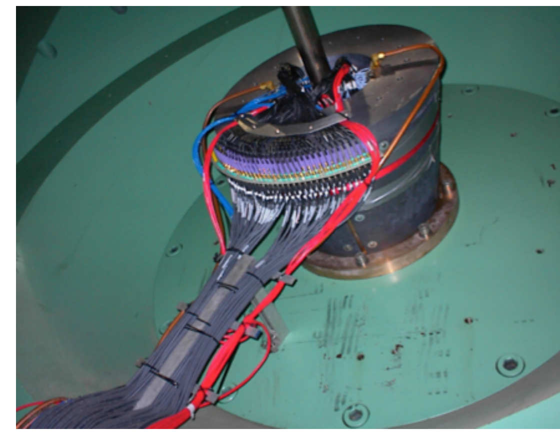

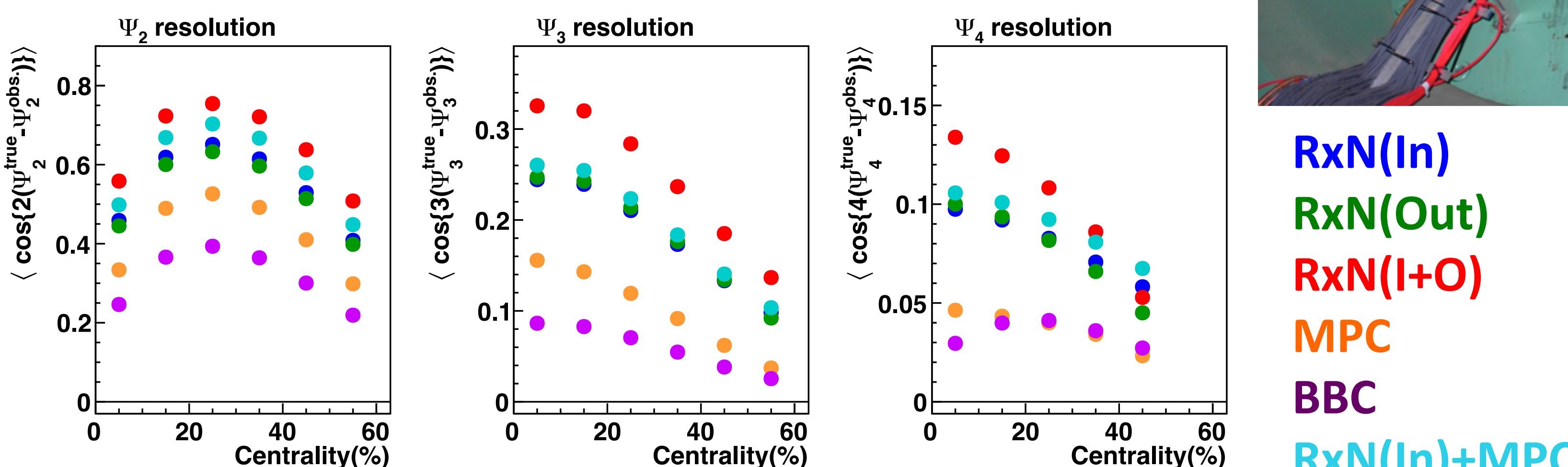

Photon reconstruction

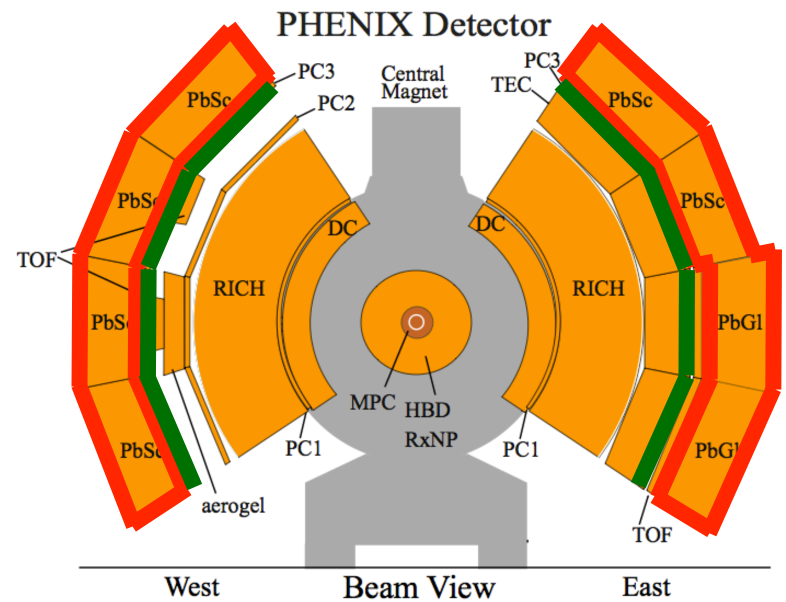

Pad chamber (PC) : space point of charged particle track

Electromagnetic calorimeter (EMCal)

Photons are reconstructed

- Energy threshold : E > 0.2GeV
- Shower shape : $\chi^2 < 3$
- Charged particle rejection at PC3 : $\sqrt{(dz)^2 + (r_T \sin(d\phi))^2} > 6.5$

π^0 (->$\gamma+\gamma$) reconstruction

- Asymmetry cut : $|E_1-E_2|/(E_1+E_2)<0.8$
- Photons are detected in same sector
- Invariant mass of $\gamma+\gamma$

$$Mass = \sqrt{2E_1E_2(1-\cos\theta)}$$

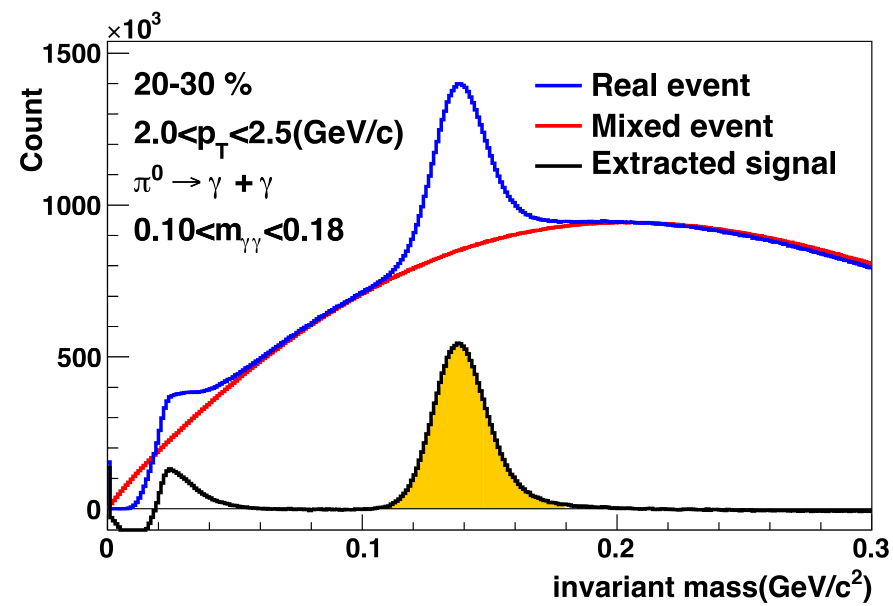

Inclusive photon v_n measurement

Inclusive photon dN/dΔφ distribution

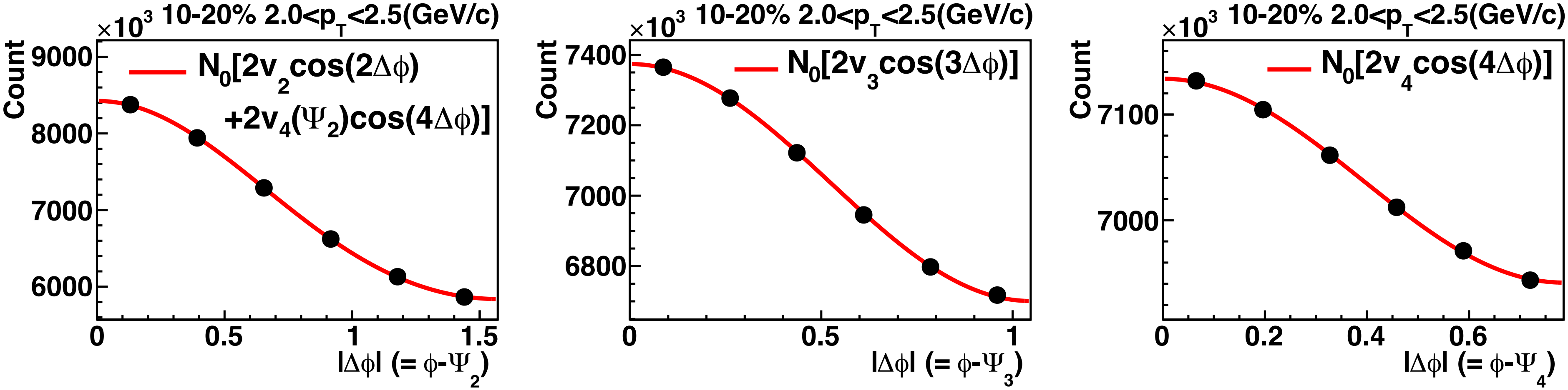

The method of extracting v_n

1. v_n=<cos{n(φ-Ψ_n)}>
2. $N_0(1+2v_n\cos\{n(\phi-\Psi_n)\})$ fitting to dN/dφ

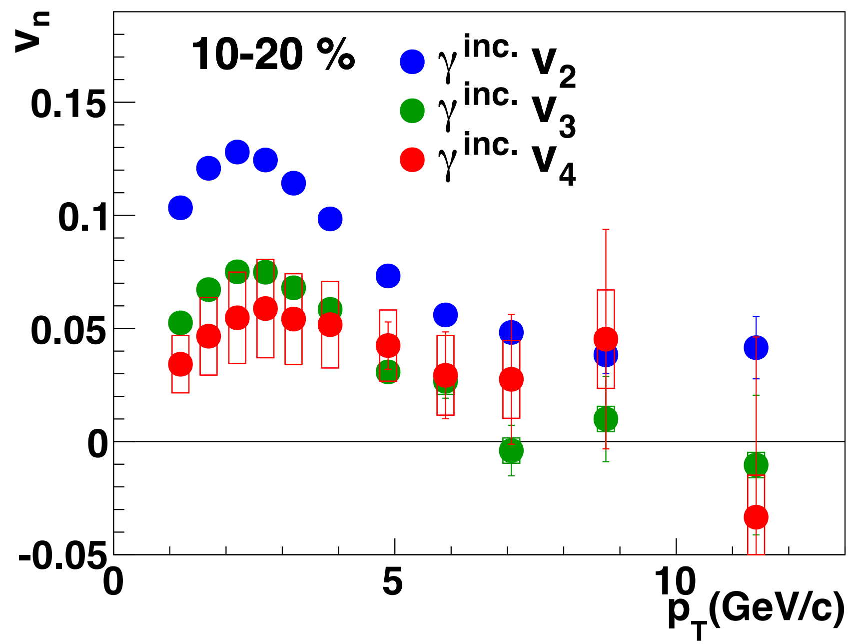

Systematic uncertainty

- Photon selection
- v_n measuring method
- Event plane determination

Neutral pion v_n measurement

Neutral pion $dN/d\Delta\phi$ distribution

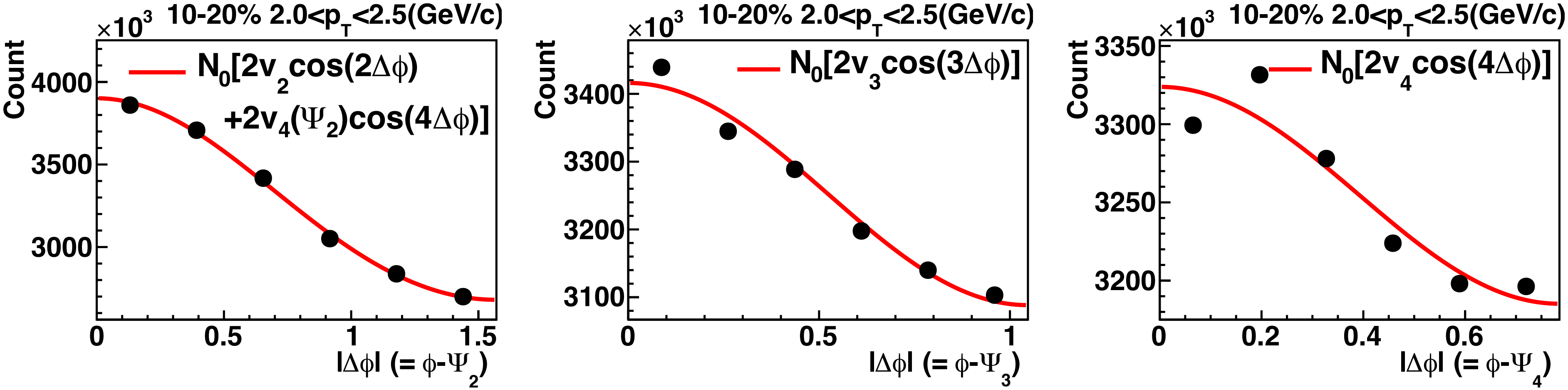

$dN/d\Delta\phi$ of π^0 is fitted by the equation.

$N_0(1+2v_n\cos\{n(\phi-\Psi_n)\})$

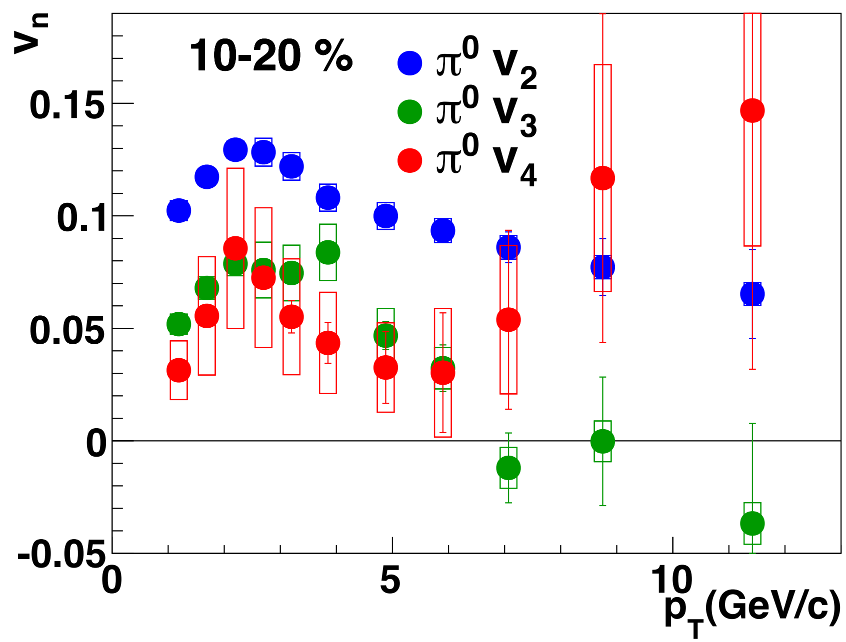

Systematic uncertainty

- Photon selection
- π^0 selection
- Event plane determination

Hadronic decay photon

We can not identify photons come from hadron decay experimentally.
They are simulated by Monte-Carlo simulation.

Particle Data Group

meson	invariant mass(MeV/c^2)	decay mode	branching ratio
π^0	134.98	2γ	(98.823 ± 0.034) %
		$e^+e^-\gamma$	(1.174 ± 0.035) %
η	547.86	2γ	(39.41 ± 0.20) %
		$\pi^+\pi^-\gamma$	(4.22 ± 0.08) %
		$e^+e^-\gamma$	$(6.9 \pm 0.4) \times 10^{-3}$
		$\pi^0 2\gamma$	$(2.7 \pm 0.5) \times 10^{-4}$
ω	782.65	$\pi^0\gamma$	(8.28 ± 0.28) %
ρ	775.26	$\pi^+\pi^-\gamma$	$(9.9 \pm 1.6) \times 10^{-3}$
		$\pi^0\gamma$	$(6.0 \pm 0.8) \times 10^{-4}$
η'	957.78	$\rho\gamma$	(29.1 ± 0.5) %
		$\omega\gamma$	(2.75 ± 0.23) %
		2γ	(2.20 ± 0.08) %
		$\mu^+\mu^-\gamma$	$(1.08 \pm 0.27) \times 10^{-4}$

Meson p_T spectra and v_n estimation

The meson p_T spectra and v_n are estimated from pion.

- **p_T spectra : m_T scaling**

$$p_{T,meson} = \sqrt{p_{T,pion}^2 + M_{meson}^2 - M_{pion}^2}$$

- **v_n : the number of constituent quark scaling (NCQ)**

$$p_{T,meson} = \sqrt{\left(\sqrt{p_{T,\pi}^2 + M_\pi^2} - M_\pi + M_{meson}\right)^2 - M_{meson}^2}$$

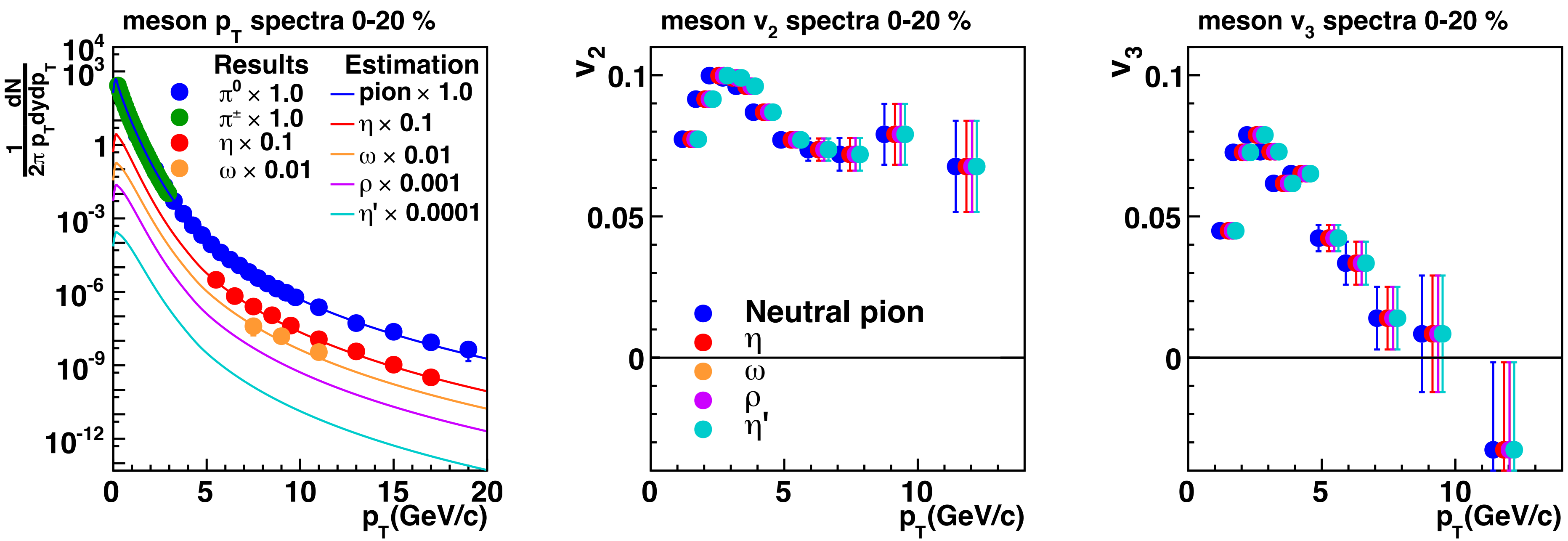

Hadronic decay photon v_n measurement

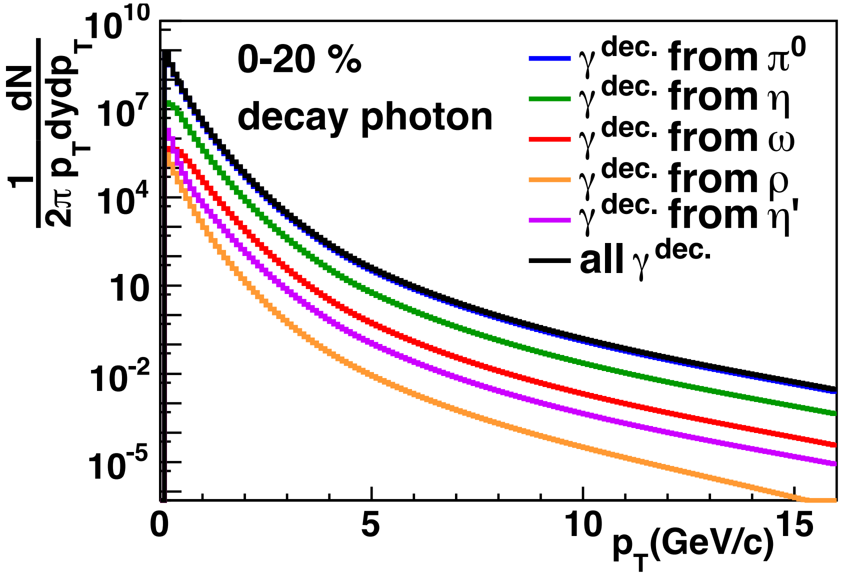

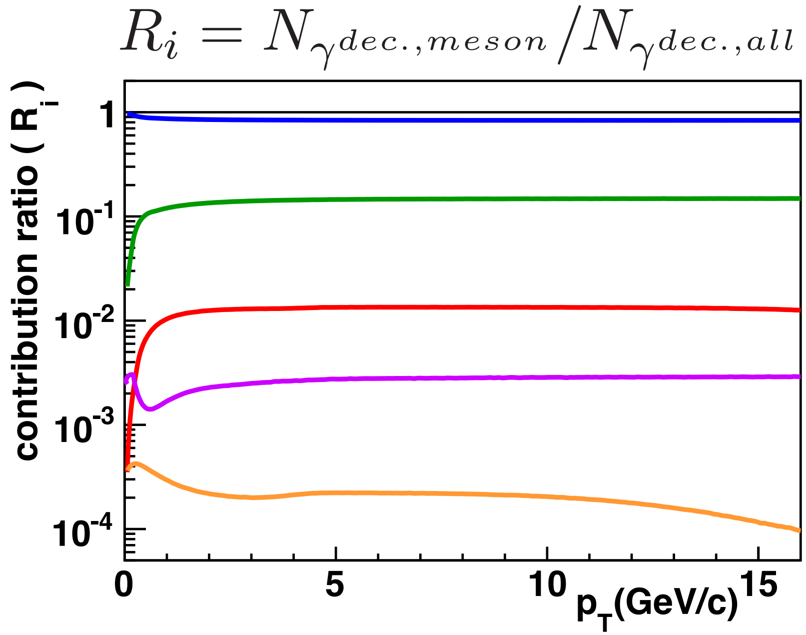

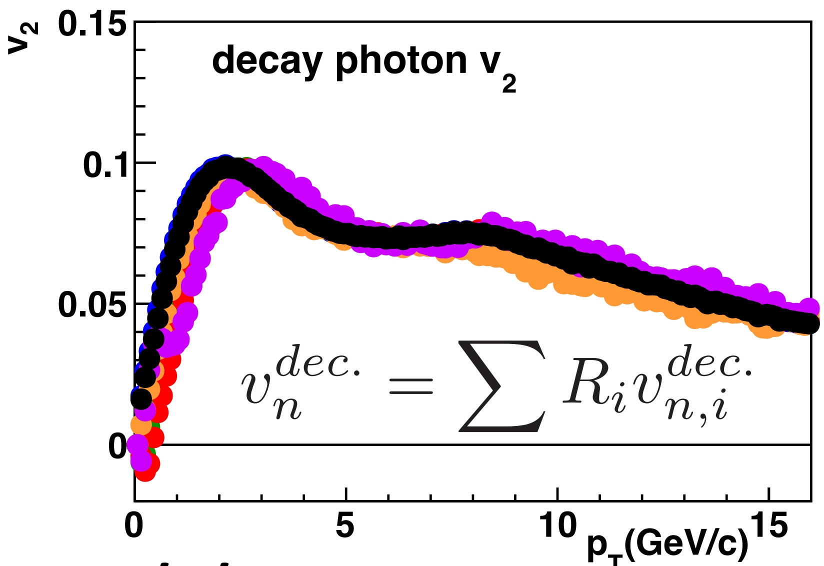

Decay photon v_n is simulated from meson input.

Systematic uncertainty

- Propagated from pion p_T spectra
- Propagated from pion v_n
- Propagated from meson input
- Event plane determination

Direct photon v_n measurement

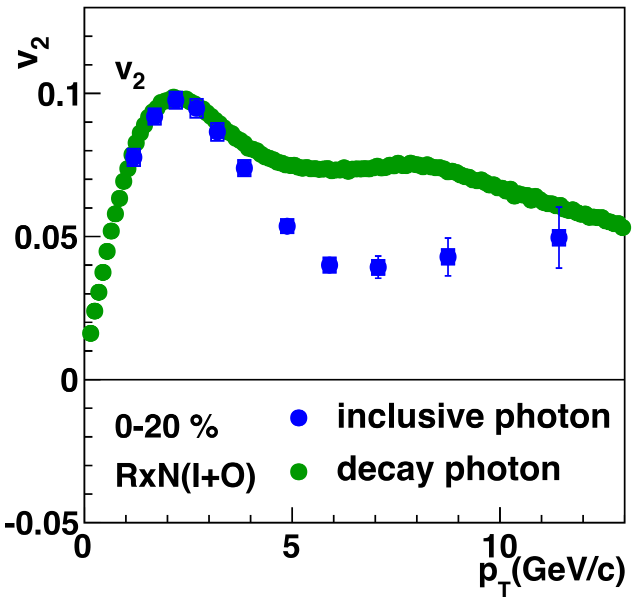

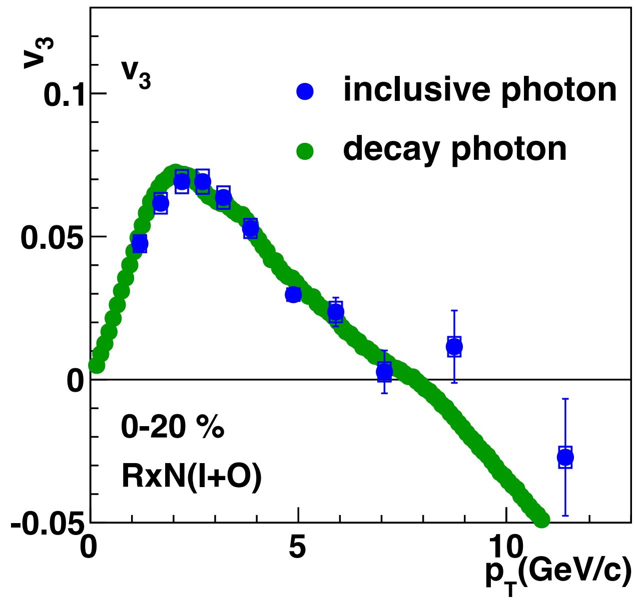

$$R_\gamma = N_{inc.}/N_{dec.}$$

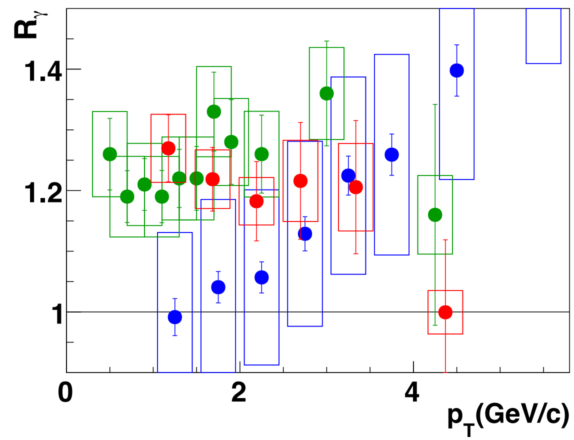

$$\nu_n^{dir.} = \frac{R_\gamma \nu_n^{inc.} - \nu_n^{dec.}}{R_\gamma - 1}$$

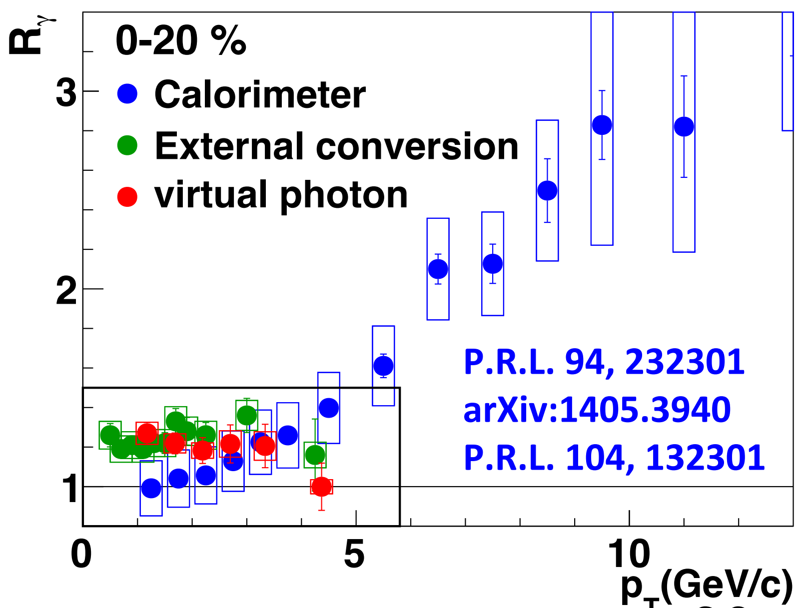

Systematic uncertainty

- Propagated from inclusive photon v_n
- Propagated from decay photon v_n
- Propagated from R_γ
- Event plane determination

Results & Discussion
Neutral pion v_n

The results of neutral pion v_n

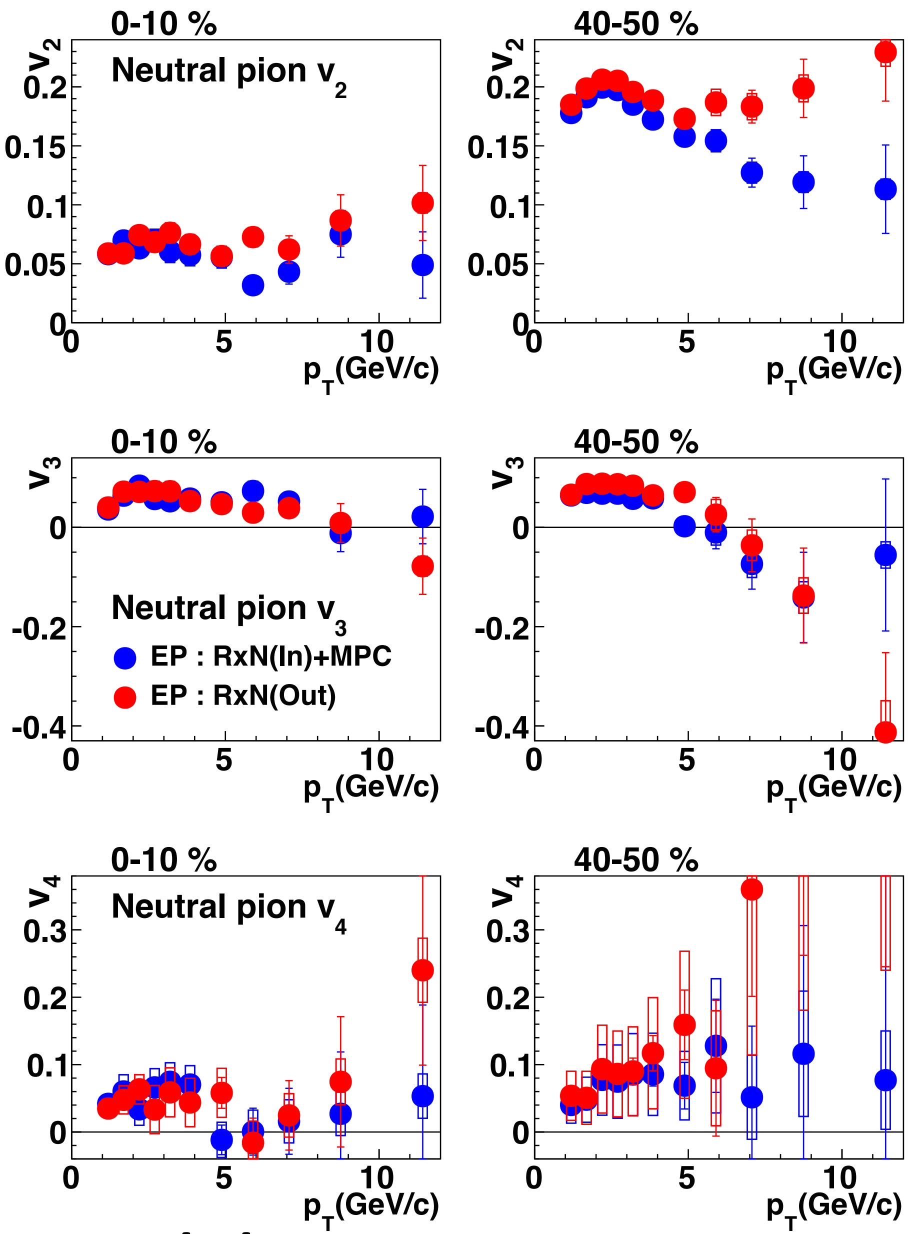

In low p_T

Consistent with charged pion v_n. Collective and radial expansion of QGP.

In high p_T

Hadrons are dominantly originated from jet fragmentation.

- **Jet kinematic and jet bias in event plane as well as jet property inside QGP**

1.0<|η|<1.5 (RxN(Out))
1.0<|η|<3.9 (RxN(In)+MPC)
|η|<0.35 (CNT)

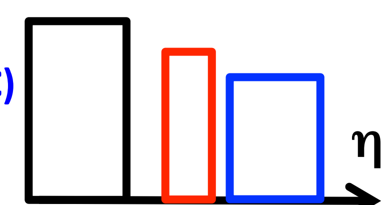

Integrated v_n of neutral pion in high p_T

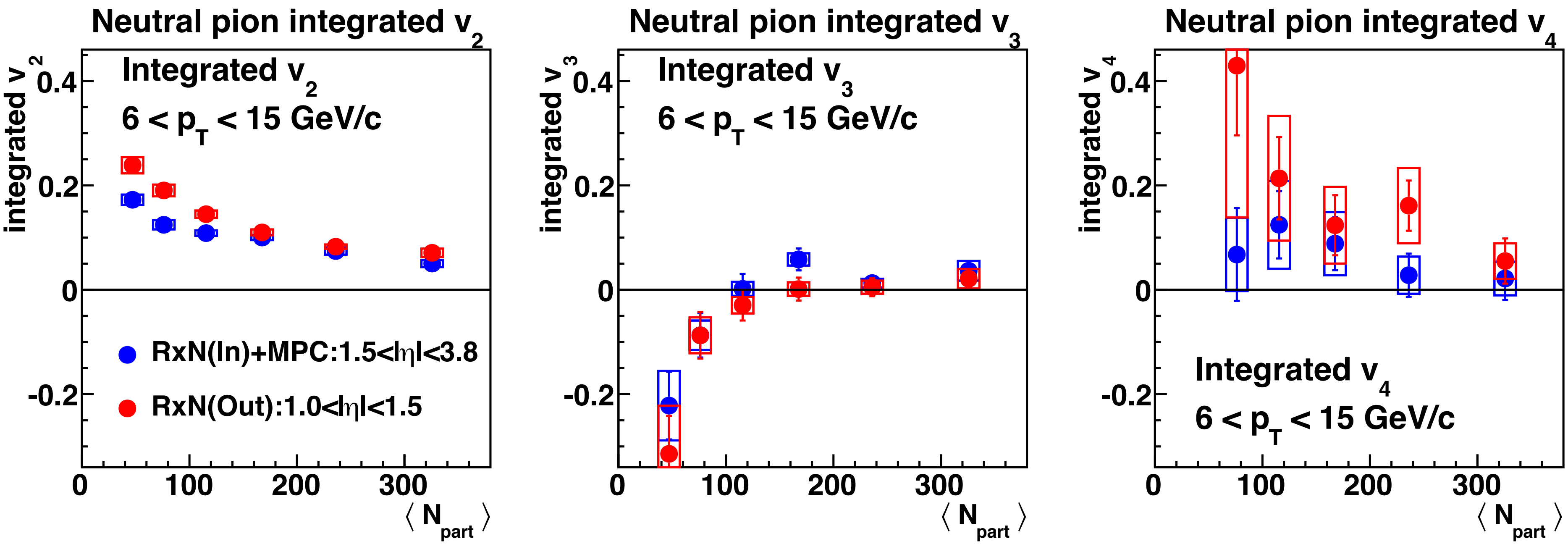

Central : v_n is positive.

Path length dependence of energy loss

Peripheral : v_2 & v_4 are positive while v_3 is negative.

Jet bias on determining event plane

It relates with initial geometry?

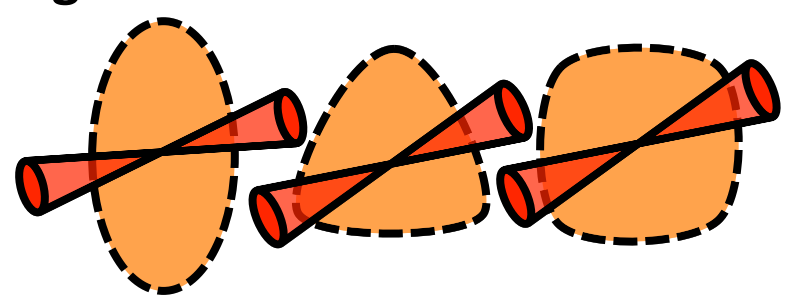

a Multiphase transport model (AMPT)

event generator (HIJING) + parton cascade (ZPC)
+ hadronization (including quark coalescence)
+ hadron cascade (P.R.C 72, 064901)

Au+Au 200 GeV are generated to test jet bias.
6.3 M events including Jet > 20 GeV are analyzed.
AMPT simulation describes v_n in low p_T region.

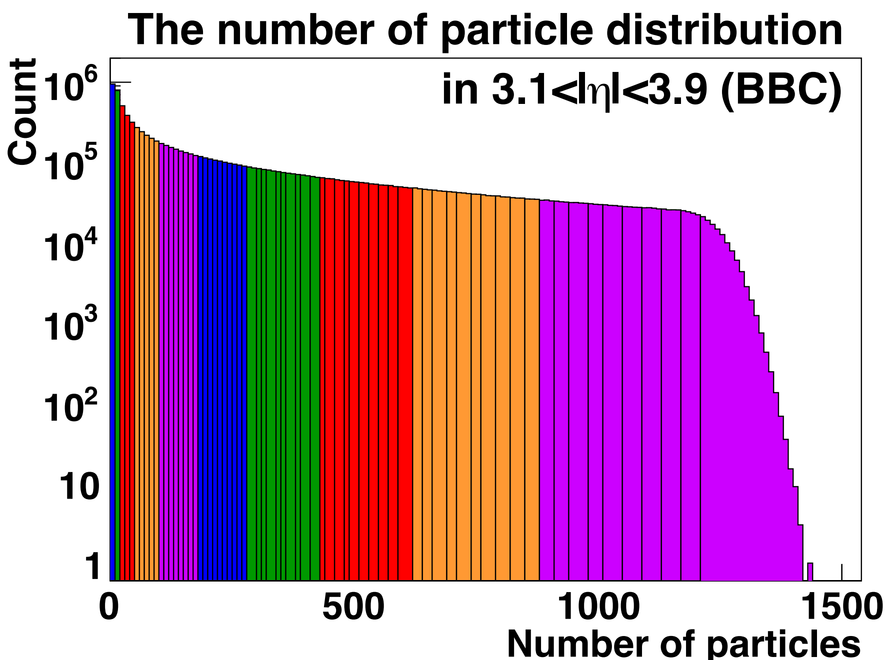

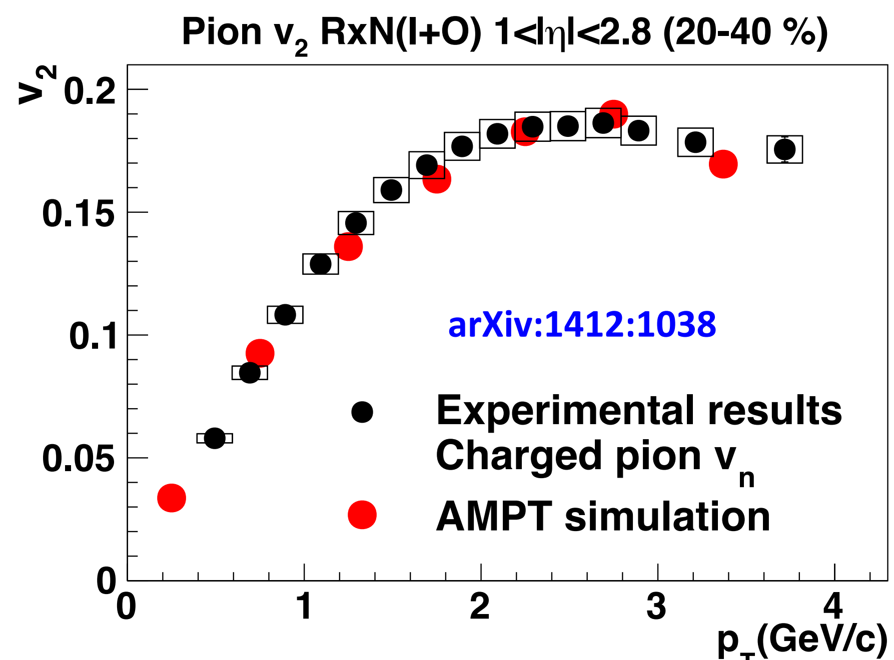

Pion v_n simulated by AMPT

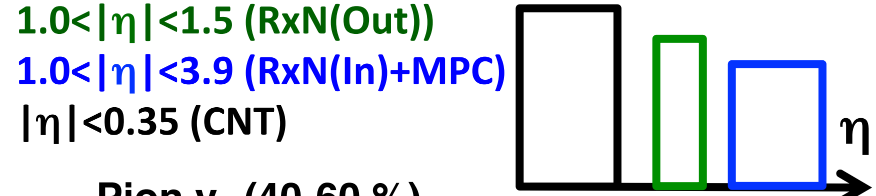

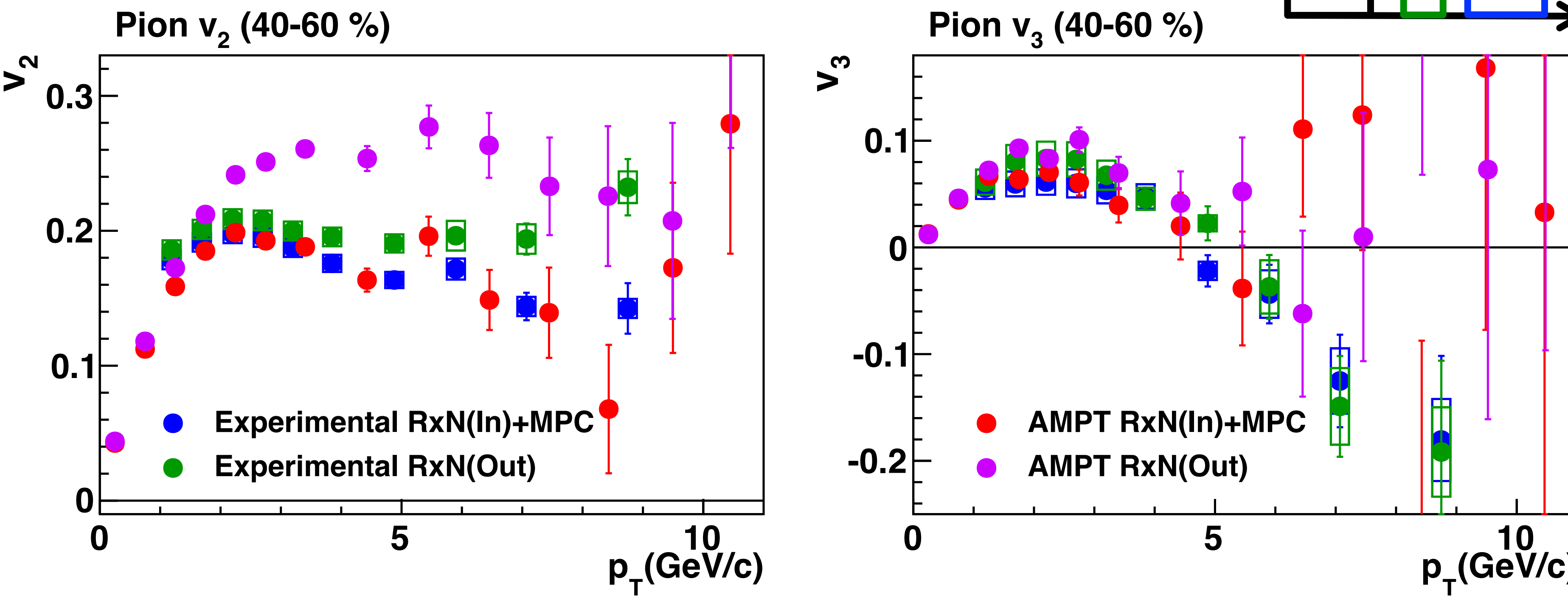

Simulation data are analyzed with the same condition analyzed in experimental measurement.

The trends of v_2 and v_3 are similar to the experimental measurement.

Event plane is defined with p_T selected particles

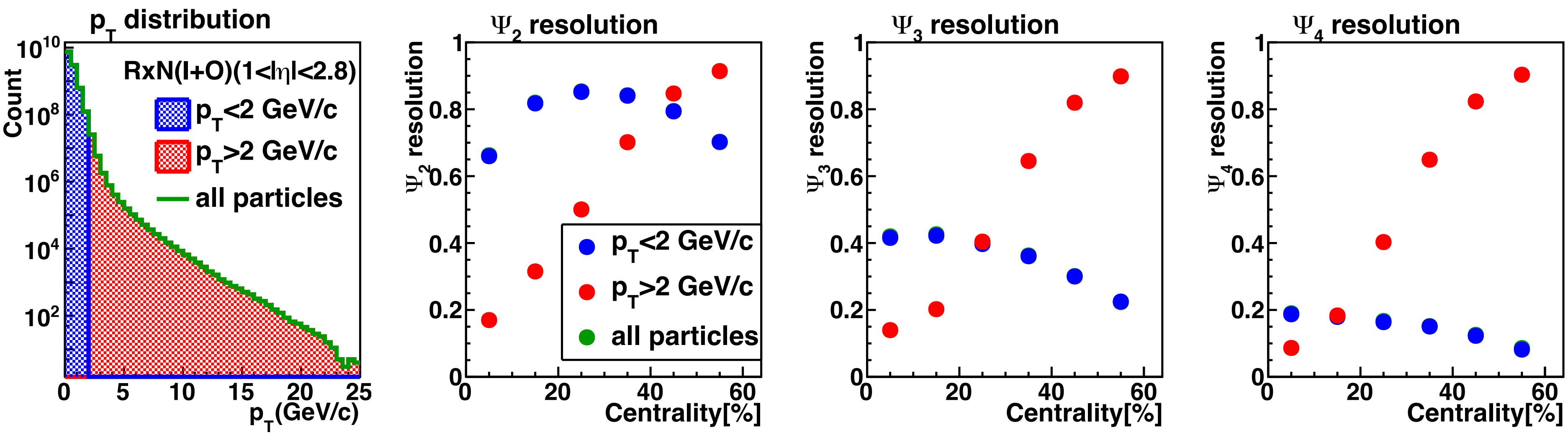

Event planes are defined at RxN (1 < |η| < 2.8) with the particles which are

- less than 2 GeV/c : dominantly come from hydrodinamic expanding medium
- larger than 2 GeV/c : dominantly originated from jet fragmentation

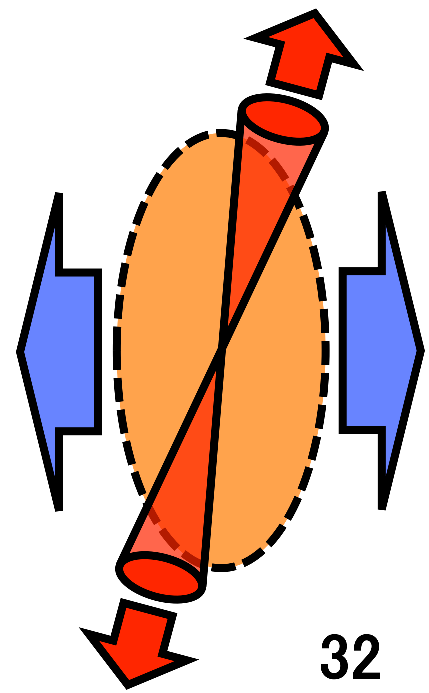

The Δη dependence of v_2 with biased event plane

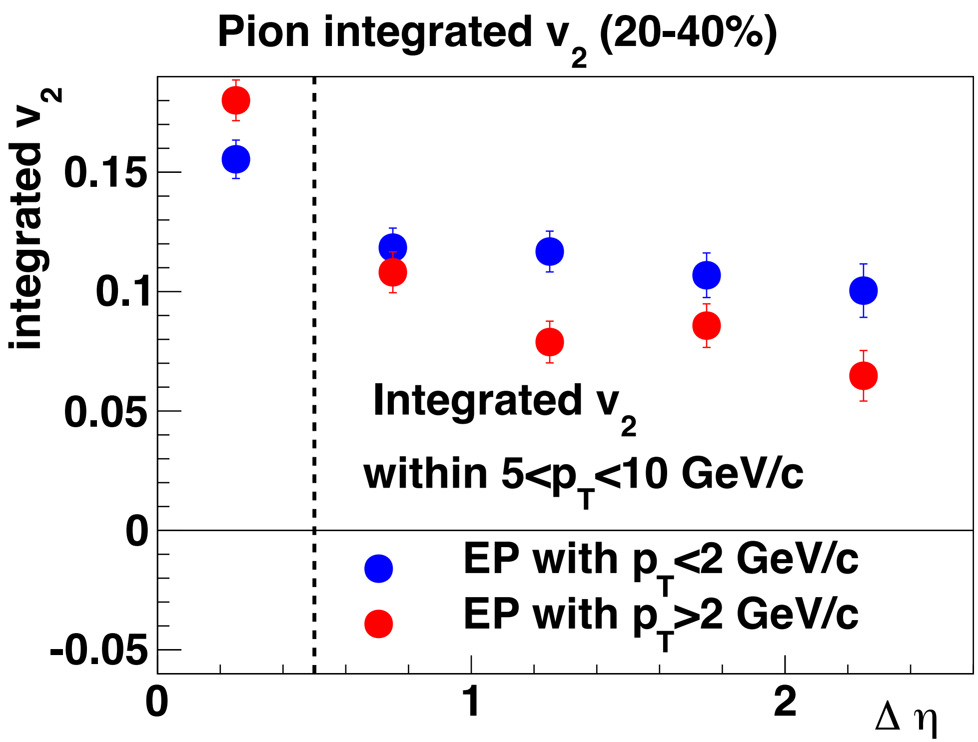

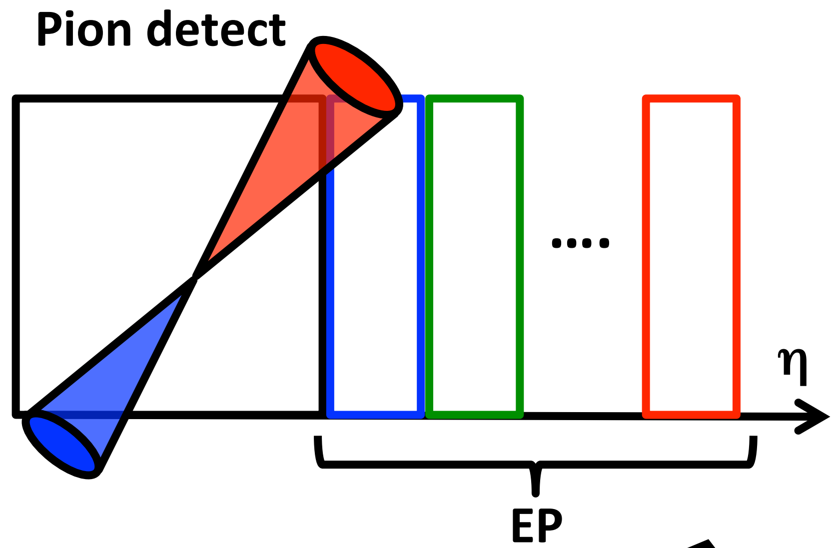

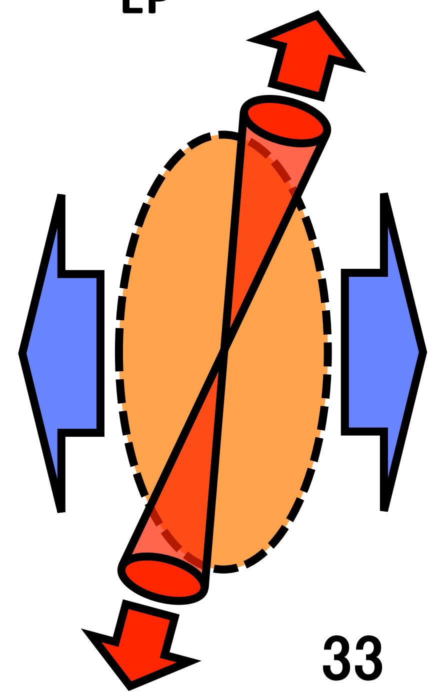

- ✓ $v_2 > 0$ (Δη > 0.5)
  Jet energy loss depending on path length
- ✓ v_2 & $v_2 > 0$ (Δη < 0.5 : near side jet)
- ✓ $v_2 > 0$ (Δη > 0.5 : away side jet)
  Jet bias on event planes

The $\Delta\eta$ dependence of v_n with biased event plane

Integrated v_n ($5 < p_T < 10$ GeV/c)

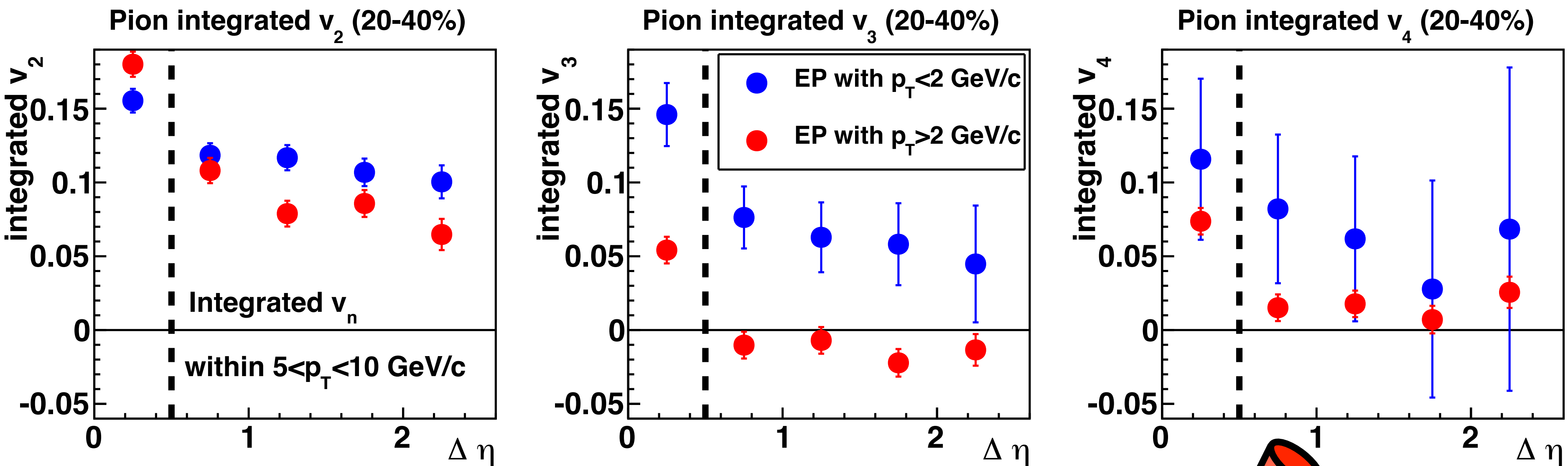

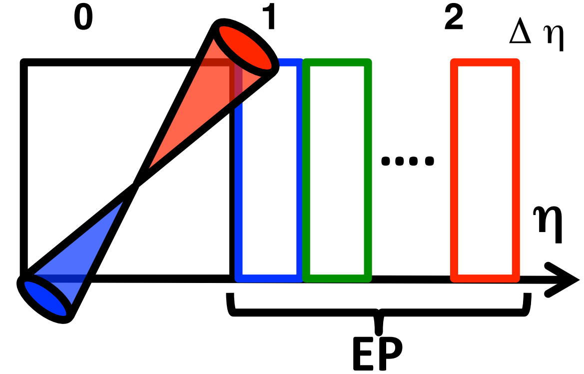

- ✓ $v_n > 0$ ($\Delta\eta > 0.5$)
  Jet energy loss depending on path length
- ✓ v_n & $v_n > 0$ ($\Delta\eta < 0.5$: near side jet)
- ✓ v_2 & $v_4 > 0$ and $v_3 < 0$ ($\Delta\eta > 0.5$: away side jet)
  Jet bias on event planes
  It relates initial geometry dependence.

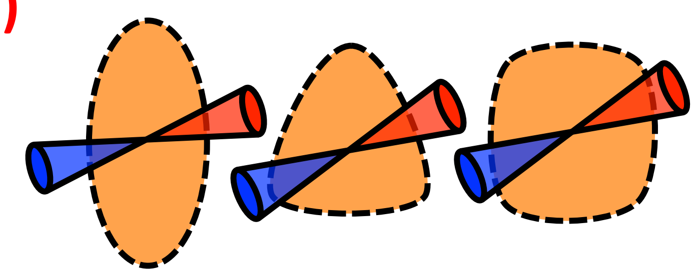

Summary (Neutral pion v_n)

- **In high p_T region**
  - Central collision : $v_n > 0$
    - ✓ jet energy loss depending on path length
  - Peripheral collision : v_2 & $v_4 > 0$ and $v_3 < 0$
    - ✓ jet bias on determining event plane

- **AMPT study for jet effect**
  - Event plane is defined with the particles mostly emitted from expanded medium.
    - ✓ jet energy loss depending on path length
  - Event plane is affected by the particles originating from jet.
    - ✓ Near side jet : v_n large.
    - ✓ Away side jet : v_2&v_4 large and v_3 small

Results & Discussion
Direct photon v_n

The comparison of neutral pion and direct photon v_n

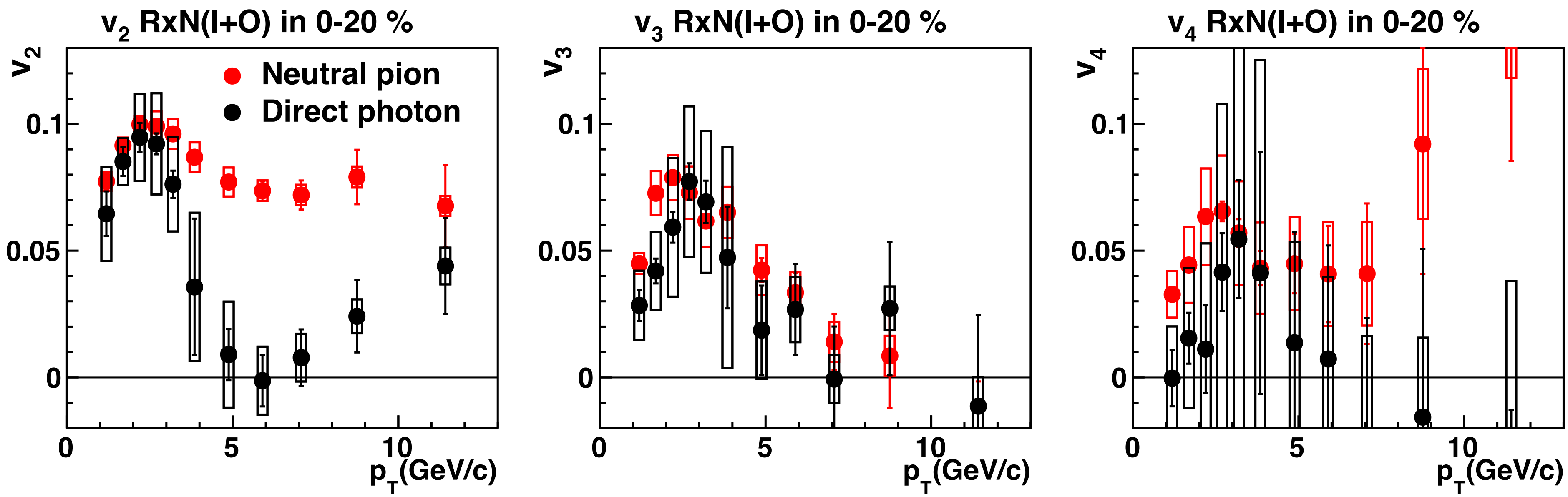

- In high p_T region
  Direct photon v_n is close to zero.

- In low p_T region
  Direct photon has non-zero and positive v_2 and v_3.

Centrality dependence of $\gamma^{dir.}$ and π^0 in high p_T

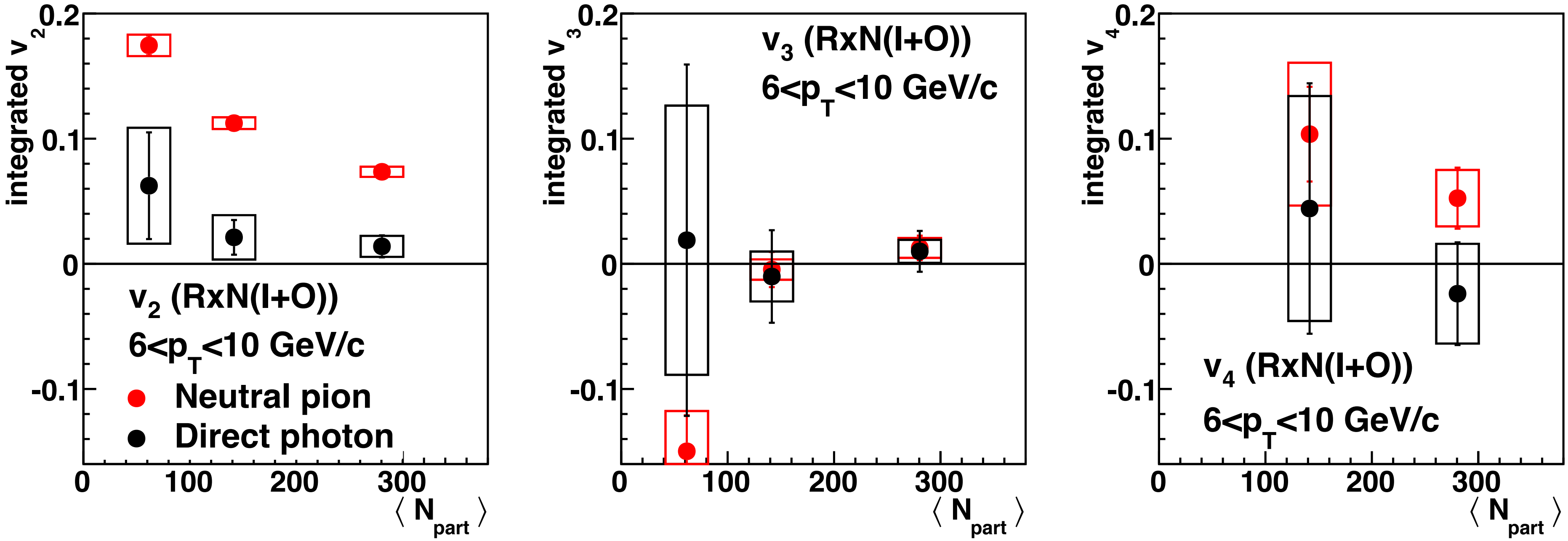

- Photon v_n is close to zero.
- There is the difference between photon and neutral pion.

It is understood that prompt photons which $v_n \approx 0$ are relatively dominant.

Centrality dependence of $\gamma^{dir.}$ and π^0 v_n in low p_T

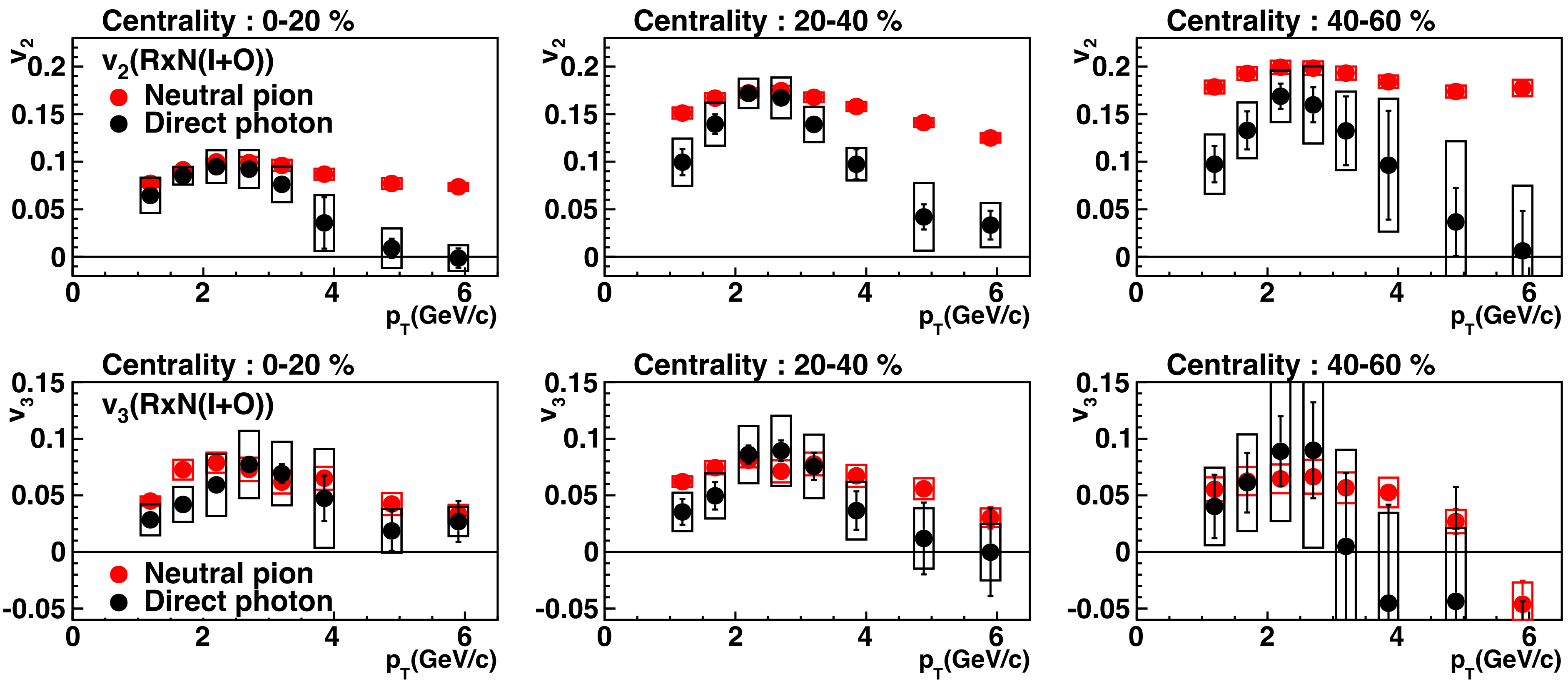

Strong dependence for v_2 : weak dependence for v_3

The strength of photon v_n in low p_T region relates with initial geometry.
It could be suggested that photons from late stage are dominant.

Blast wave model prediction for photon observables

Based on hydrodynamic model.
Observables in low p_T region are well described by the parameters when kinetic freeze-out.

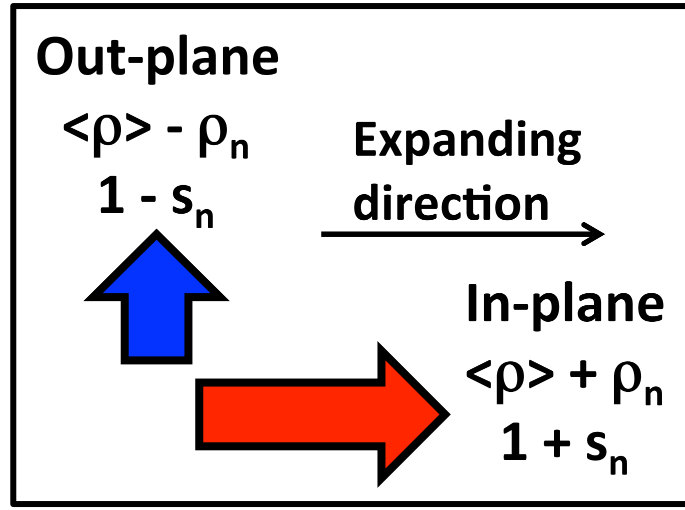

6 parameters

- Kinetic freeze-out temperature : T_f
- Average transverse rapidity : $\langle\rho\rangle$
- Transverse anisotropy : ρ_2, ρ_3
- Spatial density anisotropy : s_2, s_3

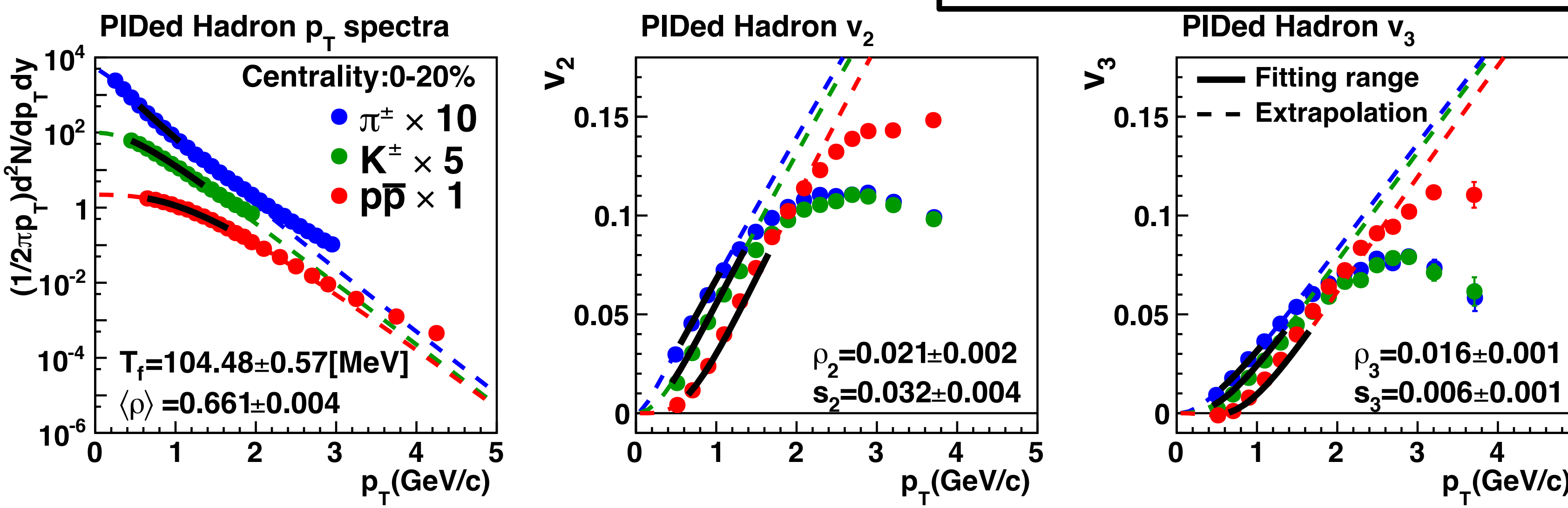

Photon observables predicted by blast wave model

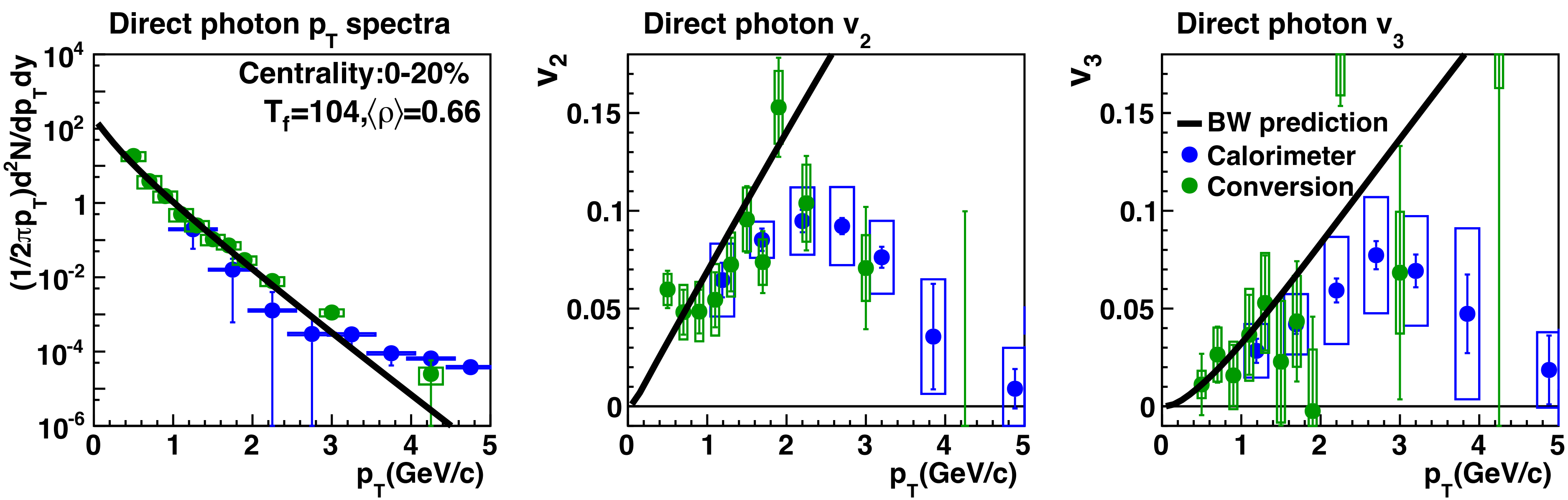

The photon p_T spectra and v_n are predicted as a massless particle.
They are well described.

The temperature (104 MeV) is much less than 240 MeV obtained by the exponential equation.
It is due to blue shift correction.

Photon observables predicted by blast wave model

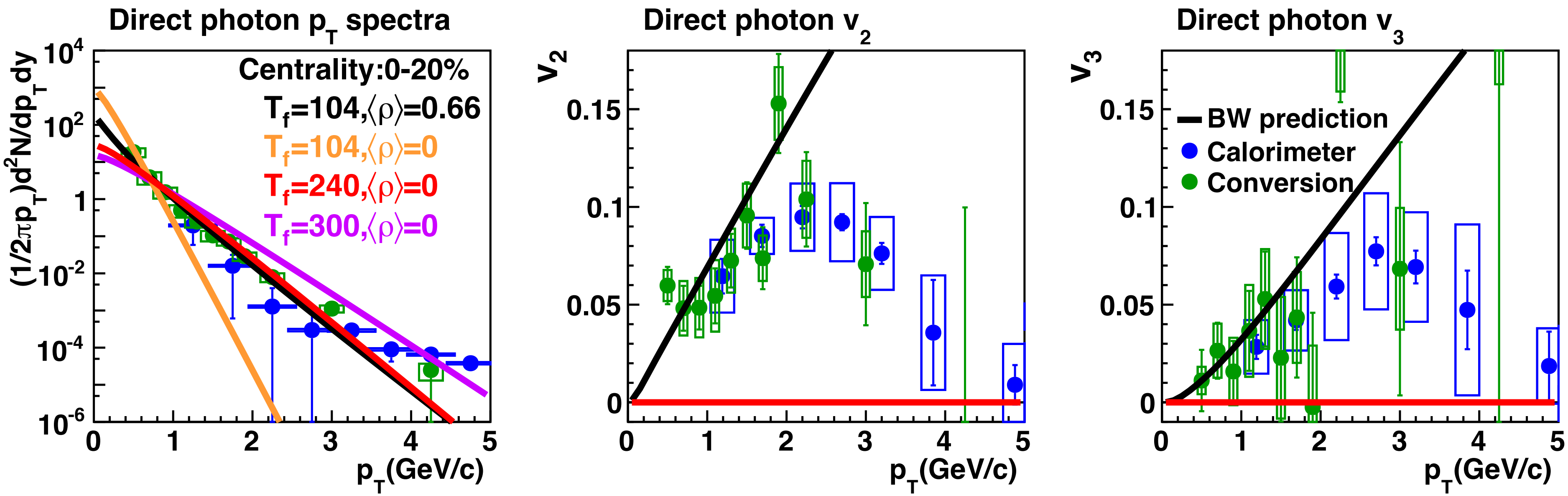

The p_T spectra is well described by

- Low temperature (T_f=104) with radial flow <ρ>=0.66
- High temperature (T_f=240) with radial flow <ρ>=0

v_n=0 with radial flow <ρ>=0

Blast wave could suggest that photon puzzle is understood by the radial flow effect.

Summary (Direct photon v_n)

- **In high p_T region**
  - Photon v_n is close to zero while hadron shows non-zero v_n.
    - ✓ Prompt photons which are $v_n \approx 0$ are relatively dominant.

- **In low p_T region**
  - It is found non-zero and positive v_3 in low p_T.
  - The centrality dependence of photon v_n similar to that of pion v_n.
    - ✓ Photon v_n also depends on the initial geometry.
    - ✓ Photons from late stage could be dominant.

- **Blast wave model**
  - Blast wave model describes photon observables well.
    - ✓ Photon puzzled could be understood by radial flow effect.

Conclusion

Neutral pion and direct photon v_n are measured in $\sqrt{s_{NN}}$ = 200GeV Au+Au collisions at RHIC-PHENIX experiment.

- **Neutral pion v_n**
  - ✓ **The trends in high p_T region are understood with the superimposition of jet effects.**

- **Direct photon v_n**
  - ✓ **Photons in high p_T are dominantly originated from hard scattering.**

  - ✓ **Photon from late stage of collisions could be dominant.**
  - ✓ **The possible explanation of "photon puzzle" could be strong radial flow effect.**

Identification photon sources from p_T spectra

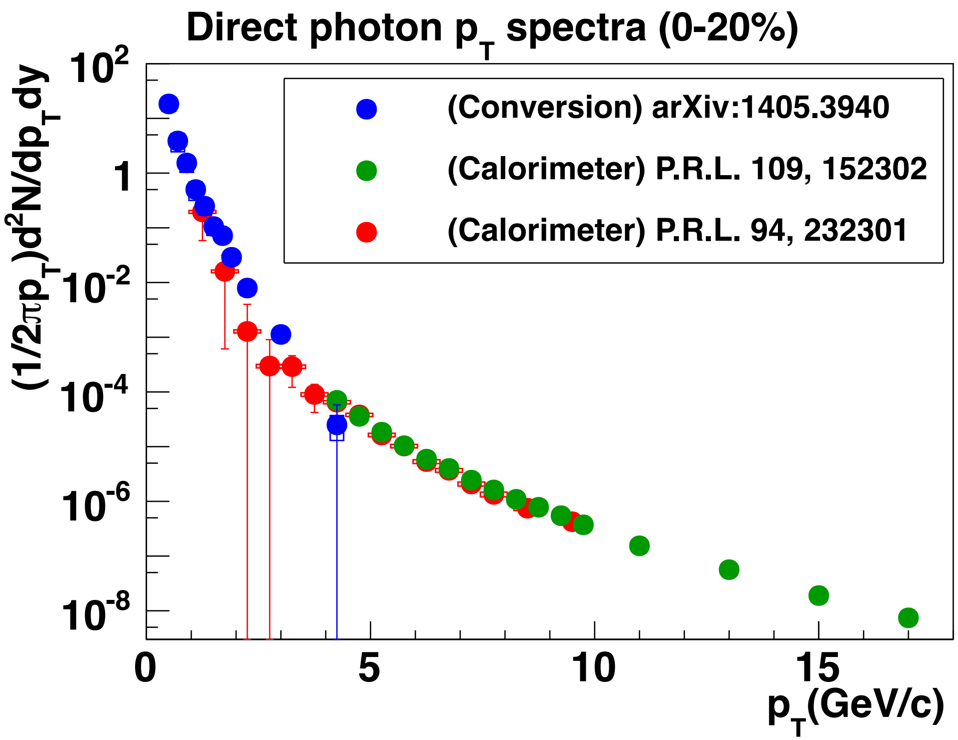

P.R.C 84, 054906(2011)

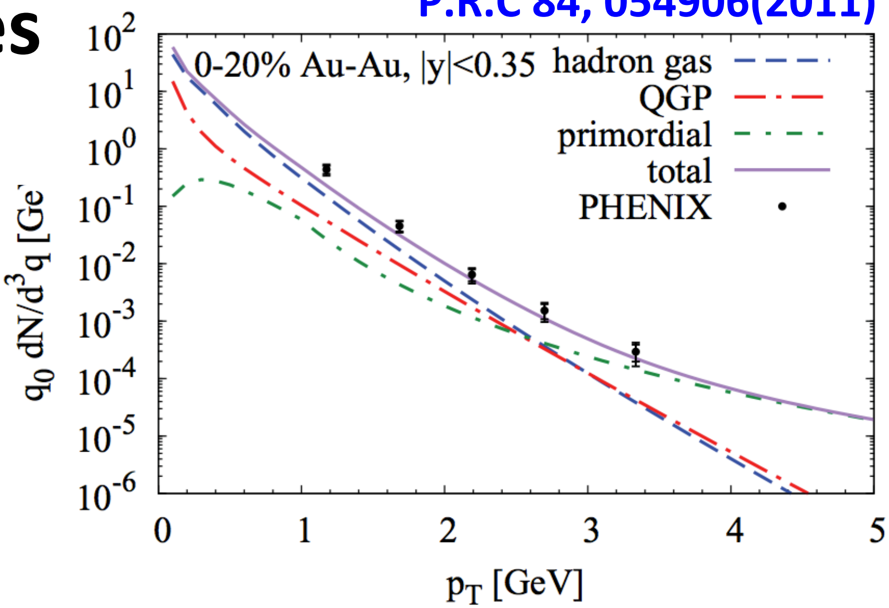

P.R.C 89, 034908(2014)

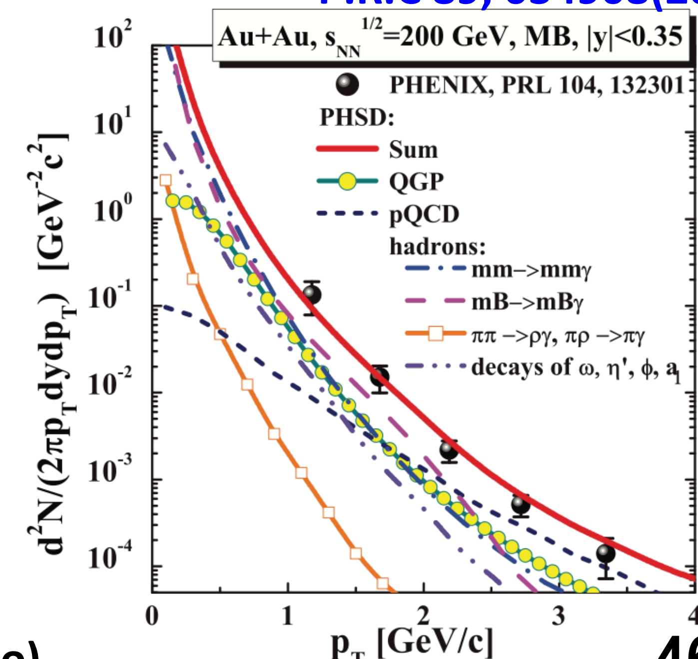

The photon sources are identified via the p_T spectra.

Medium effect (R_{AA})

$$R_{AA} = \frac{(1/N_{AA}^{evt})d^2N_{AA}/dp_Tdy}{< N_{coll} > /\sigma_{pp}^{inel} \times d^2\sigma_{pp}/dp_Tdy}$$

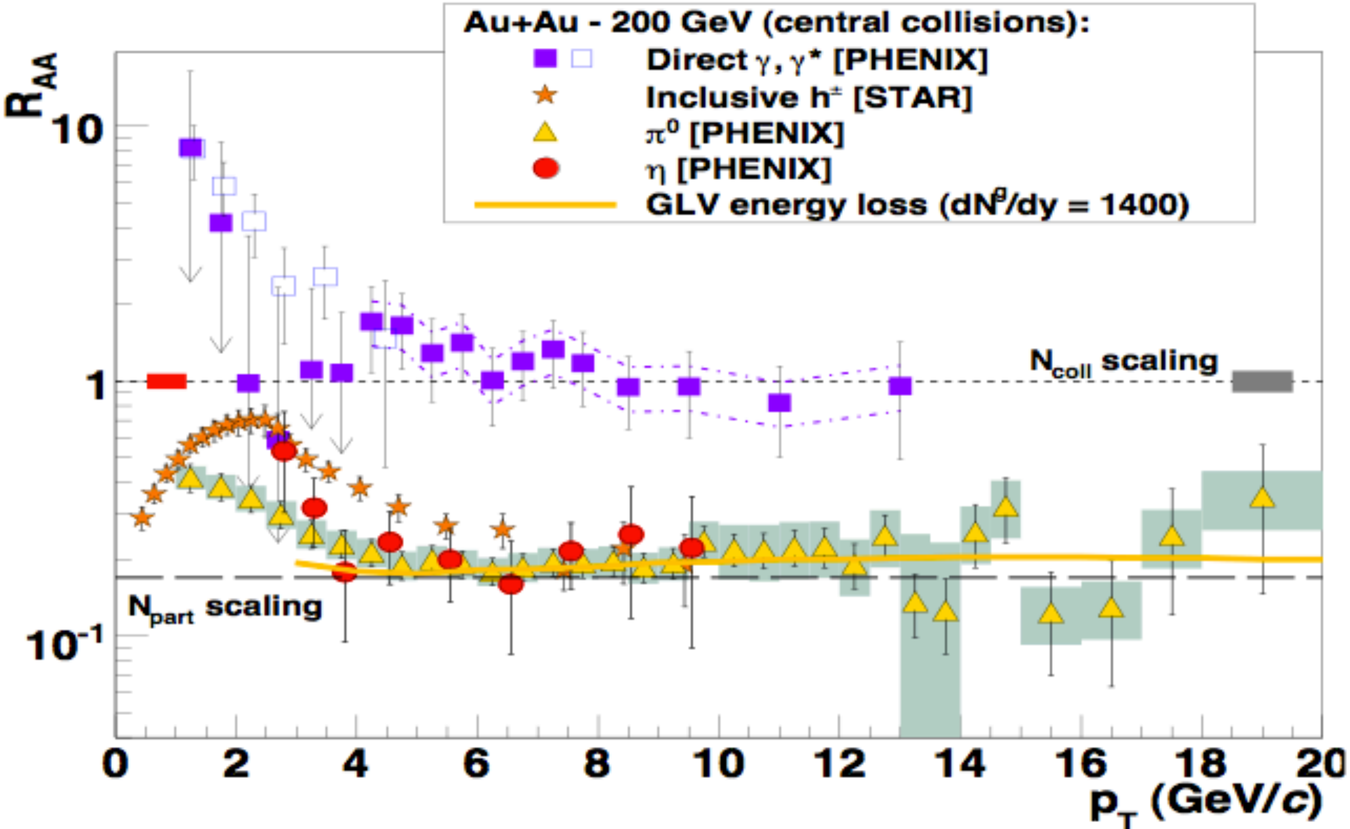

R_{AA}=1
not modified
R_{AA}≠1
medium effect

Hadron
less than unity
-> medium effect

photon

R_{AA}=1 : not modified

-> Emitted from initial hard scattering

R_{AA}>>1 : There are other photon sources which are not in p+p collisions.

Charged hadron v_n

P.R.L. 107, 252301 (2011)

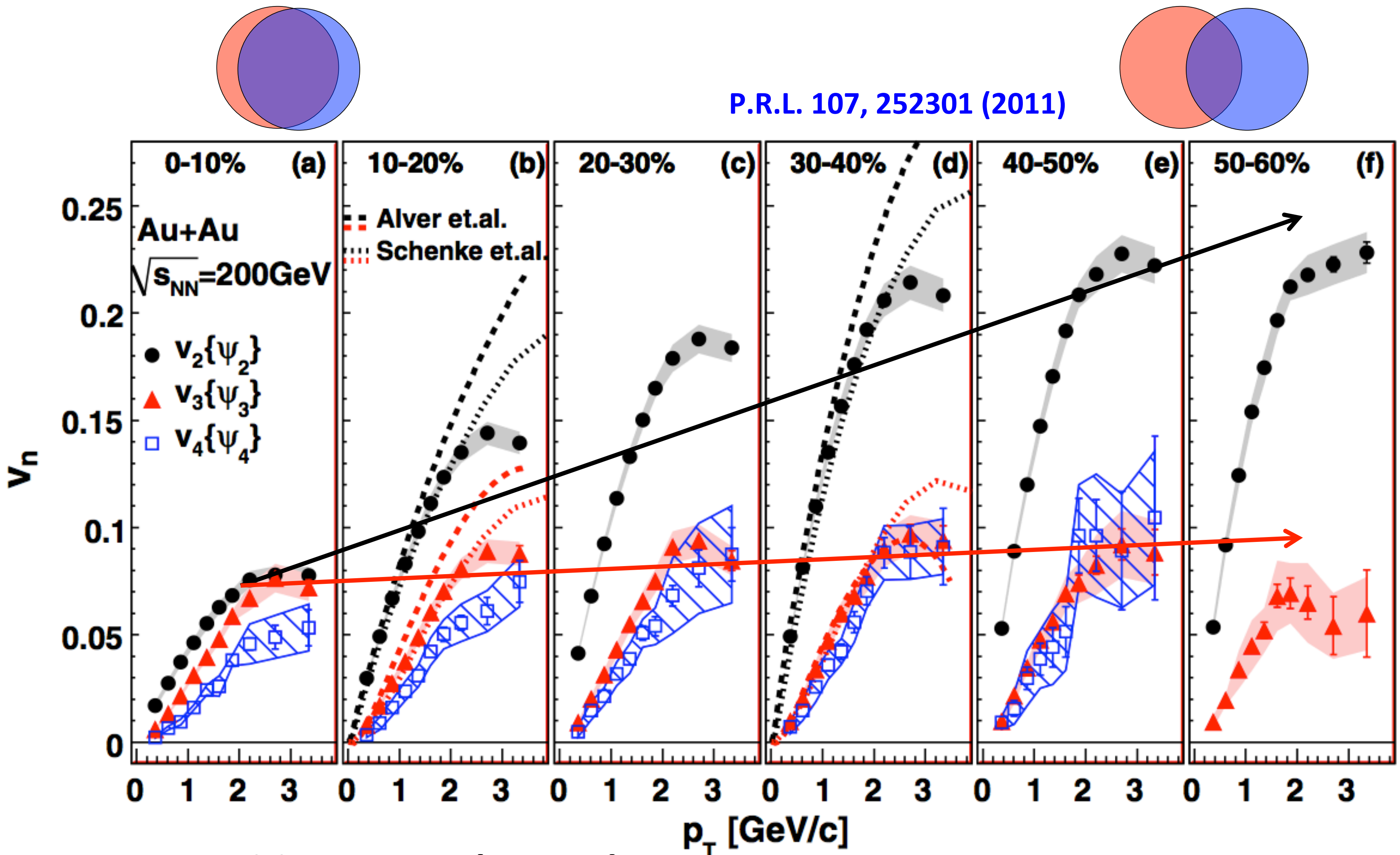

Non-zero positive v_n are observed.

The trend of centrality dependence of v_n is similar to that of eccentricity.

Event Plane correlation between different harmonics

P.R.L. 107, 252301 (2011)

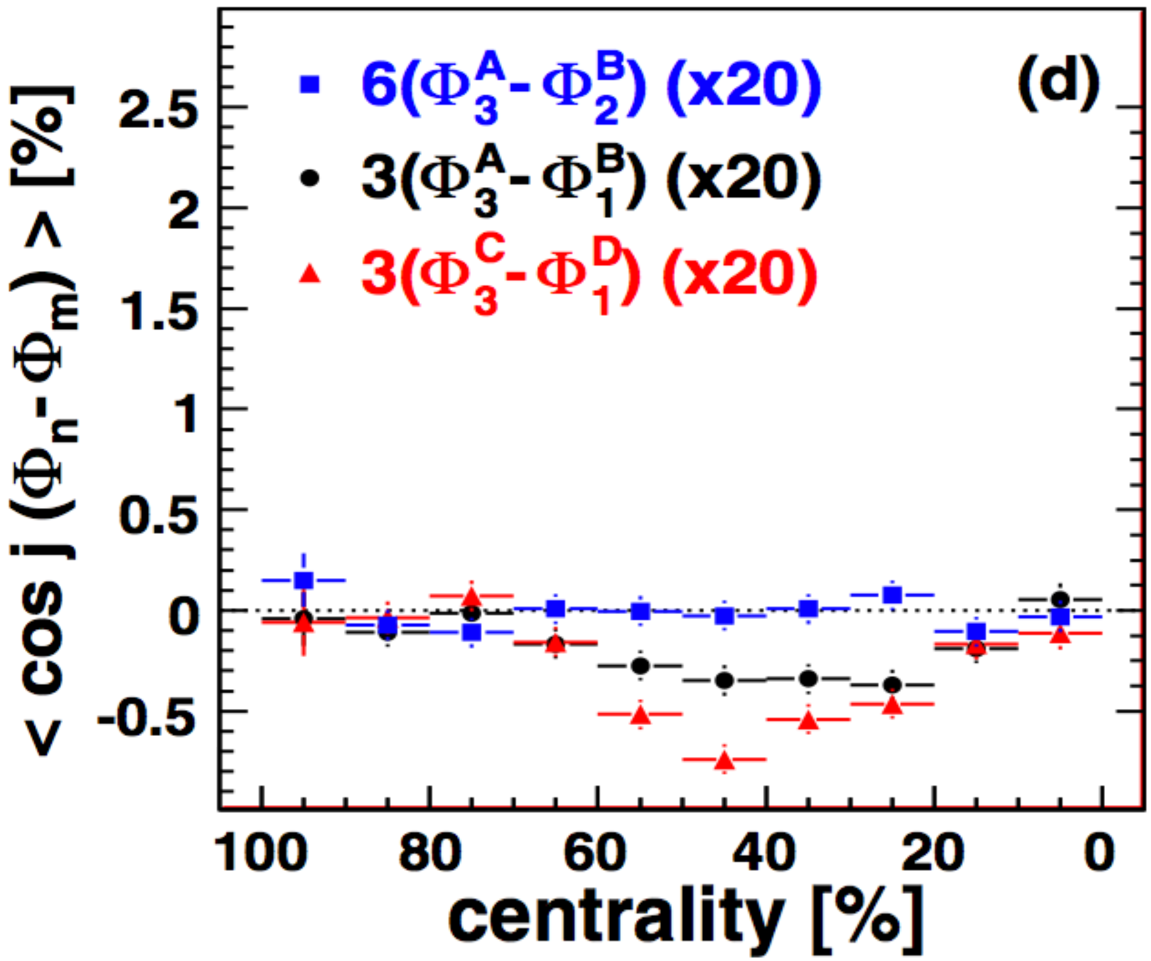

Ψ_2 and Ψ_3 are uncorrelated.

Identified charged particle v_n

arXiv:1412:1038

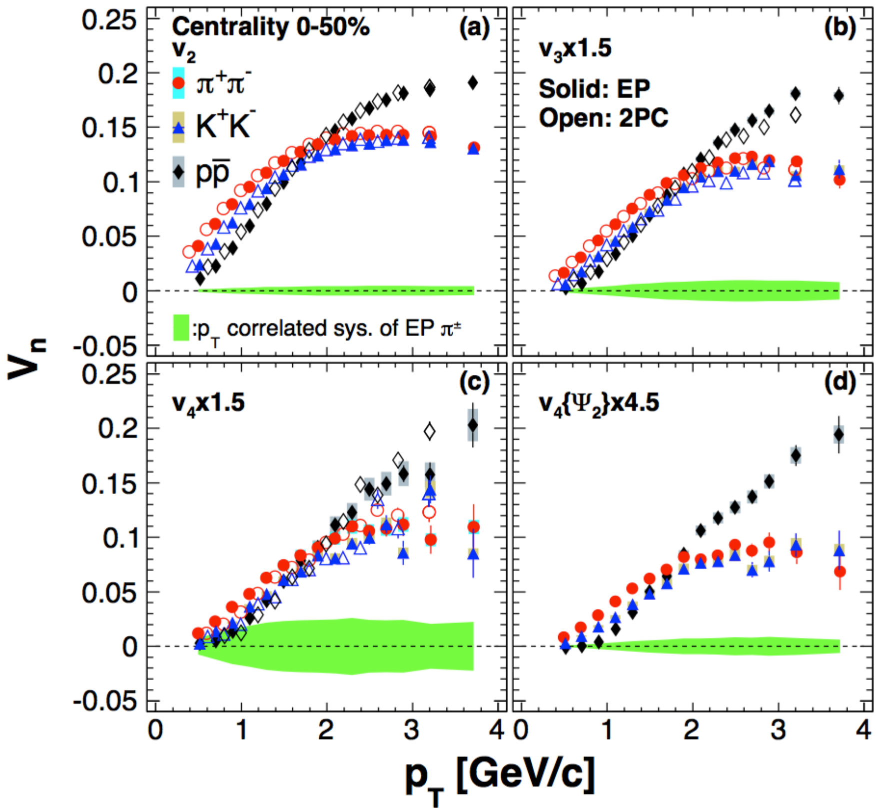

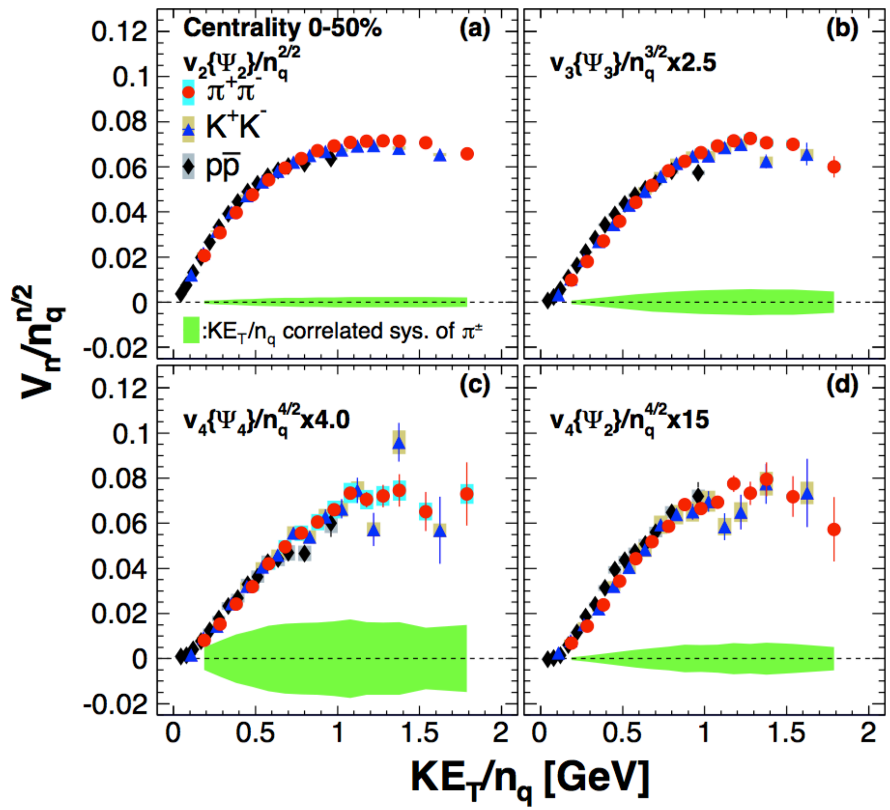

It is observed that

- all harmonics have mass ordering
- there are meson and baryon splitting

All particles are scaled by modified NCQ scaling.

(a) : $v_2(KE_T)/n_q$
(b) : $v_n^{1/n}$ scaling
(a)+(b) : $v_n(KE_T)/n_q^{n/2}$

Photon emitting angle dependence

Photon	Property	p_T range	v_2
Prompt	Initial of collision	high p_T	$v_2 = 0$
Jet fragmentation	Jet quenching Fragmentation	intermediate	$v_2 > 0$
Jet energy loss	Path length	intermediate	$v_2 < 0$
Thermal radiation (QGP)	Medium expanding	low	$v_2 \geq 0$
Thermal radiation (HG)	Medium expanding	low	$v_2 > 0$

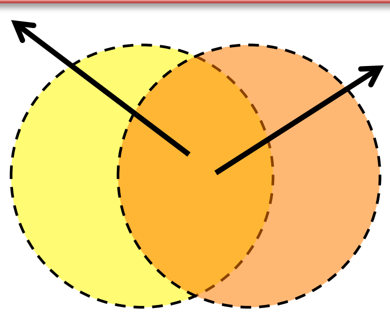

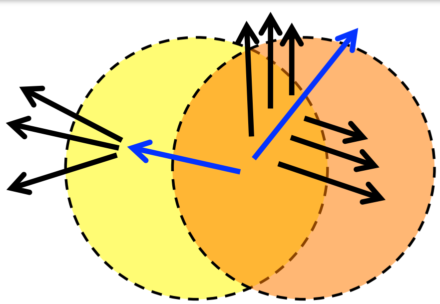

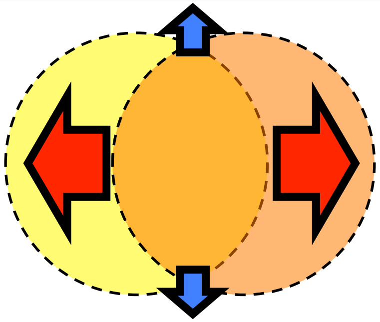

Jet quenching

High p_T hadrons are originated from jet fragmentation.
Away side jet deposits its energy inside QGP.

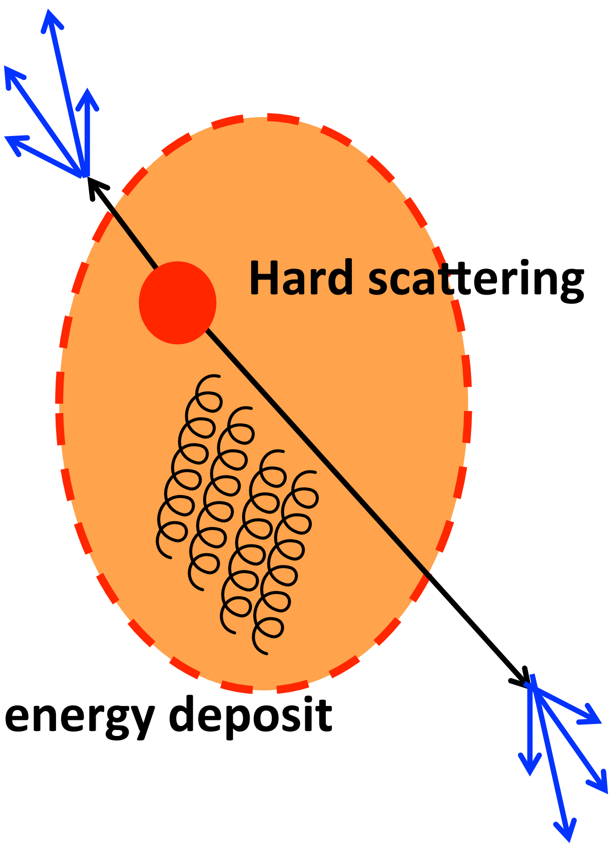

P.R.L. 91, 072304 (2003)

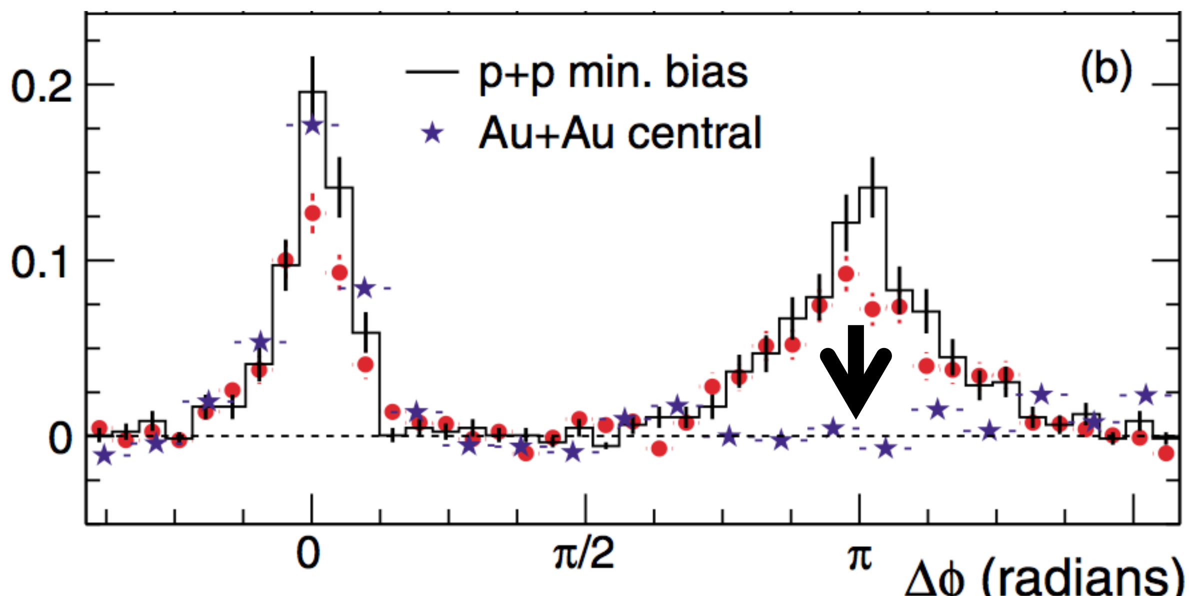

v_n measurement in high p_T at LHC

Single hadron v_2, v_3 and v_4 are measured up to 40-60 GeV/c at CMS.
Jet v_2 is measured up to p_T=200 GeV/c at ATLAS.

They are used to study jet energy loss depending on path length inside of QGP.

arXiv:1306.6469

CMS PAS HIN-12-010

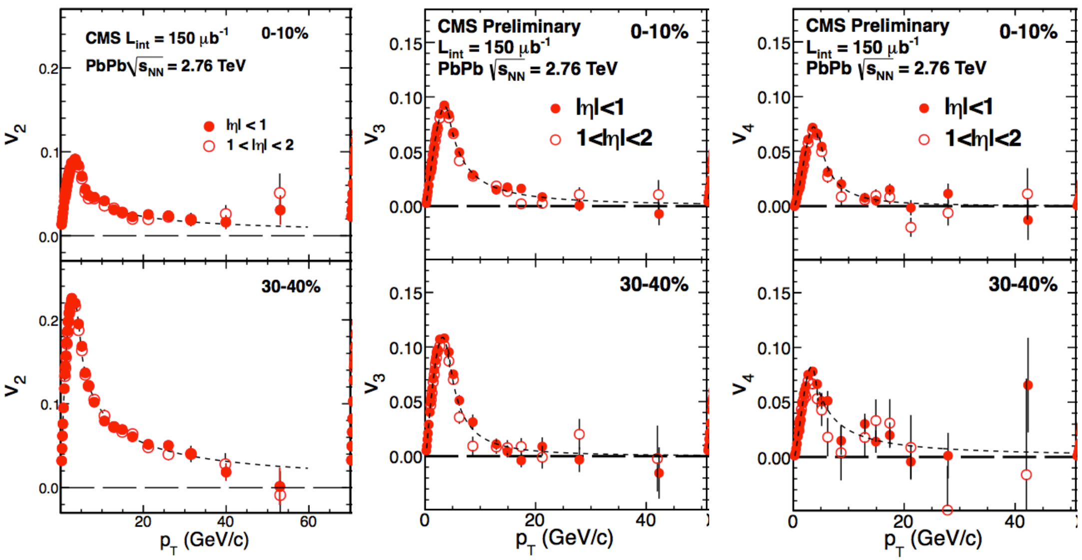

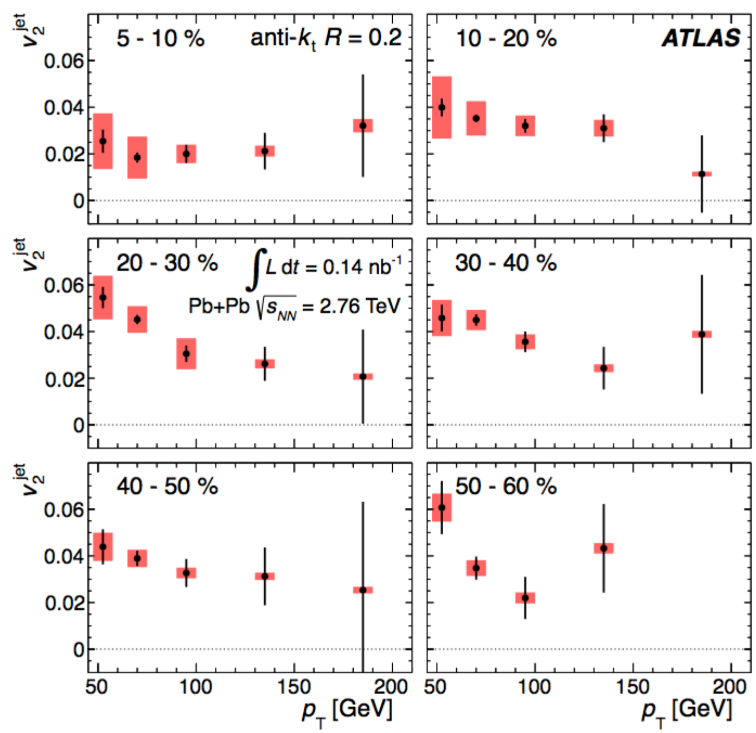

Meson p_T spectra estimation

$$p_{T,meson} = \sqrt{p_{T,pion}^2 + M_{meson}^2 - M_{pion}^2}$$

$$\begin{aligned}
\frac{d\sigma}{p_T dp_T} &= T(p_T)F_0 + (1 - T(p_T))F_1, \\
T(p_T) &= \frac{1}{1 + \exp\{(p_T - t)/w\}}, \\
F_0 &= \frac{c}{\{\exp(-ap_T - bp_T^2) + p_T/p_0\}^n}, \\
F_1 &= \frac{A}{p_T^m},
\end{aligned}$$

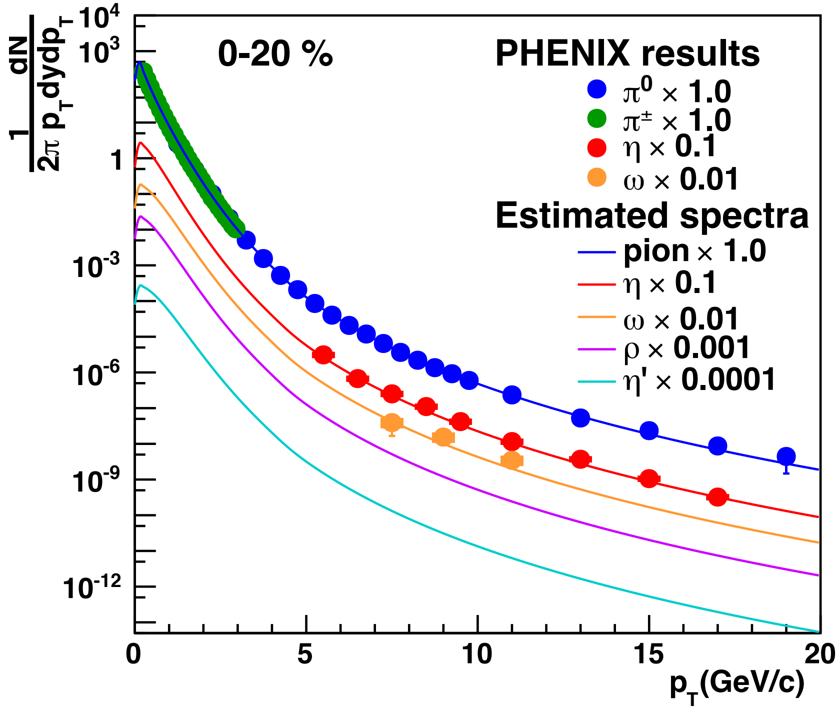

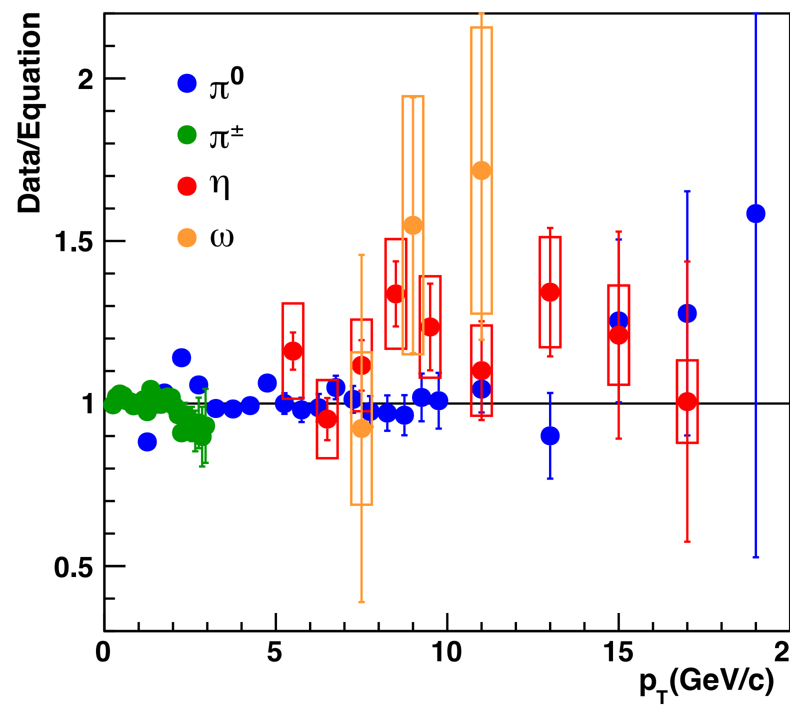

Since it is difficult to measure mesons except for pion, the other mesons p_T spectra are estimated by m_T scaling from pion experimental data.

P.R.C 69,034909
P.R.L. 101,232301
P.R.C 82,011902
P.R.C 84,044902

Meson v_n estimation

It has been known that hadron v_n as a function of KE_T are scaled by the number of constituent quark.
Meson v_n is estimated from pion v_n.

$$p_{T,meson} = \sqrt{\left(\sqrt{p_{T,\pi}^2 + M_\pi^2} - M_\pi + M_{meson}\right)^2 - M_{meson}^2}$$

The number of constituent scaling

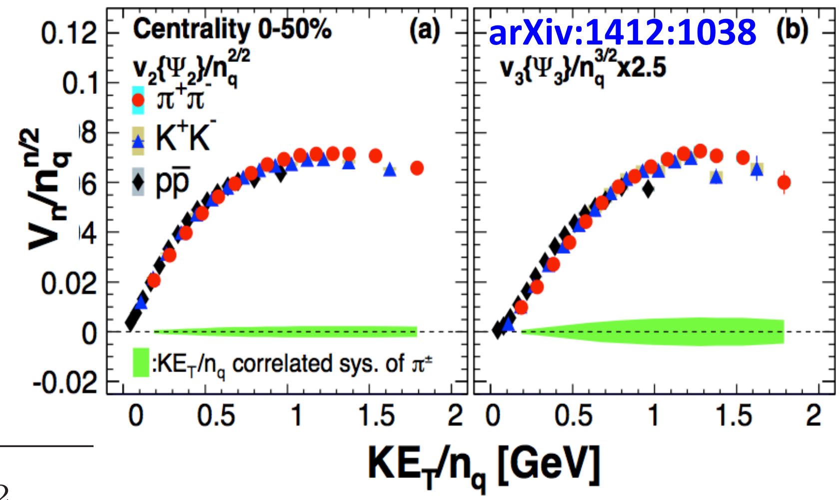

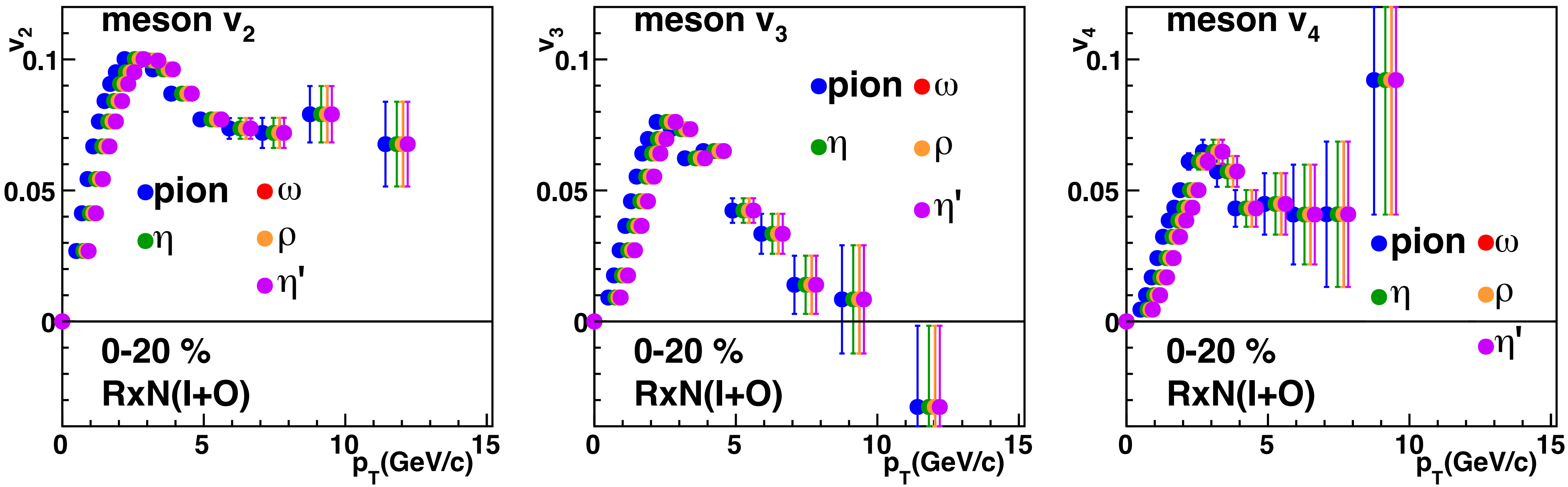

AMPT simulation for pion v_n

arXiv:1412:1038

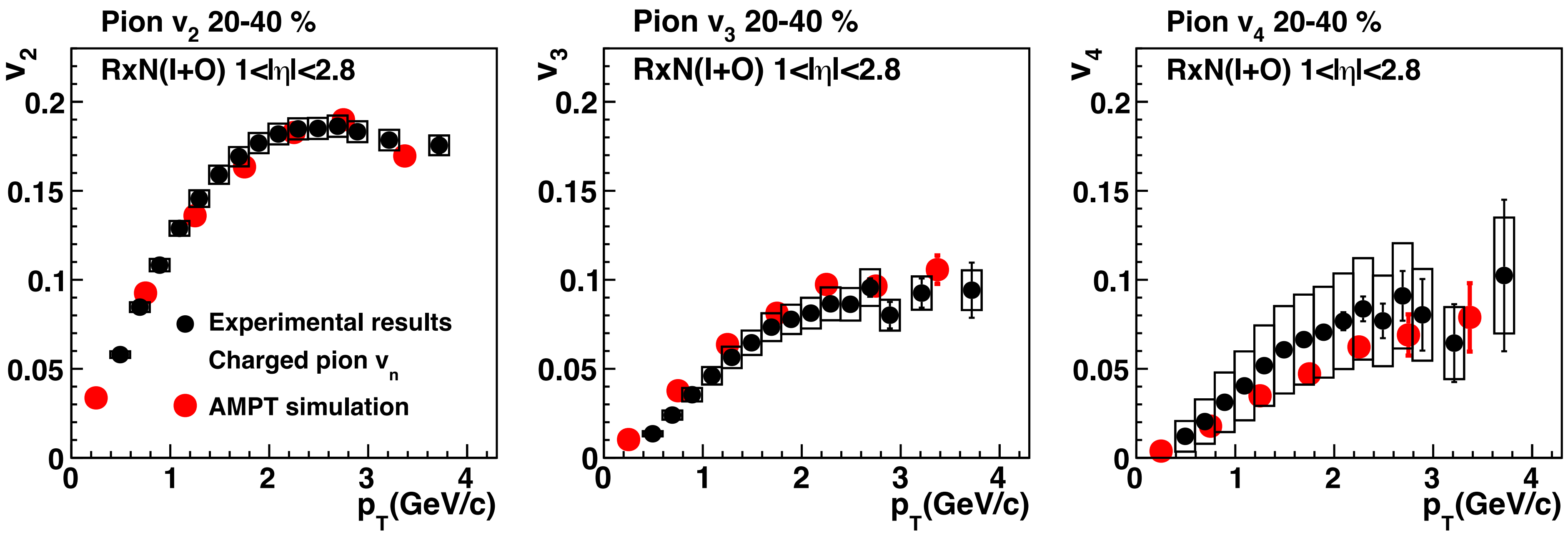

Pion v_n from AMPT simulation agrees well with charged pion v_n.

Jet bias on determining event plane

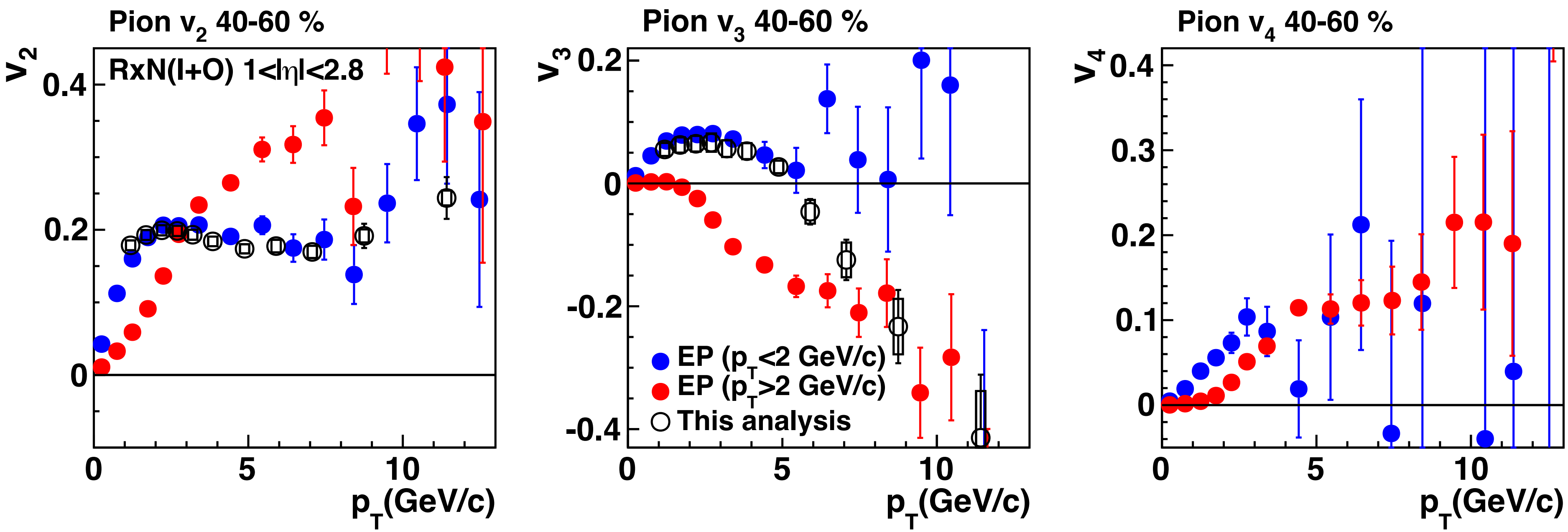

In low p_T :

$v_n(EP : p_T<2) > v_n(EP : p_T>2)$

In high p_T :

$v_2(EP : p_T<2) < v_2(EP : p_T>2)$

$v_3(EP : p_T<2) > v_3(EP : p_T>2)$

Jet bias on determining event plane

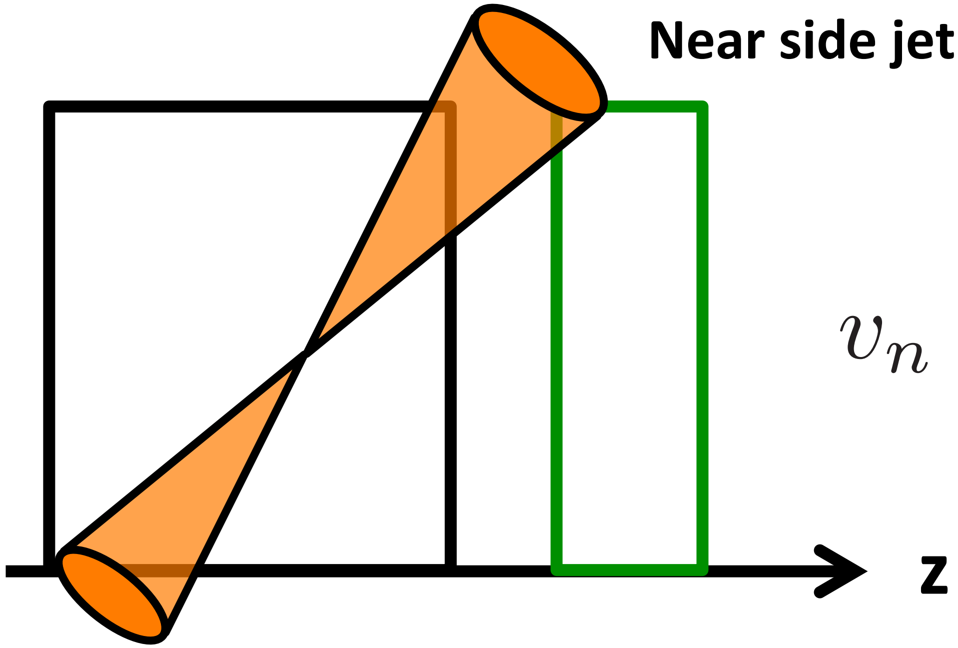

Near side jet : $v_n > 0$

$$v_n = \langle \cos\{n(\phi - \Psi_n)\}\rangle$$

Away side jet : depending on harmonics
v_2 & v_4 positive and v_3 negative

It appears in peripheral event due to the low multiplicity.

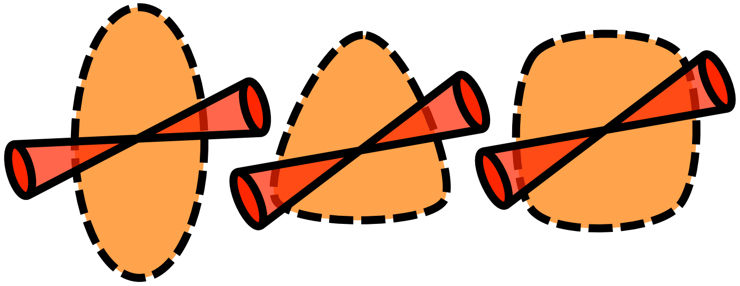

Integrated v_n with biased event plane

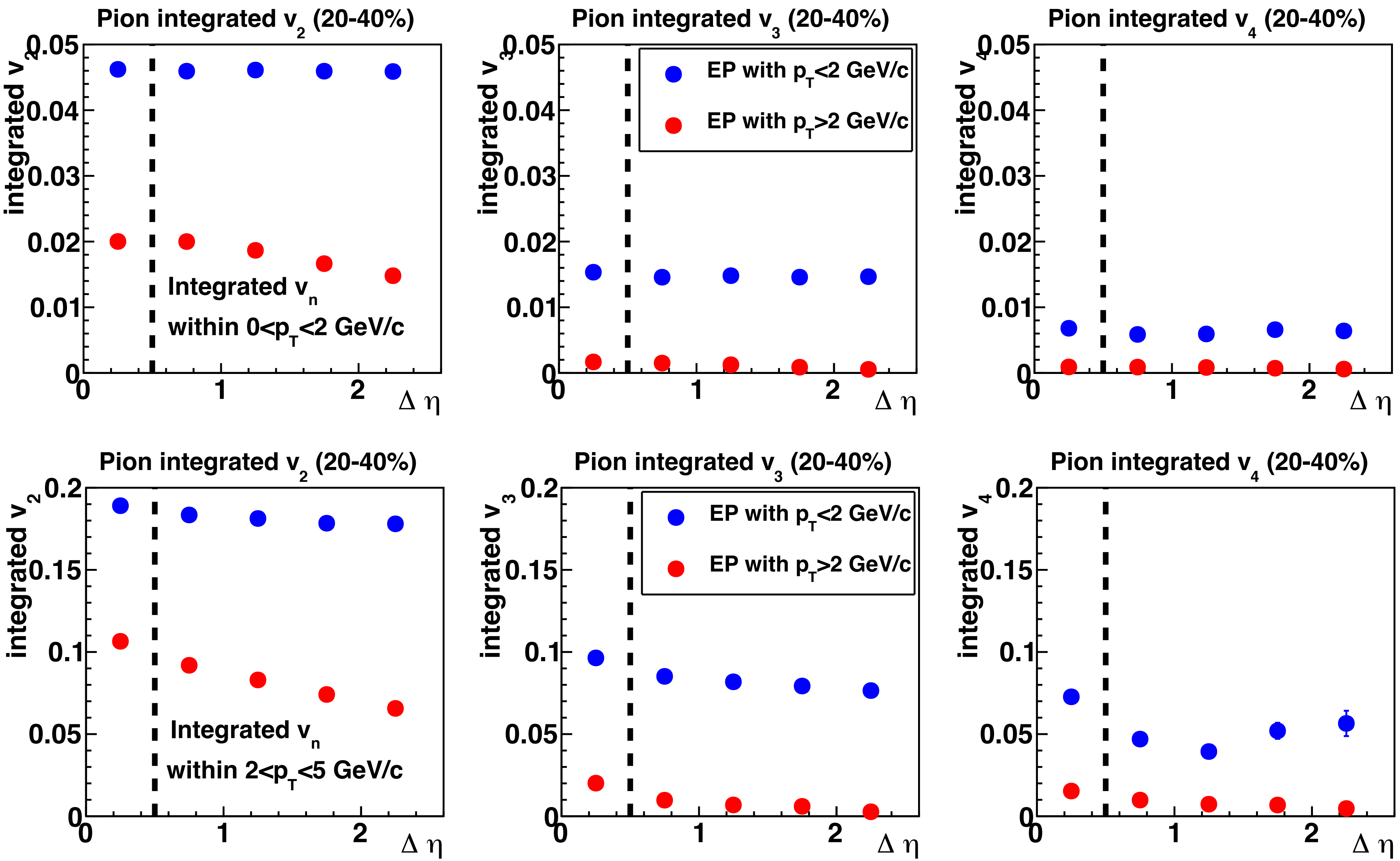

Model comparison of photon v_2

PRC 84,054906
PRC 89,034908

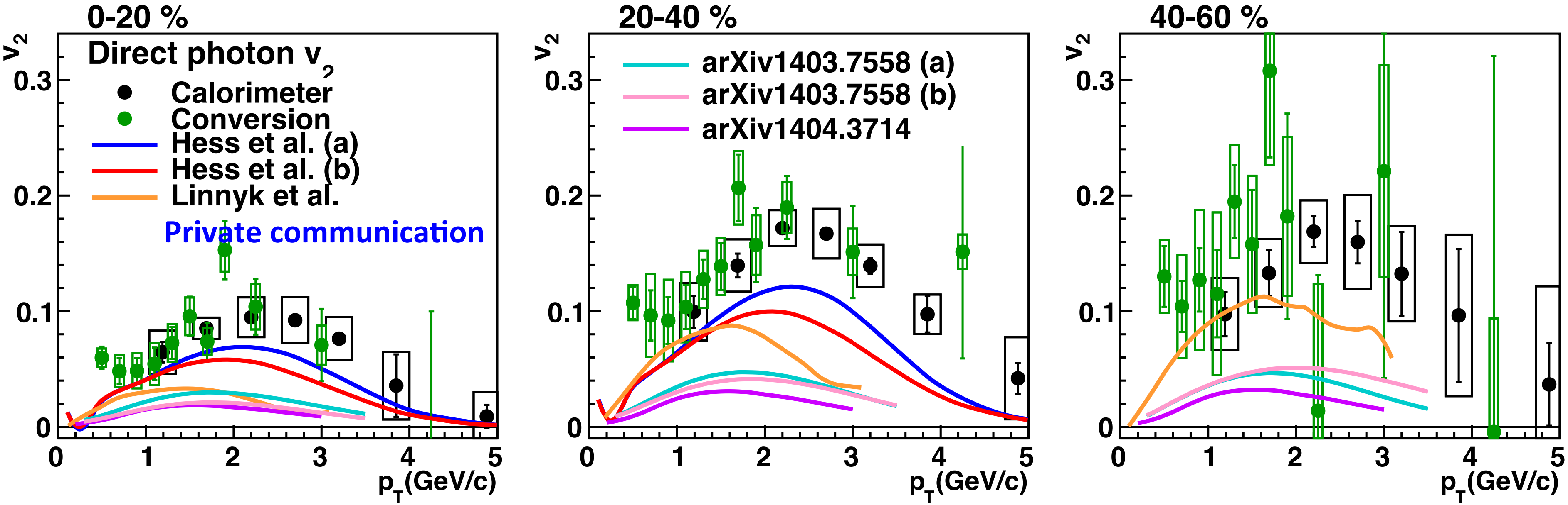

(Orange) Transport model considering photons from hadron phase
(Blue, red) Fireball model
Hydrodynamic calculations (cyan, pink, and violet) including photons from late state, are much underestimated.

Model comparison of v_2 and v_3

PRC 84,054906
PRC 89,034908
P.R.D 89,026013
arXiv:1404.3714

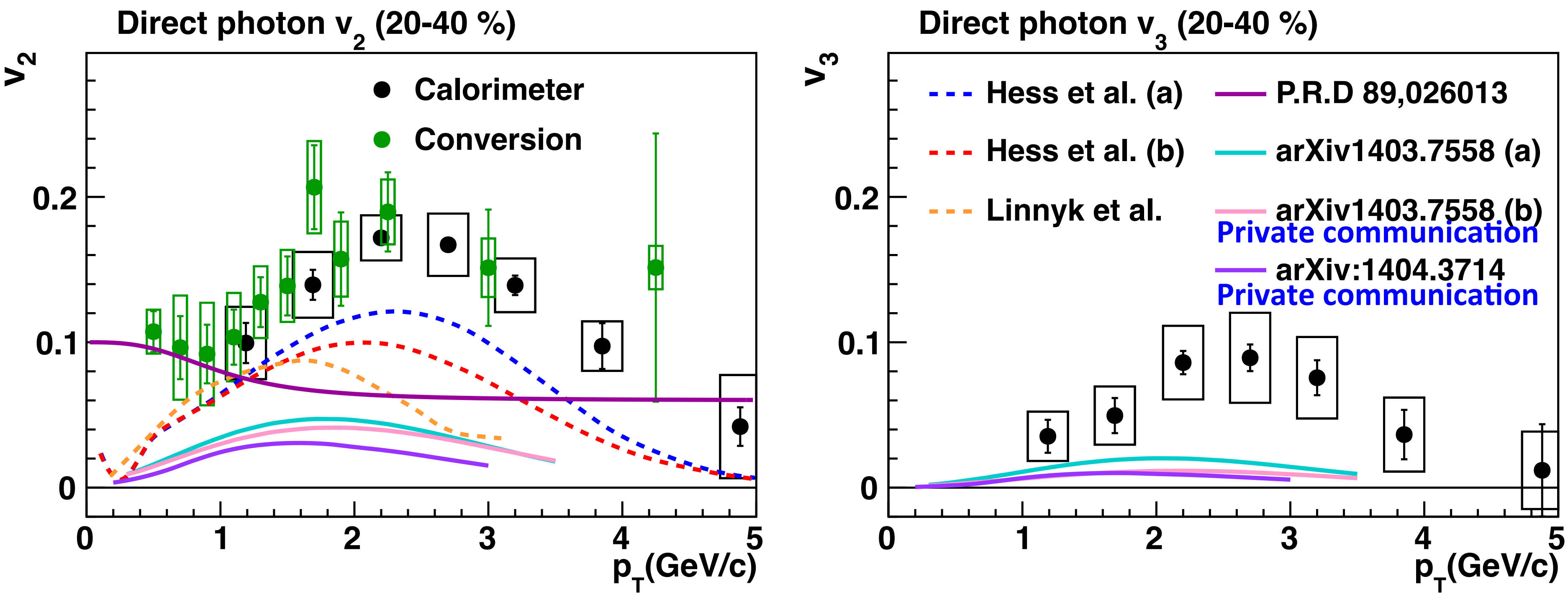

Dark violet is based on magnetic field effect, upper limit is shown.
Model calculations of photon v_3 are much smaller than experimental data.
The data of v_3 may help to constrain parameters in model calculations.

External photon conversion method

M_{HBD}: Real track
M_{vtx} : Measured track

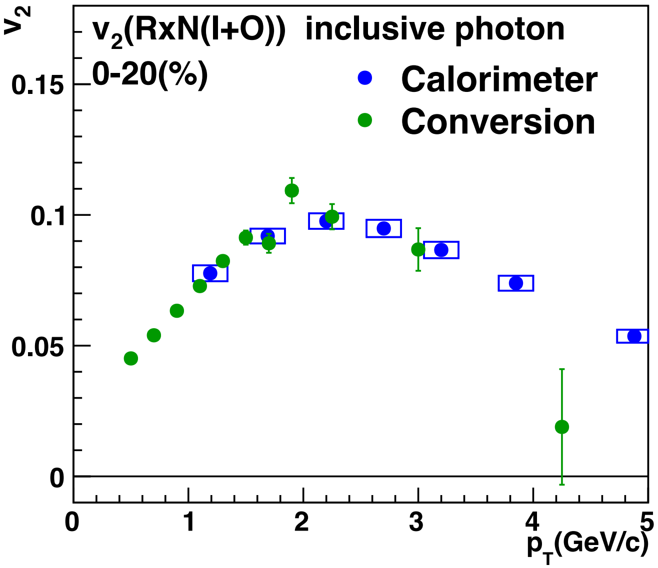

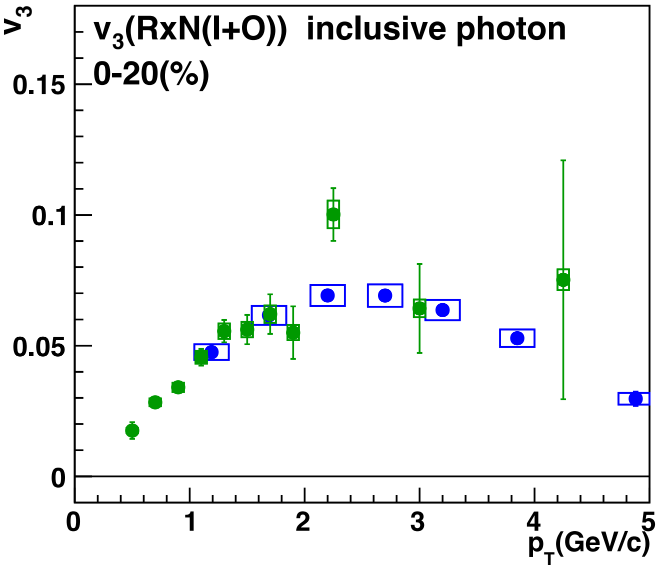

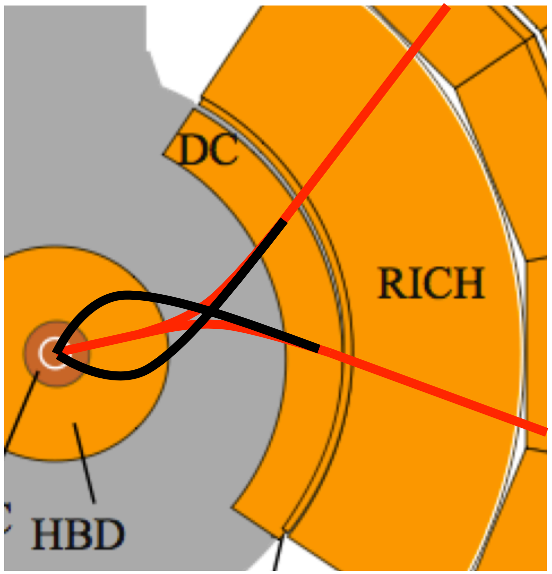

γ Invariant mass of e^++e^- pair

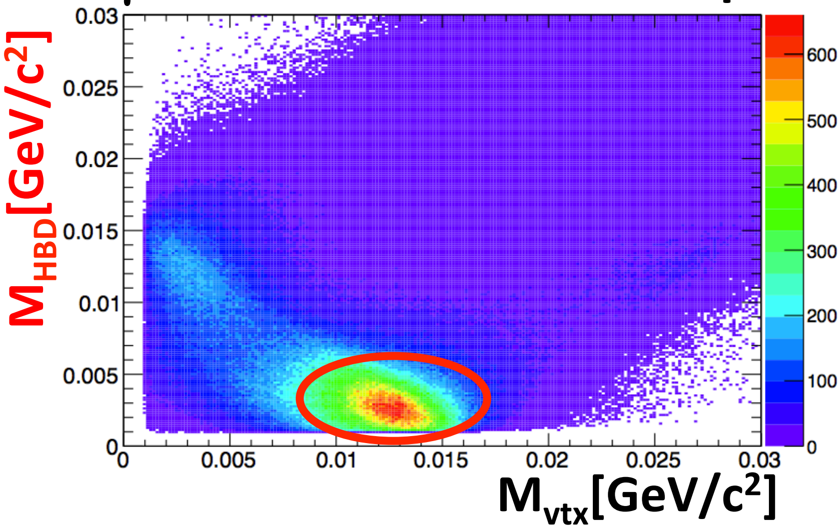

Real photons from external photon conversion at the Hadron Blind Detector (HBD) readout plane are detected.

- Extend low p_T limit

Consistent inclusive photon v_n well

External photon conversion method

Real track
estimated track

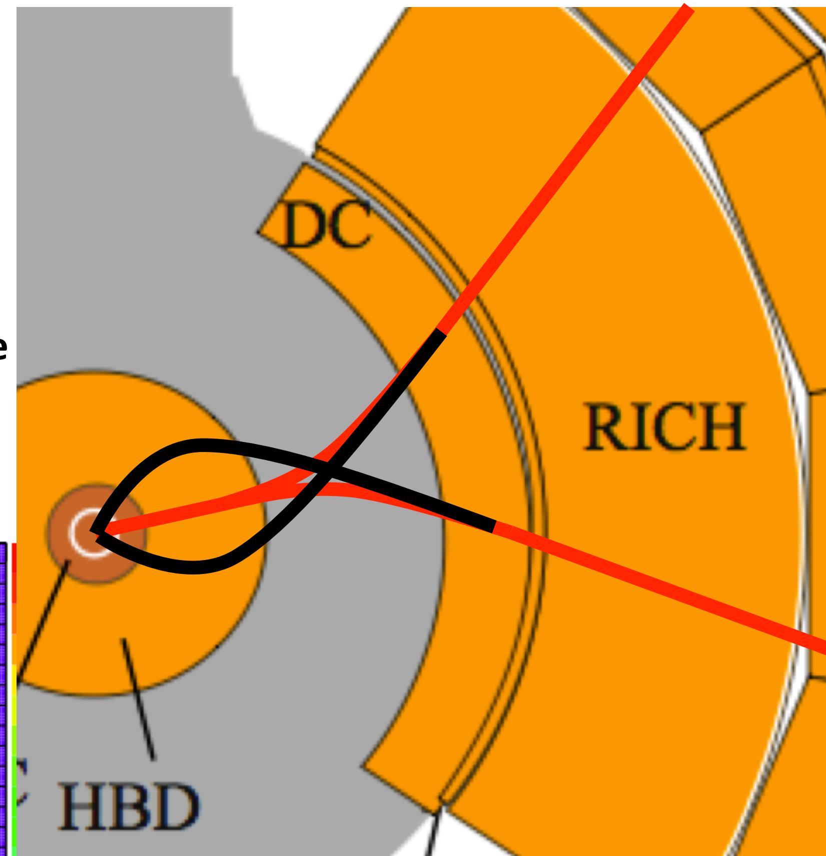

1) real photon converts to e^+e^- in HBD backplane
2) default assumption: track come from the vertex
3) momentum of the conversion tracks will be
   mis-measured (see black tracks)
4) apparent pair-mass (about 12MeV) will be measured
   for phtons
5) assume the same tracks originate in the HBD backplane
6) re-calculate momentum and pair mass with this
   "alternate tracking model"
7) for true converted photons M_{atm} will be around zero

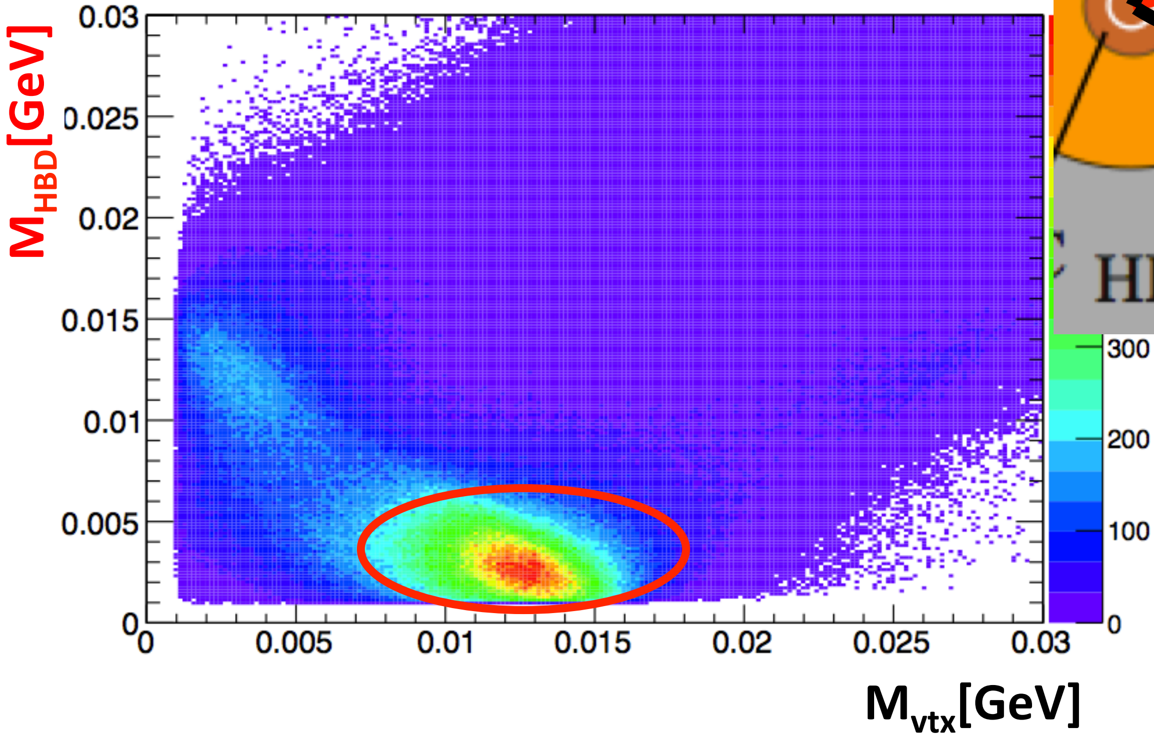

The ratio of v_2 to v_3 in p_T region

$\pi^{\pm}$: arXiv:1412:1038
Model : arXiv:1403.7558
Private communication

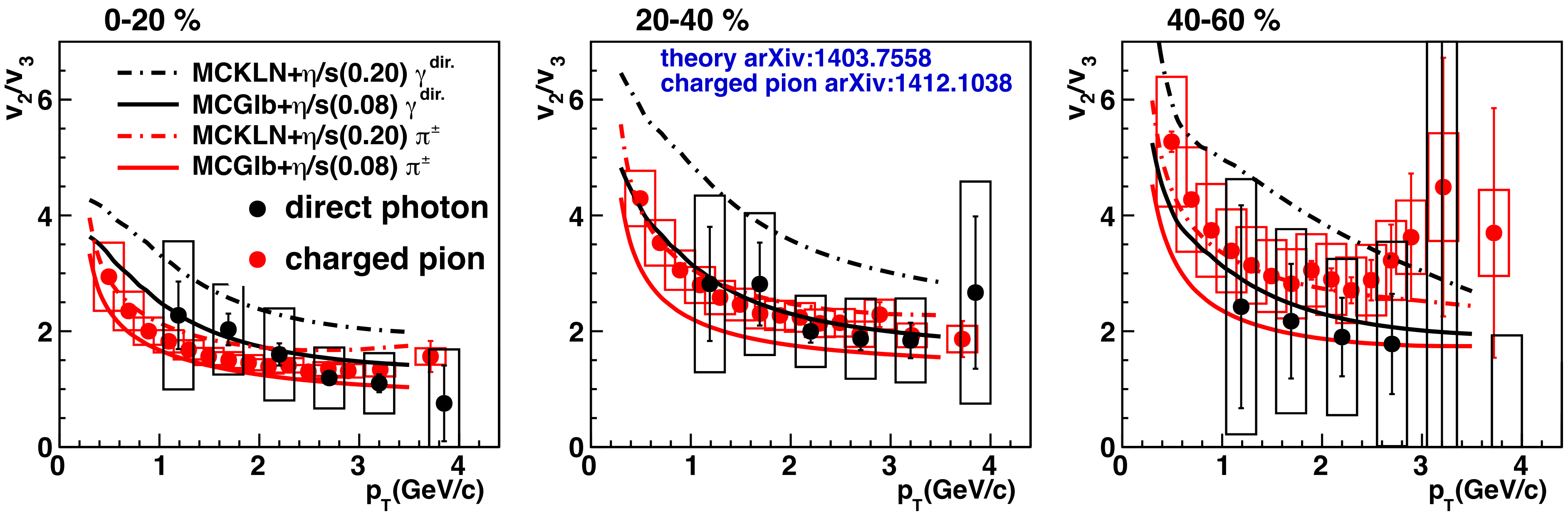

- Photons don't have strong centrality dependence at around 2-3 GeV/c
- Pions increase from central to peripheral

Photon and pion show different centrality dependence.

The event plane dependence of direct photon v_n

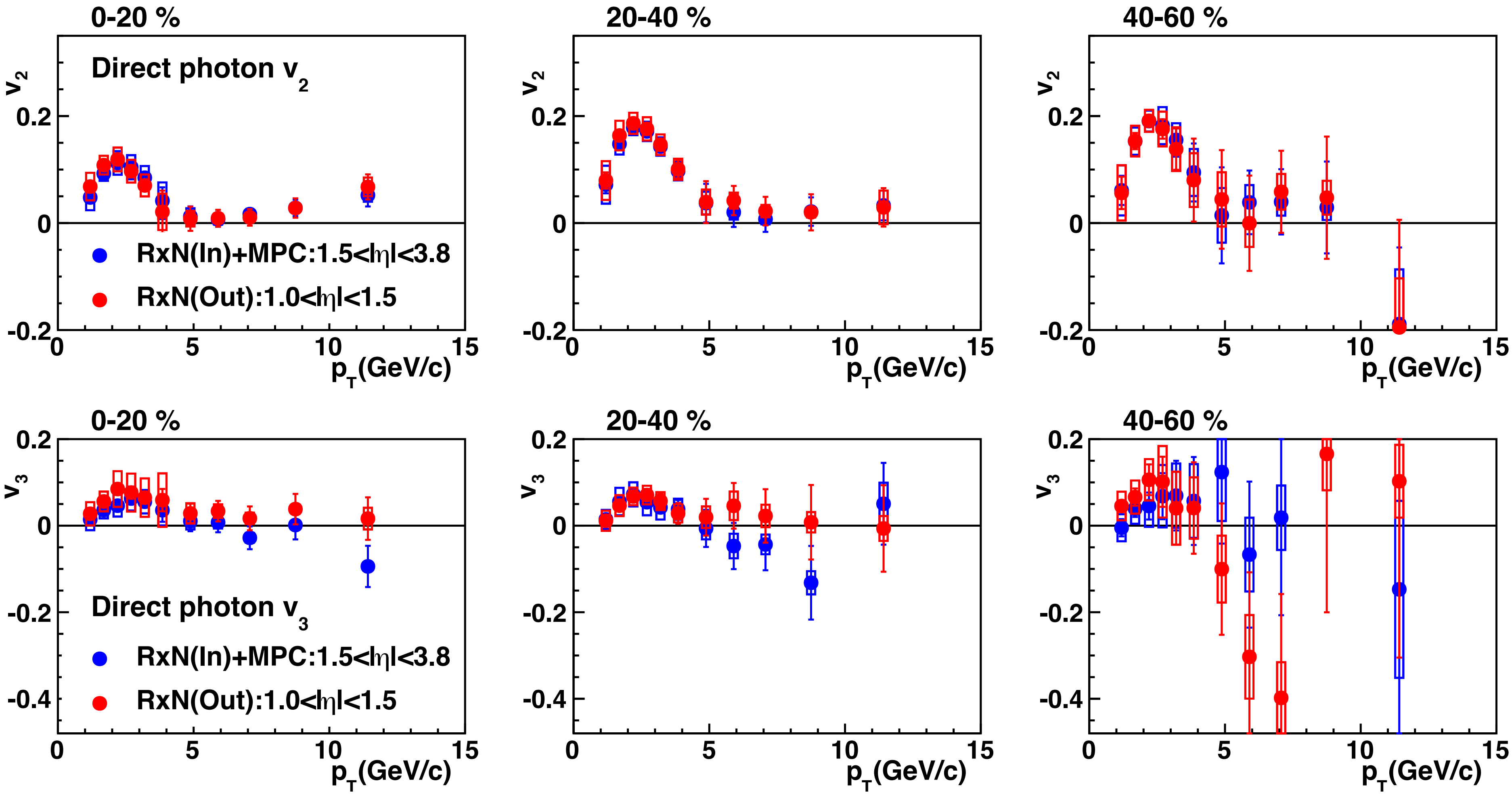

π^0 and $\gamma^{dir.}$ v_2 measurement by STAR

Ahmed M. Hamed
shown at QM

✓ BEMC: |η| < 1.0, FTPC: 2.5 < |η| < 4.0

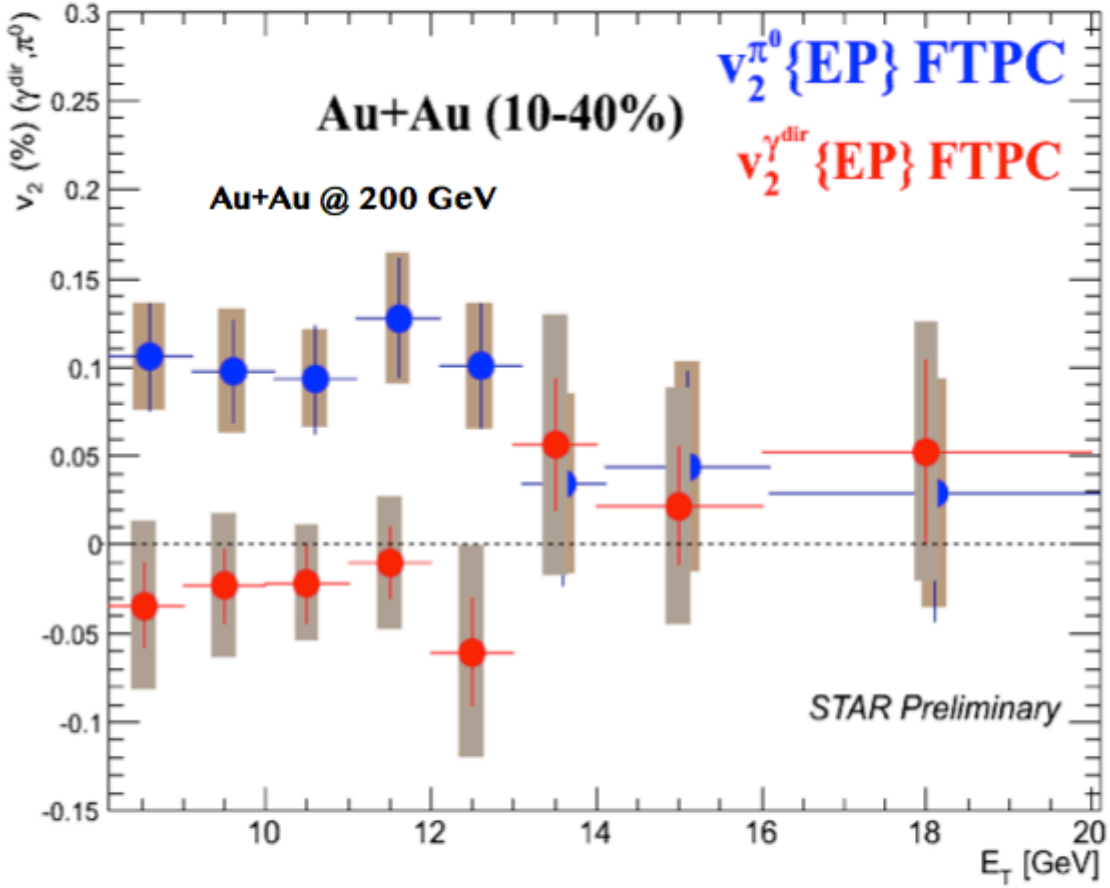

$\gamma^{dir.}$ v_2 in high E_T region are consistent with 0 within systematic uncertainty, while π^0 has positive v_2.

photon v_n measurement by ALICE

arXiv:1212.3995v2

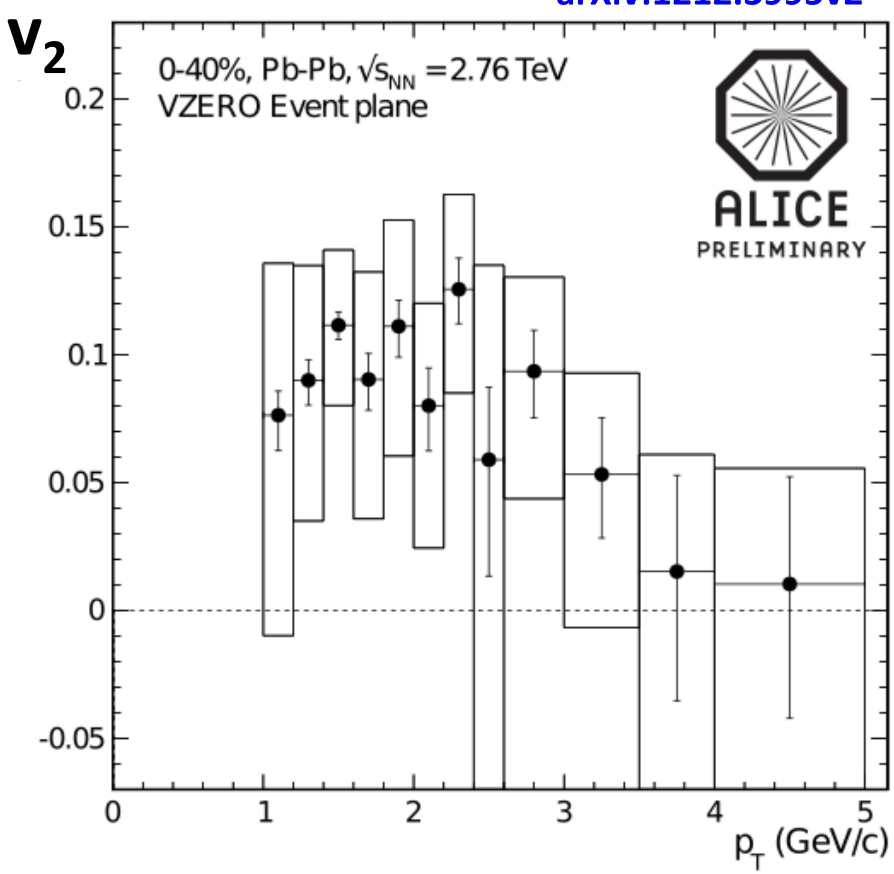

Friederike shown at QM

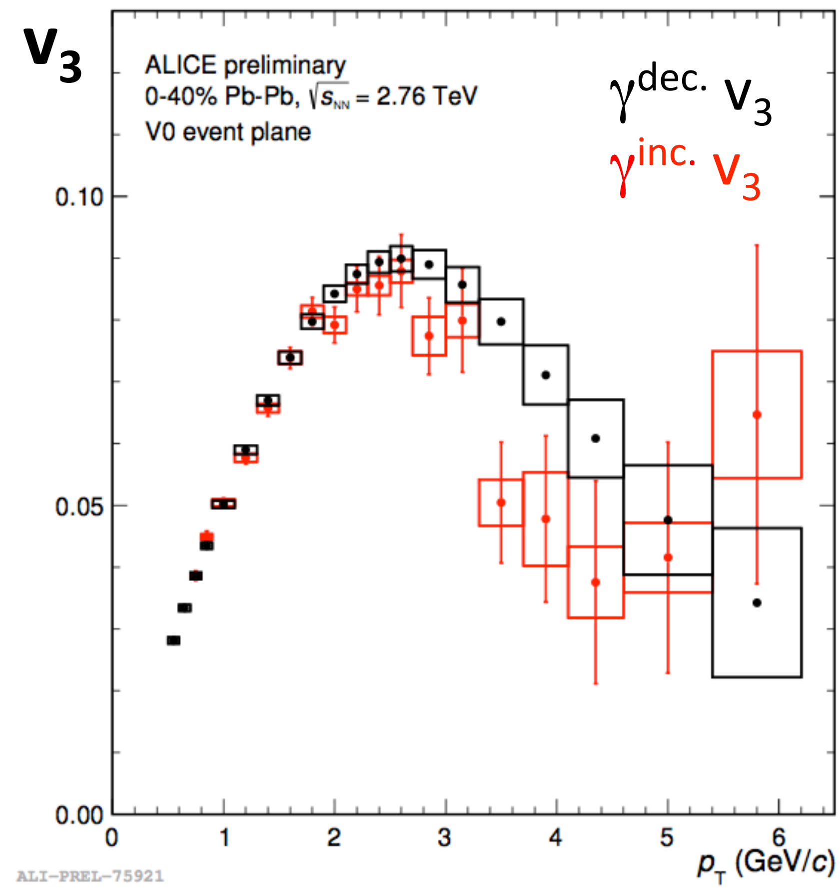

It is also observed that $\gamma^{dir.}$ v_2 is positive in low p_T at LHC-ALICE.
v_3 measurement is ongoing.

Photon p_T spectra and v_n with blue shift effect

Assumption of photon source

- **temperature decreases with the time : T(t)**
- **acceleration increases with the time : a(t)**
- **azimuthal anisotropy increases with the time $v_n(p_T, t)$**
- **thermal photon momentum distribution :**

$$n(p_T, t) = \frac{p_T}{\exp\left(p_T/T(t)\right) - 1}$$

p_T spectra and v_n at final state are calculated as :

$$n^{\text{fin.}}(p_T) = \int dt n(p_T, t) \qquad v_n^{\text{fin.}}(p_T) = \frac{\int dt n(p_T, t) v_n(p_T, t)}{\int dt n(p_T, t)}$$

Effective temperature is taken via fitting by exponential equation to p_T spectra.
The difference with experimental measurement is estimated as :

$$(V_{\text{obs.}} - V_{\text{cal.}})/E(\text{stat.} \oplus \text{sys.})$$

$V_{obs.}$: experimental measurement
E : error of $V_{obs.}$
$V_{cal.}$: calculation result

Basic assumption for yield, velocity, and anisotropy

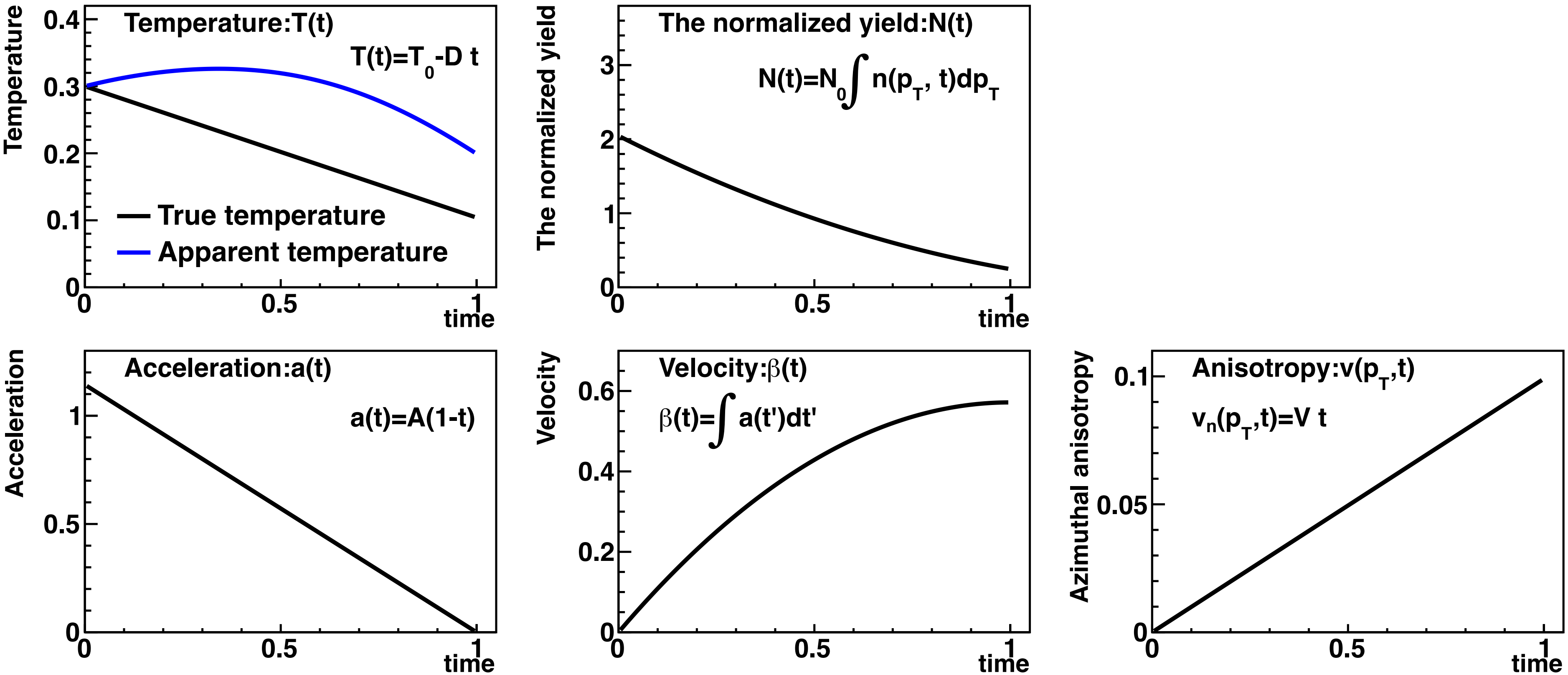

The temperature is decreased from 300 MeV to 100 MeV.
The time is defined by temperature.

Calculation with basic assumption

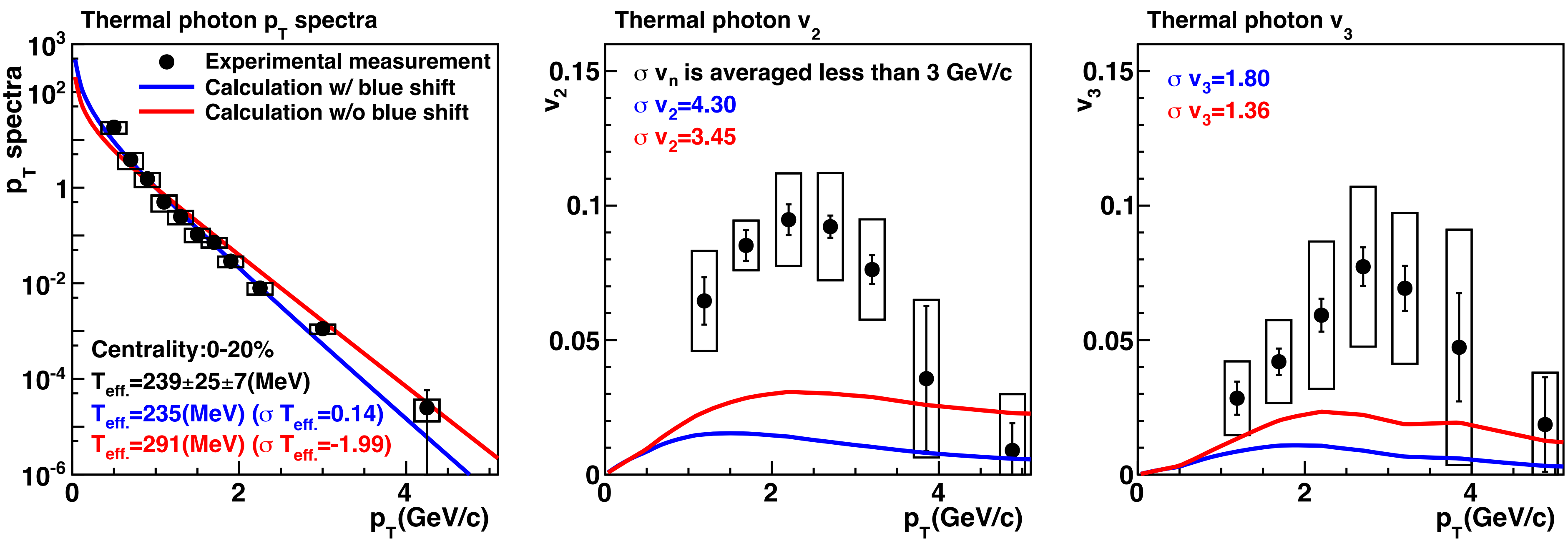

The effective temperature and v_n with blue shift is higher than those without correction.
The photons from late stage relatively increase in high p_T region due to blue shift correction.

Additional assumption

- **Yield dependence**

Since photon source expands, the yield is assumed to get large with time.

$$N(t) = \int dp_T t^b n(p_T, t)$$

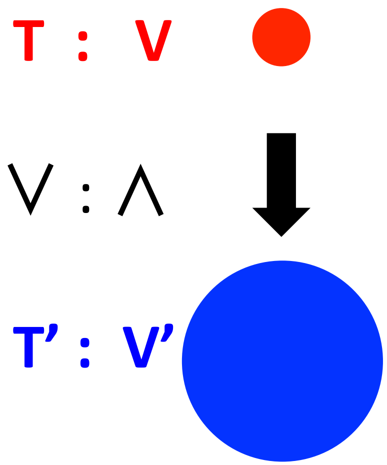

- **Anisotropy (velocity) dependence**

$$a(t) = A(1 - t^\alpha)$$

- **Azimuthal anisotropy dependence**

$$v_n(p_T, t) = V(p_T) \cdot t^c$$

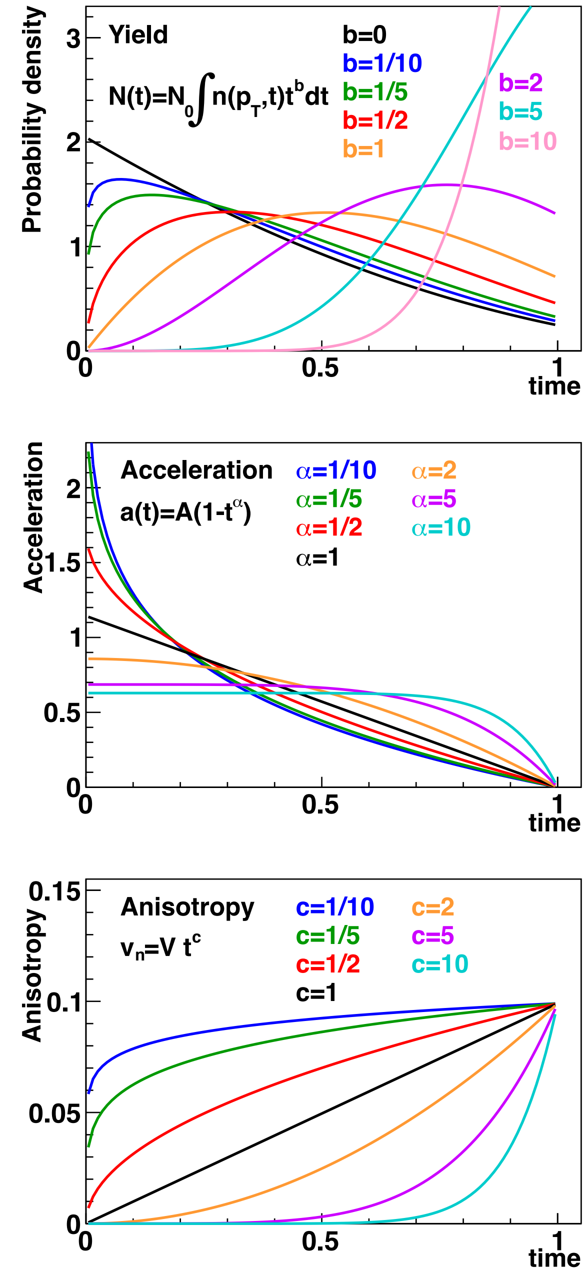

p_T spectra and v_n with relative yield dependence

$$N(t) = \int dp_T t^b n(p_T, t)$$

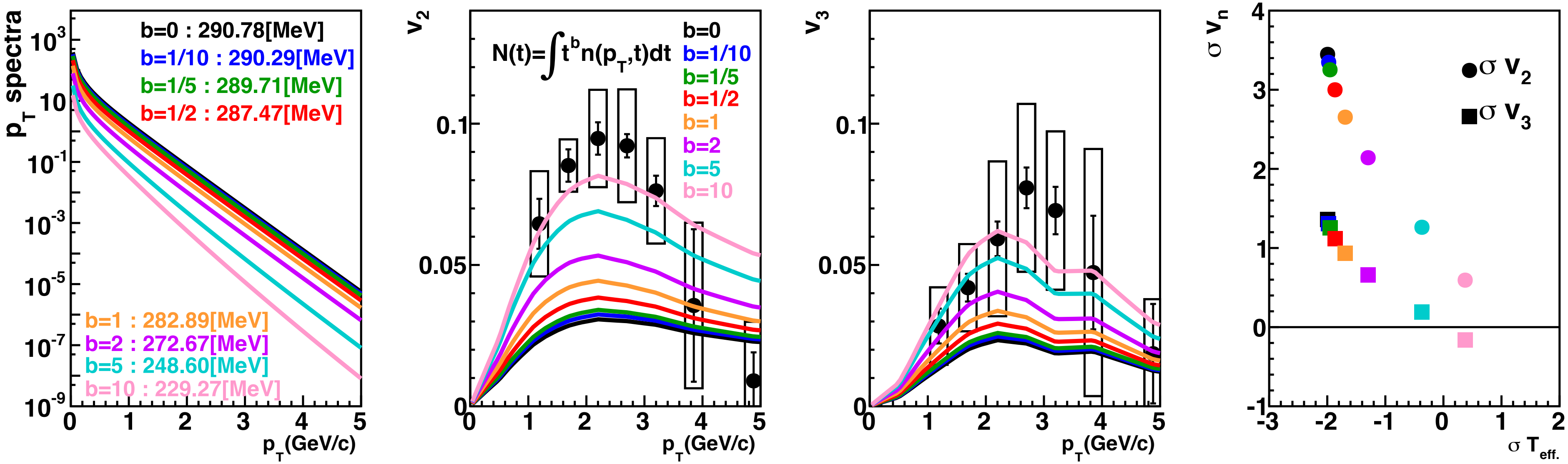

Photons from late stage : low temperature & large v_n

The both of effective temperature and v_n are affected.

p_T spectra and v_n with acceleration dependence

$$a(t) = A(1 - t^{\alpha})$$

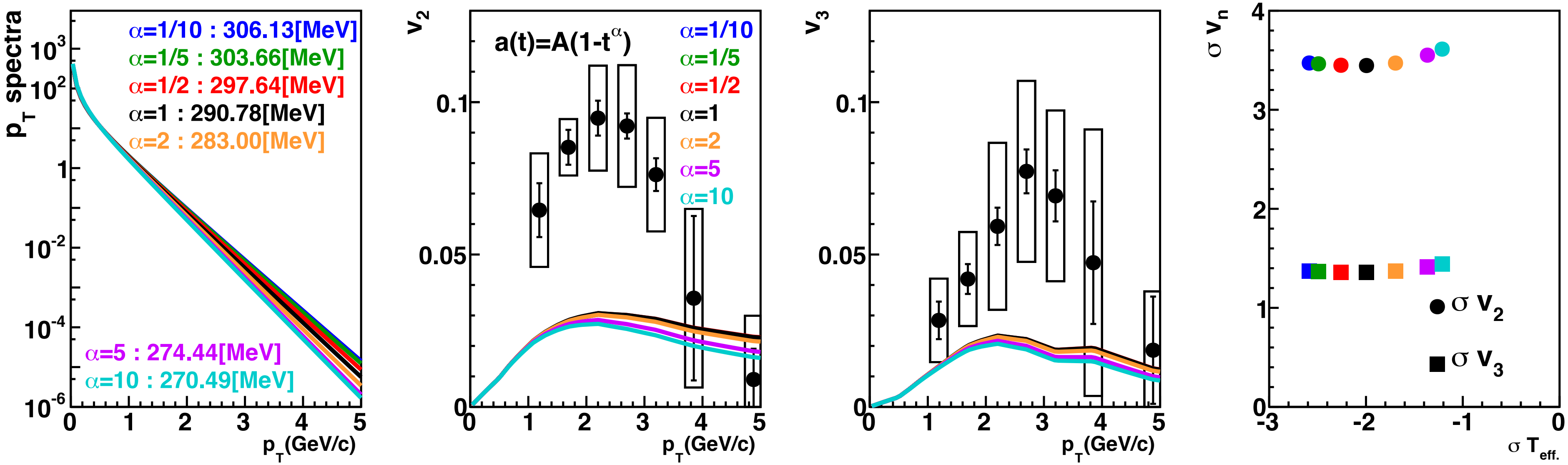

Effective temperature significantly decreases with increasing "α".
The v_n is a slightly affected.

p_T spectra and v_n with anisotropy dependence

$$v_n(p_T, t) = C(p_T) \cdot t^c$$

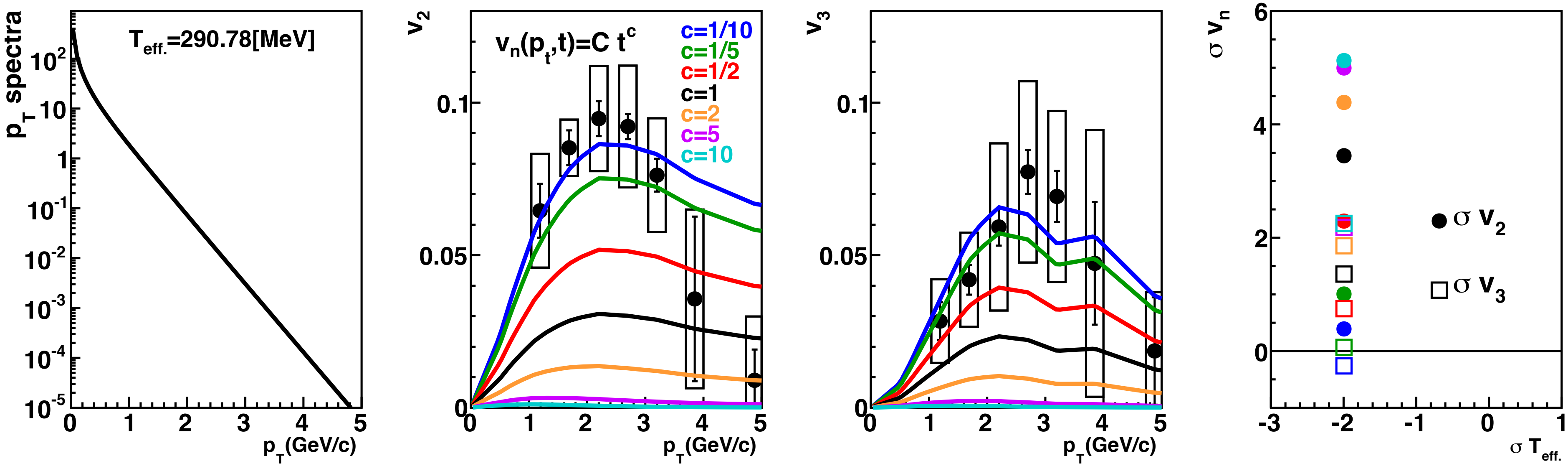

Since p_T spectra is not affected, effective temperature is not varied.

The v_n increases with "c" decreasing.

Comparison with experimental measurement

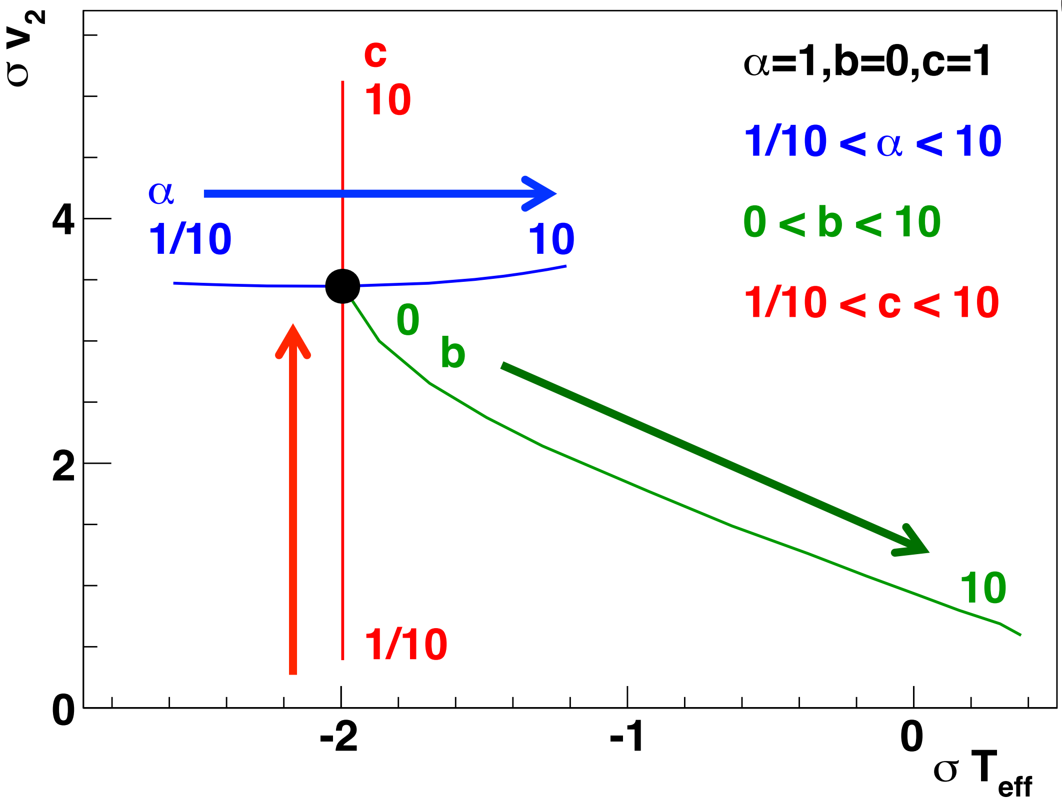

$$(V_{\rm obs.} - V_{\rm cal.})/E({\rm stat.} \oplus {\rm sys.})$$

$V_{obs.}$: experimental measurement
E : error of $V_{obs.}$
$V_{cal.}$: calculation result

$$N(t) = \int dp_T t^b n(p_T, t)$$

$$a(t) = A(1 - t^{\alpha})$$

$$v_n(p_T, t) = C(p_T) \cdot t^c$$

The differences (σT_{eff} and σv_2) are varies uniquely with the parameters "α", "b", and "c".
They are selected so that $T_{eff.}$ and v_2 are comparable to the experimental measurement.

The “b” and “c” are constrained

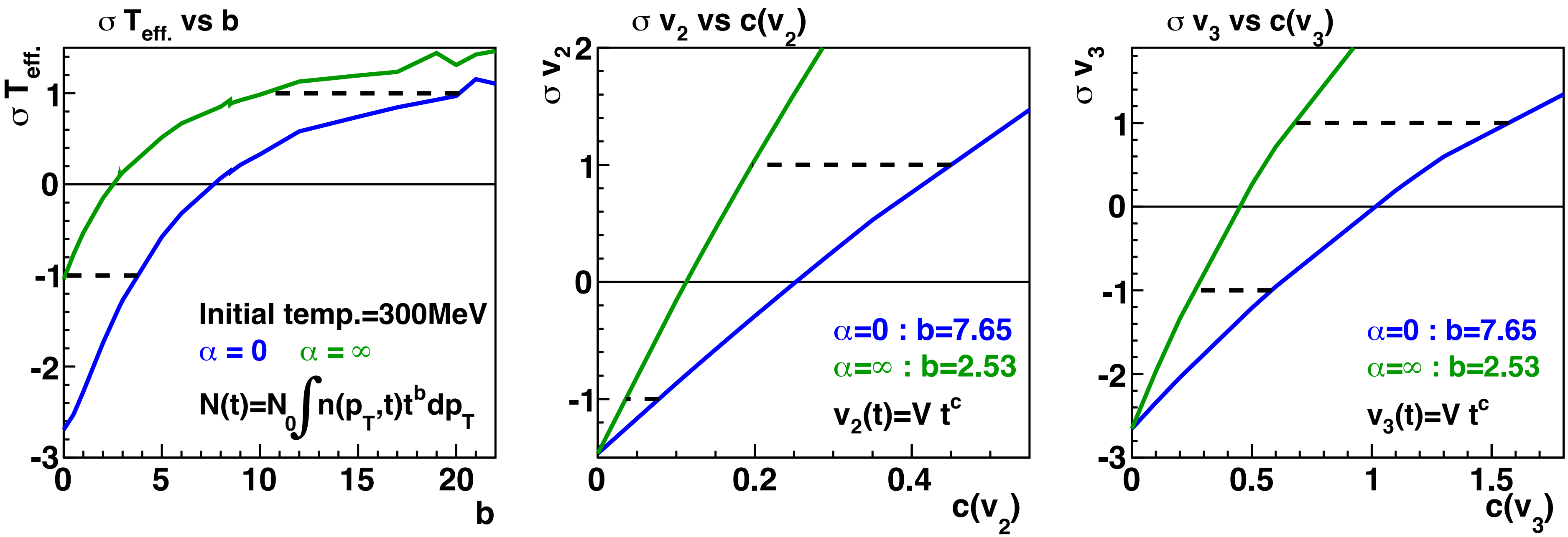

The parameters “b” and “c” are limited so that the calculations agree with experimental measurements within 1 σ.

The limitation of time evolution

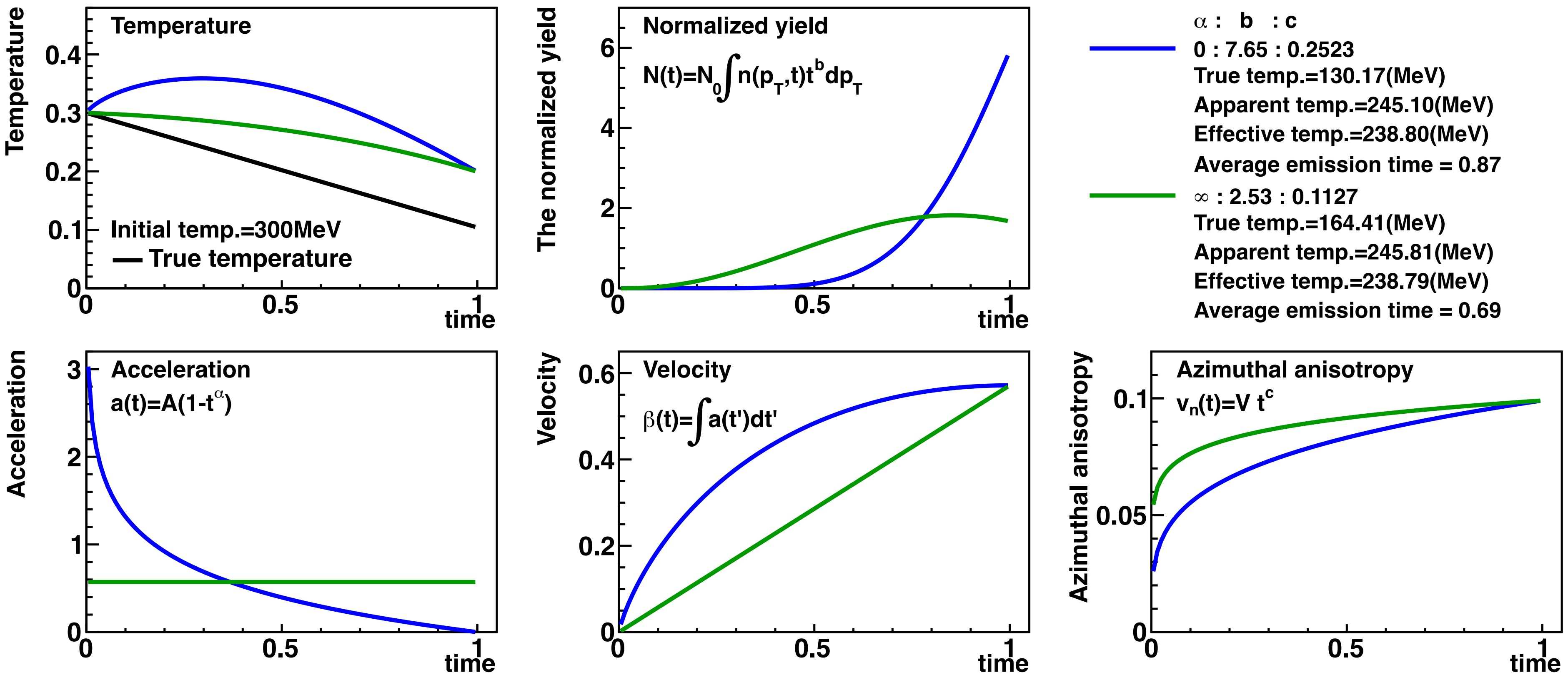

The development of photon yield and azimuthal anisotropy are constrained.

The p_T spectra and v_n with selected parameters

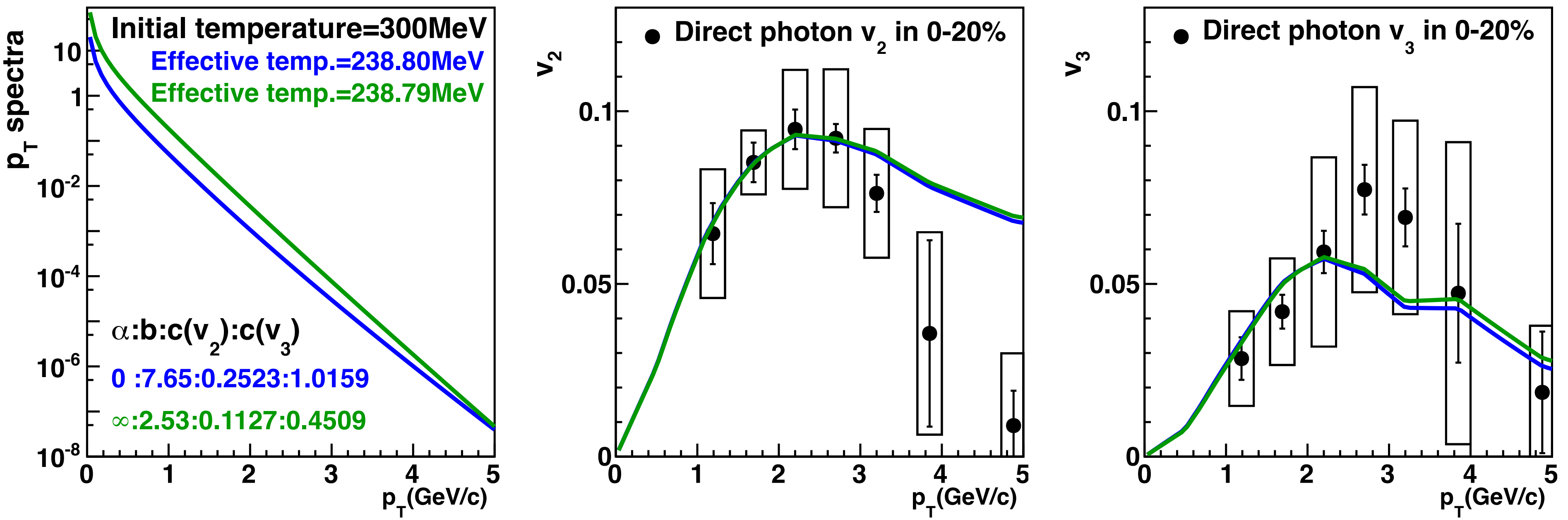

Parameter "b" is selected so that effective temperature is comparable to experimental measurement.
The "c" is chosen to be comparable to v_2.

The summary of calculations

The summary of calculations			
Initial temperature	Effective temperature	True temperature	Average emission time
300 (MeV)	238.79 - 238.80 (MeV)	130.17 - 164.41 (MeV)	0.69 - 0.87
400 (MeV)	237.29 - 240.38 (MeV)	128.61 - 146.09 (MeV)	0.86 - 0.92
500 (MeV)	237.97 - 238.08 (MeV)	128.52 - 138.59 (MeV)	0.91 - 0.94
600 (MeV)	236.27 - 236.72 (MeV)	128.15 - 135.28 (MeV)	0.94 - 0.95

Table 5.3: The summary of true temperature and average emission time. The time of freeze-out is defined as 1.

Thermal photon contribution

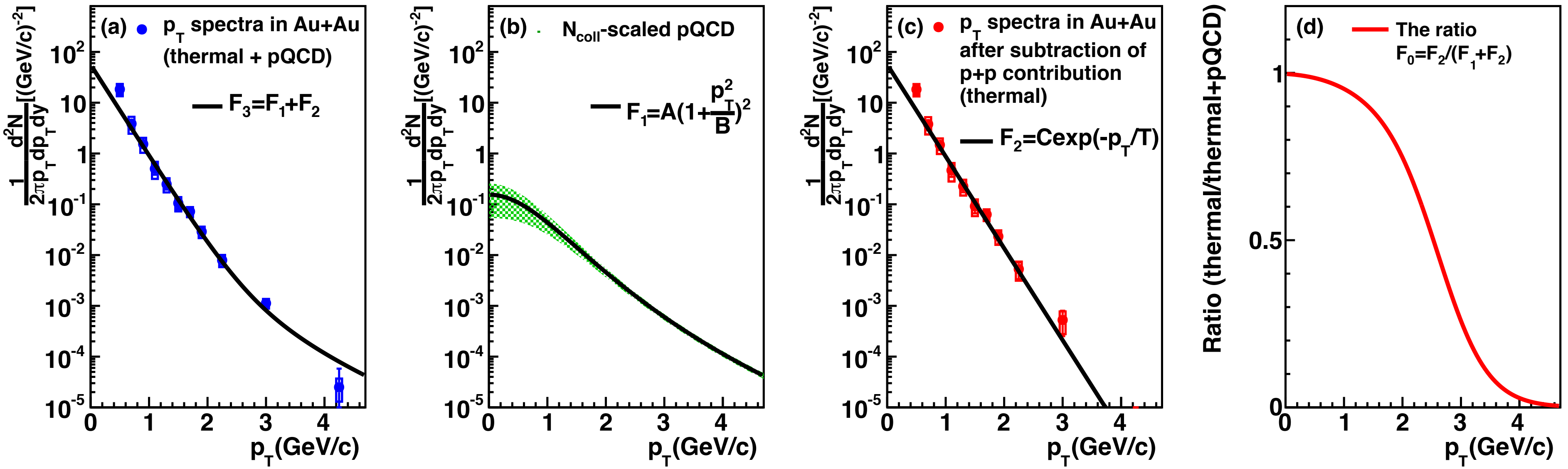

Thermal photon contribution to all photons are estimated.

It is found that thermal photons significantly drop down at around 2 GeV/c.

(Thermal + pQCD) photon v_n

$$v_n^{dir.} = \frac{N^{\rm thermal} v_n^{\rm thermal} + N^{\rm qQCD} v_n^{\rm pQCD}}{N^{\rm thermal} + N^{\rm pQCD}}$$

$$v_n^{dir.} = \frac{N^{\rm thermal} v_n^{\rm thermal}}{N^{\rm thermal} + N^{\rm pQCD}} \quad v_n^{\rm pQCD} = 0$$

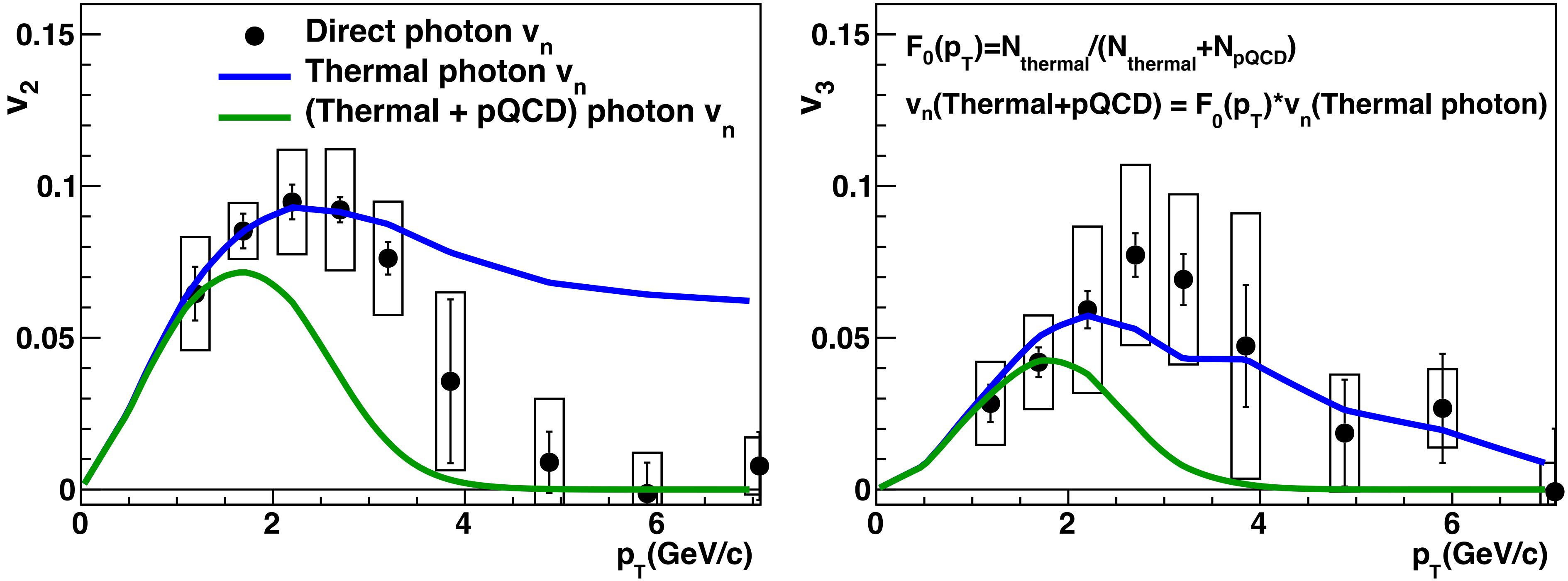

(Thermal + pQCD) photon v_n is smaller than experimental results.
The other photon contribution such as jet could be dominant in the region of $2 < p_T < 5$ GeV/c.

Comparison of neutral pion v_2 with previous results

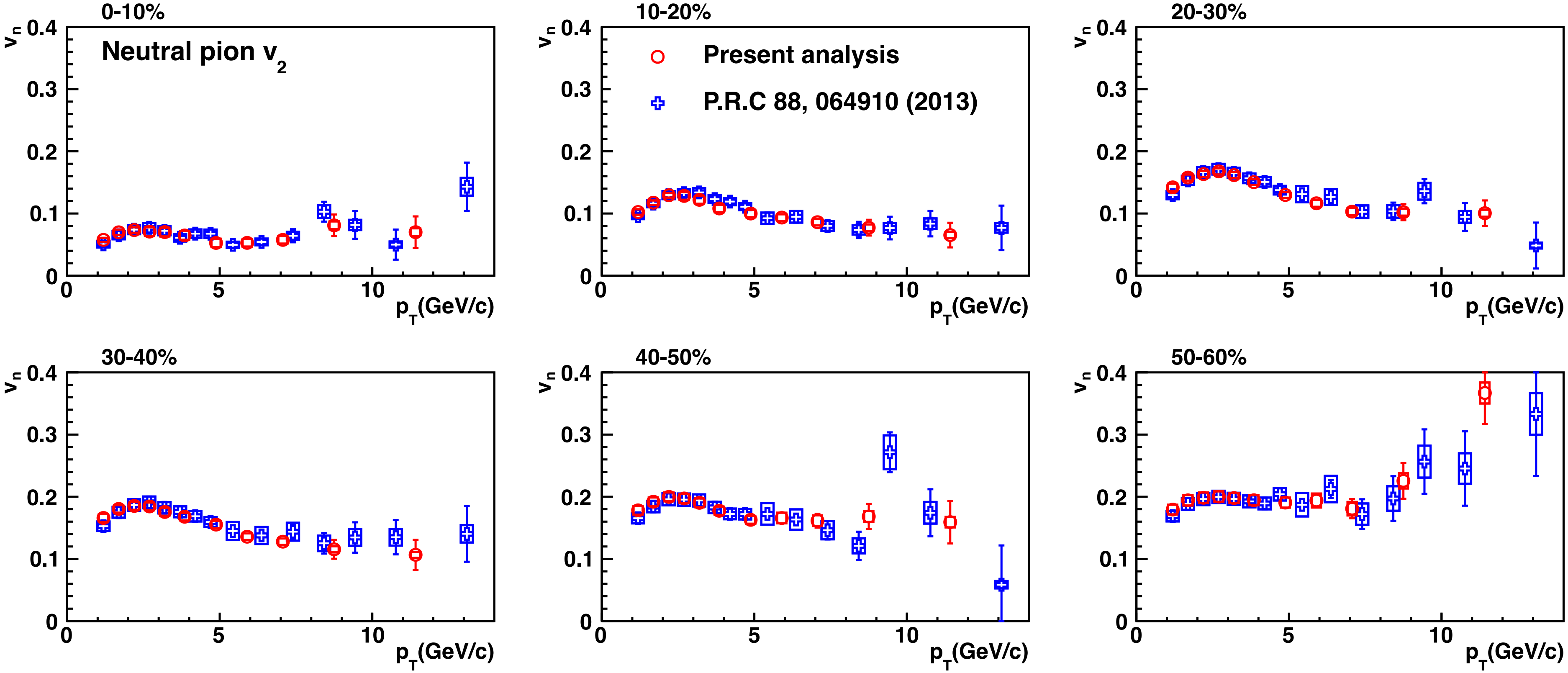

They are consistent within systematic uncertainty.

Comparison of neutral pion v_2 with previous results

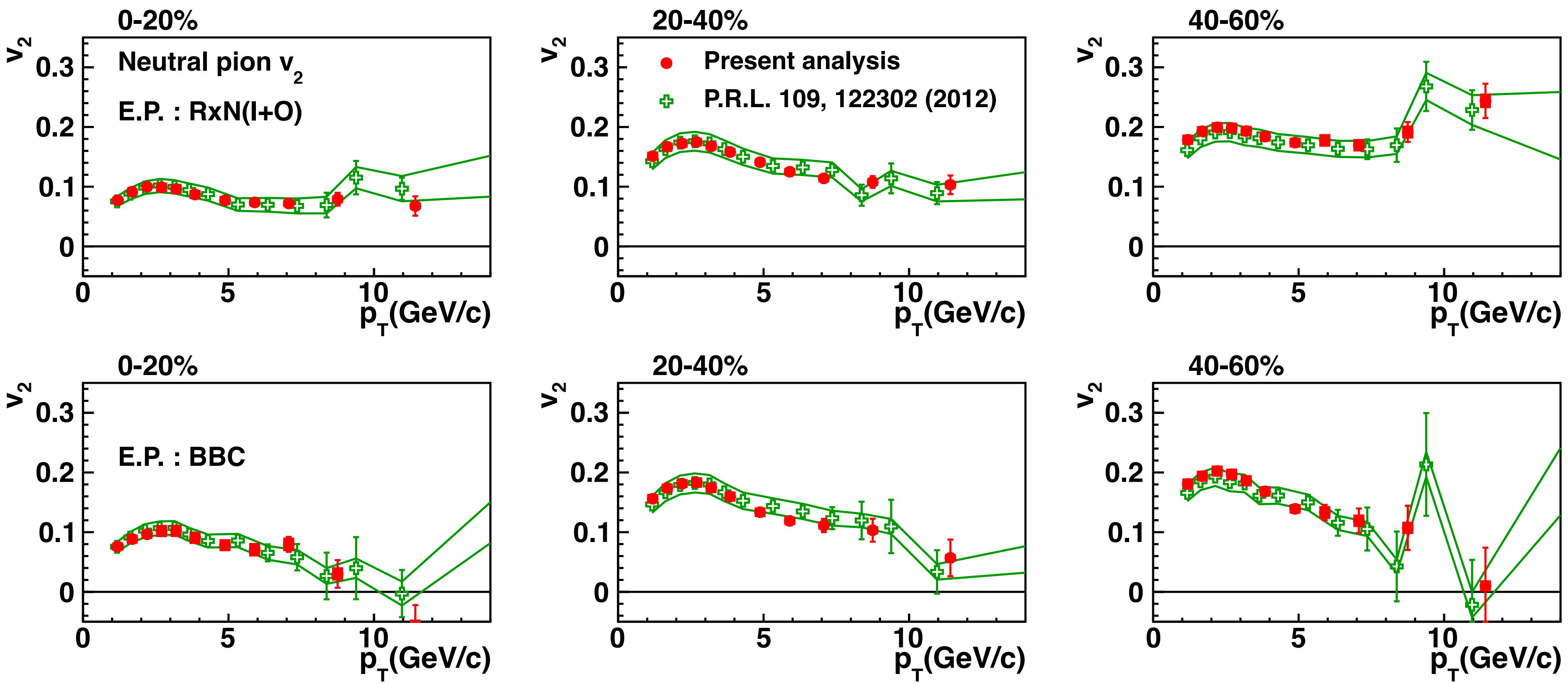

They are consistent within systematic uncertainty.

Comparison of inclusive photon v_2 with previous results

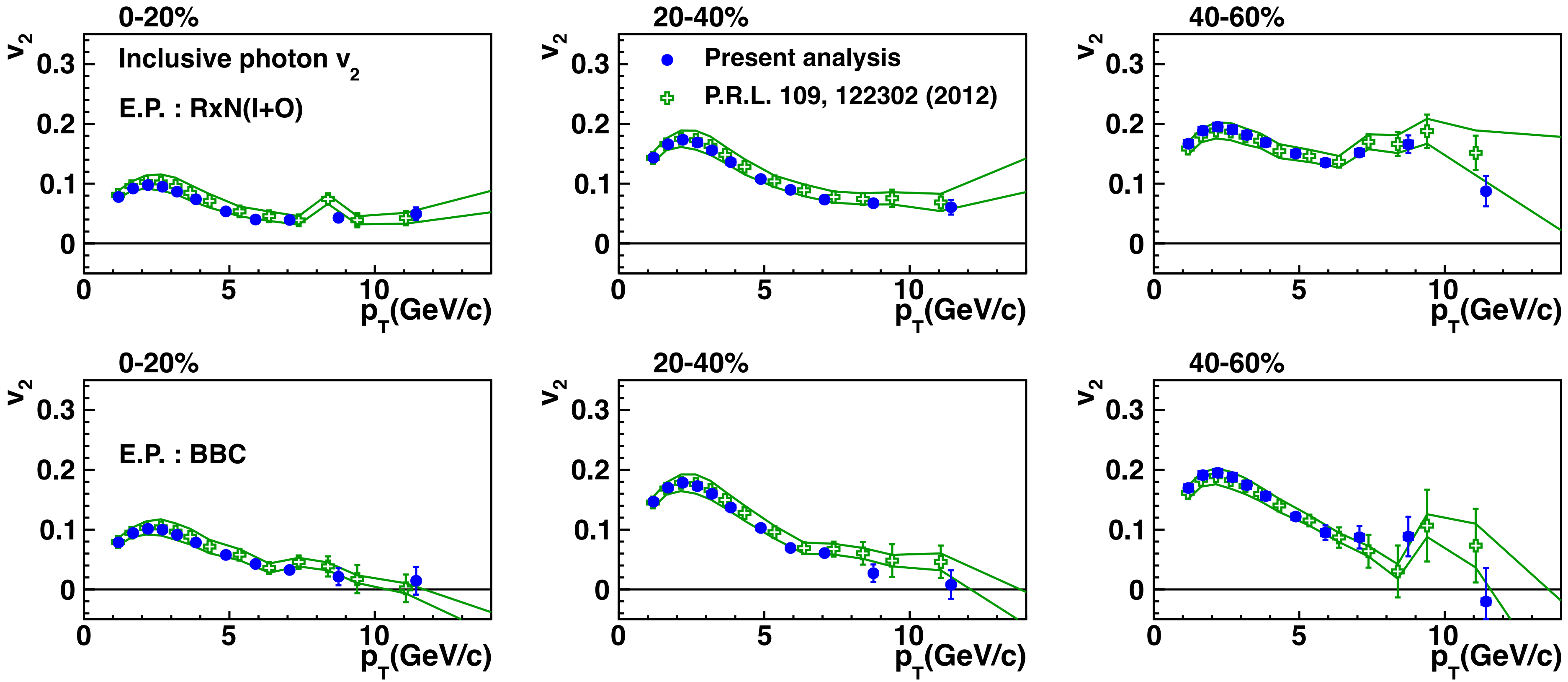

They are consistent within systematic uncertainty.

Comparison of neutral pion v_2 with charged pion v_2

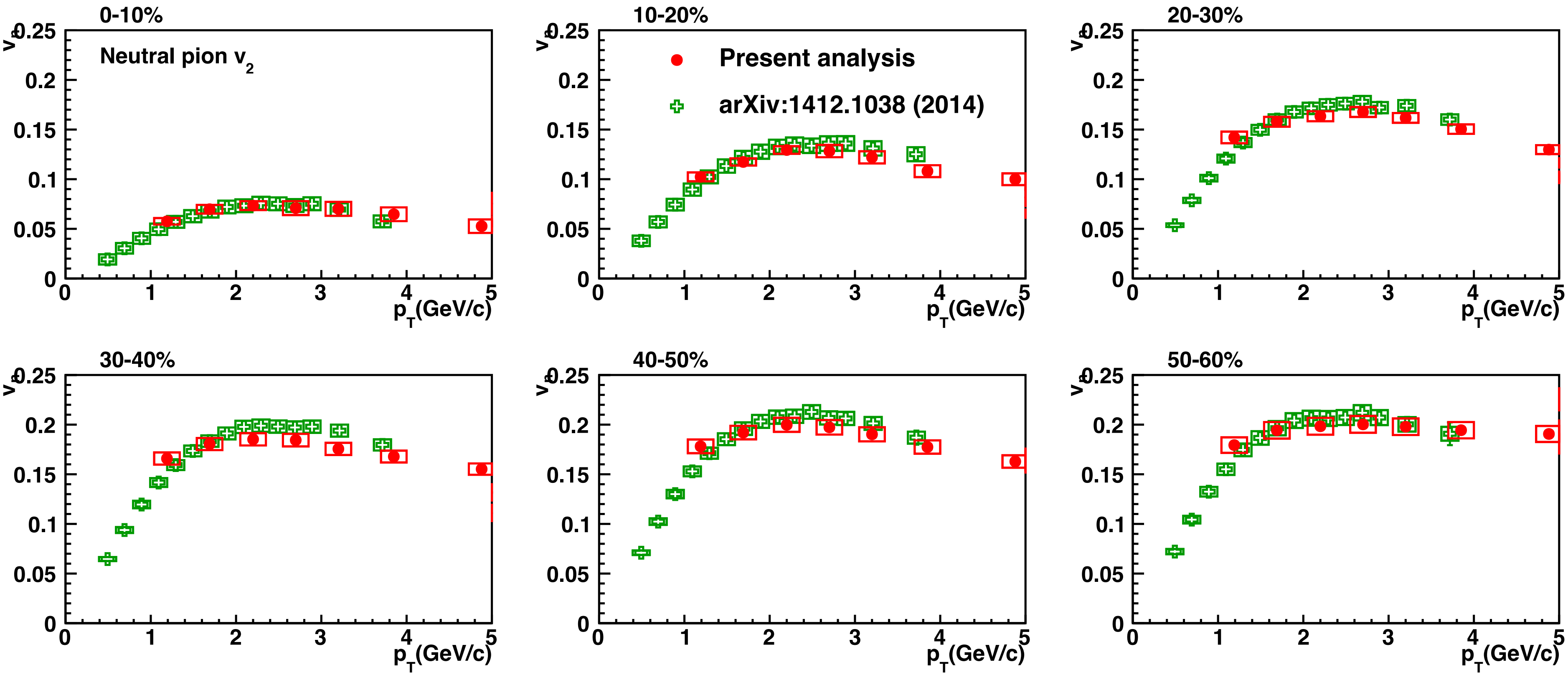

They are consistent within systematic uncertainty.

Comparison of neutral pion v_3 with charged pion v_3

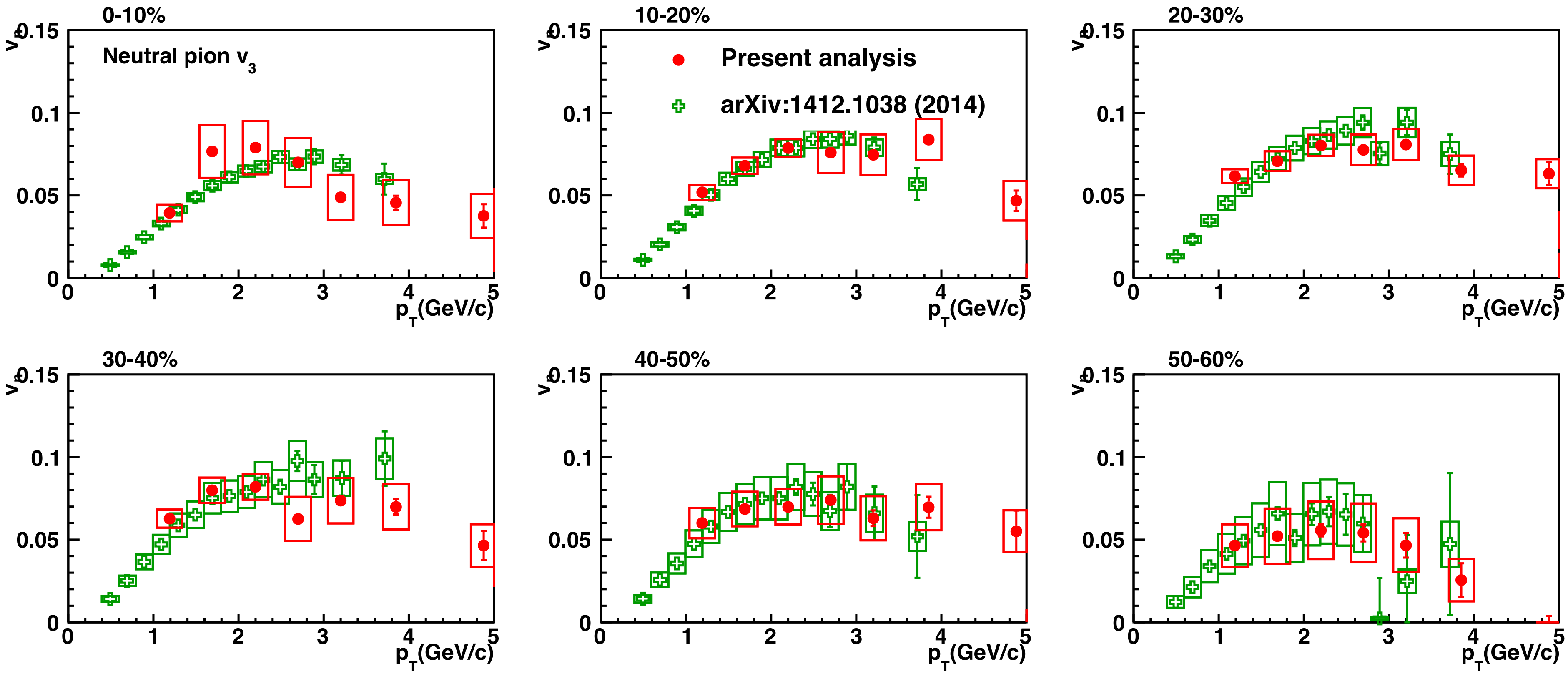

They are consistent within systematic uncertainty.

Comparison of neutral pion v_3 with charged pion v_3

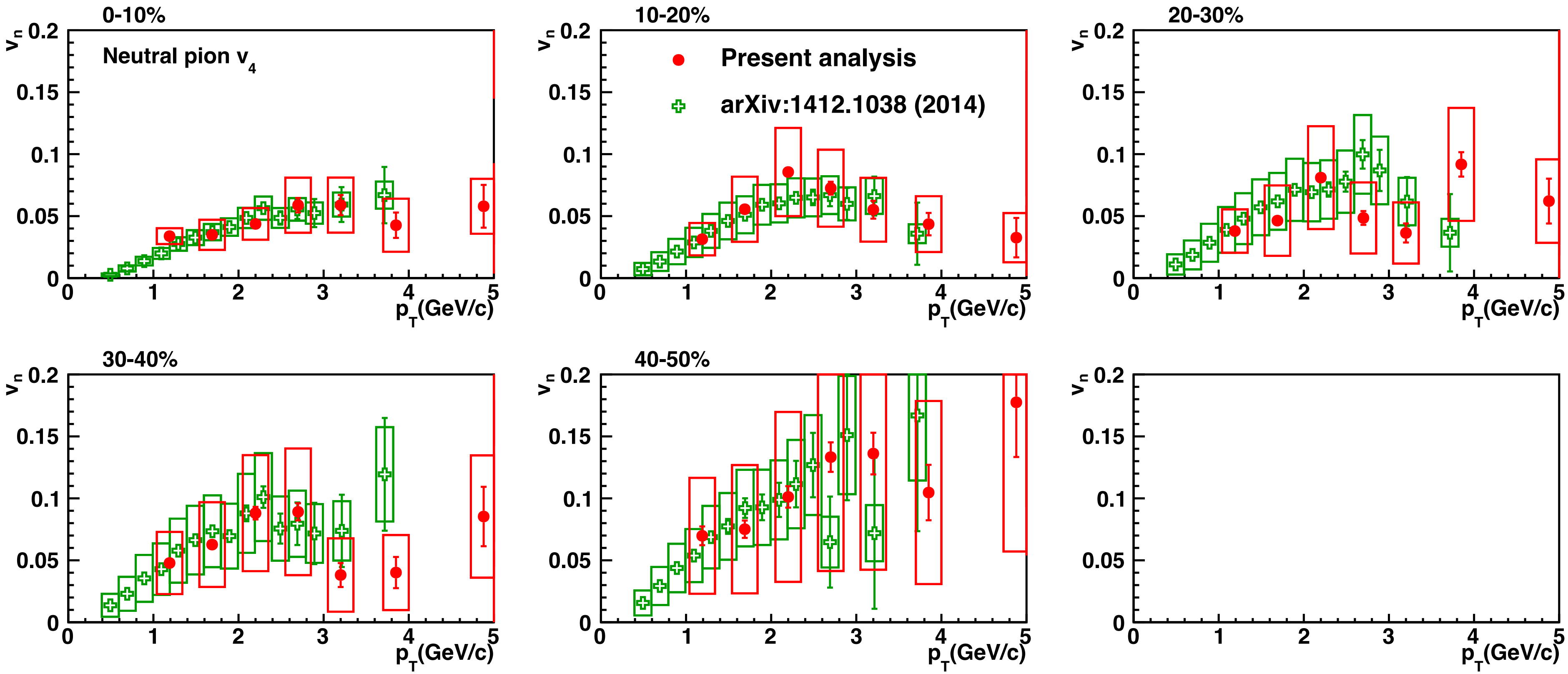

They are consistent within systematic uncertainty.

Comparison of direct photon v_2 with previous results

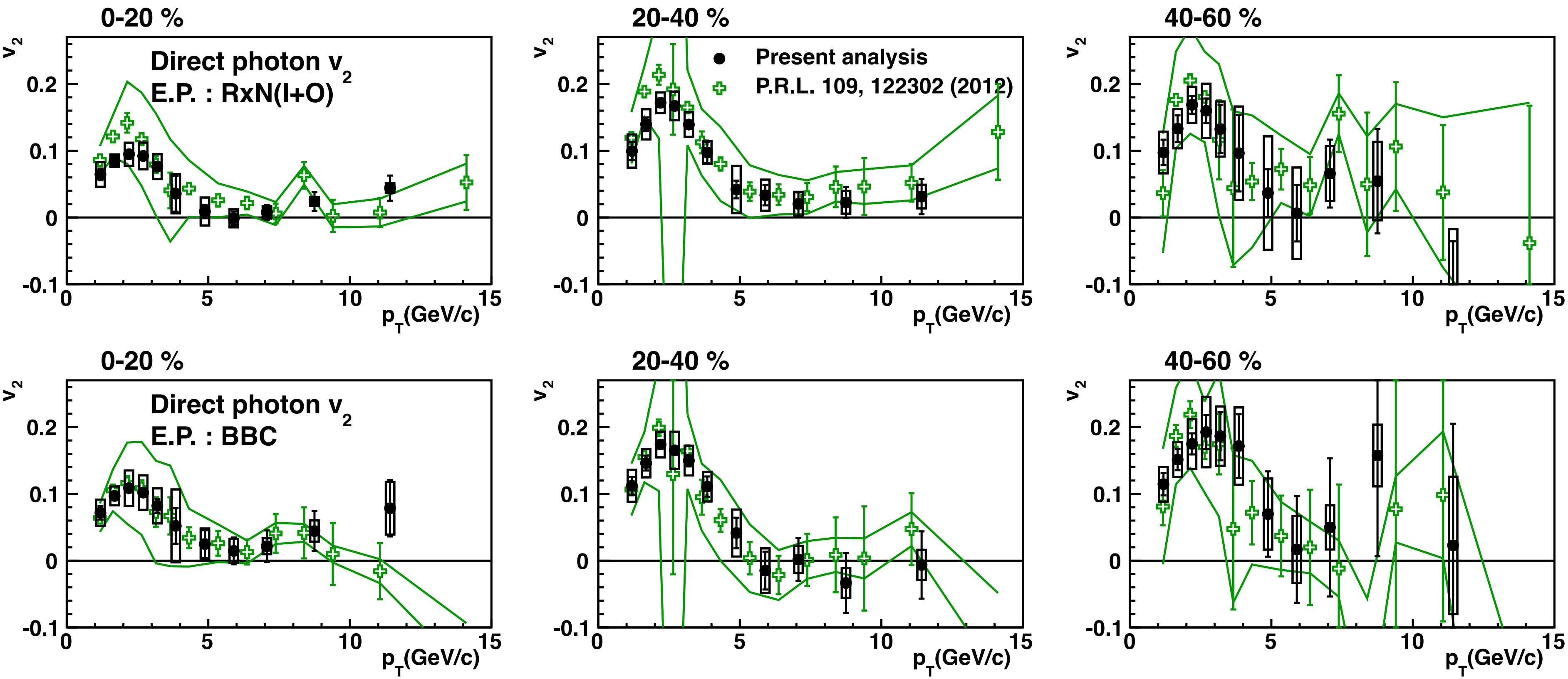

They are consistent within systematic uncertainty.